

ADAPTATION OF TURBULENCE MODELS
TO A NAVIER-STOKES SOLVER

A THESIS SUBMITTED TO
THE GRADUATE SCHOOL OF NATURAL AND APPLIED SCIENCES
OF
MIDDLE EAST TECHNICAL UNIVERSITY

BY

EMRE GÜRDAMAR

IN PARTIAL FULFILLMENT OF THE REQUIREMENTS
FOR
THE DEGREE OF MASTER OF SCIENCE
IN
MECHANICAL ENGINEERING

SEPTEMBER 2005

Approval of the Graduate School of Natural and Applied Sciences

Prof. Dr. Canan ÖZGEN
Director

I certify that this thesis satisfies all the requirements as a thesis for the degree of Master of Science.

Prof. Dr. Sıtkı Kemal İDER
Head of Department

This is to certify that we have read this thesis and that in our opinion it is fully adequate, in scope and quality, as a thesis for the degree of Master of Science.

Dr. Ali Ruhşen ÇETE
Co-Supervisor

Prof. Dr. Mehmet Haluk AKSEL
Supervisor

Examining Committee Members

Prof. Dr. Kahraman ALBAYRAK (METU, ME) _____

Prof. Dr. Mehmet Haluk AKSEL (METU, ME) _____

Dr. Ali Ruhşen ÇETE (TAI) _____

Prof. Dr. Zafer DURSUNKAYA (METU, ME) _____

Asst. Prof. Dr. Cüneyt SERT (METU, ME) _____

I hereby declare that all information in this document has been obtained and presented in accordance with academic rules and ethical conduct. I also declare that, as required by these rules and conduct, I have fully cited and referenced all material and results that are not original to this work.

Emre GÜRDAMAR

ABSTRACT

ADAPTATION OF TURBULENCE MODELS TO A NAVIER-STOKES SOLVER

GÜRDAMAR, Emre

M.S., Department of Mechanical Engineering

Supervisor : Prof. Dr. Mehmet Haluk AKSEL

Co-Supervisor: Dr. Ali Ruhşen ÇETE

September 2005, 151 pages

This thesis presents the implementation of several two-equation turbulence models into a finite difference, two- and three-dimensional Navier-Stokes Solver. Theories of turbulence modeling and the historical development of these theories are briefly investigated. Turbulence models that are defined by two partial differential equations, based on $k-\omega$ and $k-\varepsilon$ models, having different correlations, constants and boundary conditions are selected to be adapted into the base solver. The basic equations regarding the base Navier-Stokes solver to which the turbulence models are implemented presented by briefly explaining the outputs obtained from the solver. Numerical work regarding the implementation of turbulence models into the base solver is given in steps of non-dimensionalization, transformation of equations into generalized coordinate system, numerical scheme, discretization, boundary and initial conditions and limitations. These sections

of implementation are investigated and presented in detail with providing every steps of work accomplished.

Certain trial problems are solved and outputs are compared with experimental data. Solutions for fluid flow over flat plate, in free shear, over cylinder and airfoil are demonstrated. Airfoil validation test cases are analyzed in detail. For three dimensional applications, computation of flow over a wing is accomplished and pressure distributions from certain sections are compared with experimental data.

Keywords: Turbulence, Turbulence Modeling, Two-Equation Turbulence Models

ÖZ

TEDİRGİNLİK MODELLERİNİN İKİ BOYUTLU BİR NAVIER-STOKES ÇÖZÜCÜSÜNE UYARLANMASI

GÜRDAMAR, Emre

Yüksek Lisans, Makina Mühendisliği Bölümü

Tez Yöneticisi : Prof. Dr. Mehmet Haluk AKSEL

Ortak Tez Yöneticisi: Dr. Ali Ruhşen ÇETE

Eylül 2005, 151 sayfa

Bu tez çeşitli iki-denklemlilik tedirginlik modellerinin, sonlu farklar, iki ve üç boyutlu Navier-Stokes çözücüsüne eklenmesini sunmaktadır. Tedirginlik modellerinin teorileri ve bu teorilerin tarihsel gelişimi özetle incelenmiştir. Farklı bağıntılar, sabitler ve sınır şartları içeren, iki denklemlilik tanımlanmış k - ω ve k - ε bazlı tedirginlik modelleri seçilmiş ve temel çözücüyeye eklenmiştir. Modellerin eklendiği Navier-Stokes çözücünün temel denklemleri ve çıktıları sunulmuş kısaca açıklanmıştır. Tedirginlik modellerinin uygulanmasındaki kullanılan sayısal çalışma, birimsizleştirme, genel kordinat sistemine dönüştürme, numerik şema, ayırıklaştırma, sınır ve ilk şartlar ve sınırlandırmalar olarak adımlar halinde verilmiştir. Bu adımlar detaylı olarak, ve her adımda yapılan çalışmalar gösterilerek incelenmiş ve sunulmuştur.

Çeşitli deneme problemleri yapılmış ve deneysel veri ile doğrulanmıştır. Düz levha üzerinde akış, serbest akış ve silindir ve kanat kesiti üzerinden akışlar

için çözümler gösterilmiştir. Kanat kesit doğrulama denemeleri detaylıca incelenmiştir. Üç boyutlu uygulamalar için örnek olarak bir kanat seçilmiş ve basınç dağılımları deneysel veri ile karşılaştırılmıştır.

Anahtar Kelimeler: Tedirginlik, Tedirginlik Modellemesi, İki-Denklemli Tedirginlik Modelleri

To My Parents,
To GÜRDAMAR and BODUR families

ACKNOWLEDGMENTS

The author wishes to express his gratitude to Prof. Dr. Mehmet Haluk AKSEL and Dr. Ali Ruhşen ÇETE, since they were the pioneers of this work who oriented the author towards the correct directions every time.

The author would also like to thank Prof. Dr. Ünver KAYNAK, Mr. Yüksel ORTAKAYA, Mr. Hakan TİFTİKÇİ and Mr. Joseph MORRISON for their help during the thesis work.

Special thanks go to the colleagues of the author, Kıvanç ÜLKER, Onur BAŞ, Ali AKTÜRK, Özlem CEYHAN, Cumhuri ÖZGÜR, Umut Can DİNÇGEZ and Alkan ALTAY.

This work wouldn't be done without the support of the author's altruistic parents Işıl, Can GÜRDAMAR, his family and his dear Dilra Nazlı ERİÇ.

This study was completed by the support of the Turkish Aerospace Industries (TAI) under the name of TİDEB project ordered 3040091.

TABLE OF CONTENTS

PLAGIARISM.....	iii
ABSTRACT.....	iv
ÖZ.....	vi
DEDICATION.....	viii
ACKNOWLEDGMENTS	ix
TABLE OF CONTENTS.....	x
LIST OF TABLES.....	xii
LIST OF FIGURES	xiii
LIST OF SYMBOLS	xvii
CHAPTER	
1 INTRODUCTION	1
2 THEORY AND TURBULENCE MODELING	4
2.1 Turbulence, Definition and Properties	4
2.2 Turbulence Modeling.....	9
2.3 Brief History of Turbulence Modeling and Turbulence Models	11
3 BASE SOLVER.....	16
3.1 Governing Equations	17
3.2 Input and Output Files	19
4 MODEL IMPLEMENTATION	23
4.1 Model Equations and Correlations.....	24
4.1.1 Wilcox $k-\omega$ turbulence model.....	24

4.1.2	Chien $k-\varepsilon$ turbulence model	26
4.1.3	Abid $k-\varepsilon$ turbulence model	27
4.1.4	Menter Baseline (BSL) turbulence model	29
4.2	Numerical Framework	32
4.2.1	Non-Dimensionalization.....	33
4.2.2	Transformation to Generalized Coordinate System.....	37
4.2.3	Numerical Scheme	39
4.2.4	Discretization.....	49
4.2.5	Boundary and Initial Conditions.....	54
4.2.6	Limitations and Improvements.....	62
5	RESULTS AND DISCUSSIONS	71
5.1	Flat Plate	71
5.2	Free Shear.....	78
5.3	Cylinder	79
5.4	Airfoil	81
5.4.1	NACA0012	82
5.4.2	RAE2822	87
5.4.3	NACA63-2-415	96
5.5	Wing	99
5.5.1	ONERA M6 Wing	99
6	CONCLUSION.....	104
	REFERENCES	107
	APPENDICES.....	110

LIST OF TABLES

Table 4.1 Partial List of Schemes [3]	41
Table 4.2 List of Boundary Condition types	55
Table 5.1 C_l , C_d results for different turbulence models	86
Table 5.2 C_l , C_d results for different turbulence models	87
Table 5.3 C_l , C_d results for different turbulence models	88

LIST OF FIGURES

Figure 2.1	Leonardo da Vinci Sketch of turbulence	5
Figure 2.2	Time averaging	10
Figure 2.3	Movements of turbulence modeling [5]	15
Figure 3.1	Coordinate transformation for finite difference scheme	18
Figure 3.2	C-Grid for airfoil input for LANS2D	19
Figure 3.3	Residual graph of conservative flow variables	20
Figure 3.4	Residual graph of C_l , C_d and C_m variables	21
Figure 3.5	C_p versus x/c graph	21
Figure 3.6	Contours of C_p	22
Figure 3.7	Contours of Mach number	22
Figure 4.1	Domain representation for a solution node	49
Figure 4.2	Standard diffusion discretization nodes	52
Figure 4.3	Diffusion discretization with imaginary solution nodes	53
Figure 4.4	Boundary condition types for flat plate	55
Figure 4.5	Boundary condition types for free shear	55
Figure 4.6	Boundary condition types for cylinder	56
Figure 4.7	Boundary condition types for airfoil	56
Figure 4.8	Representation of wake boundary	59
Figure 4.9	Representation of outlet boundary	60
Figure 4.10	Symmetry boundary representation	60

Figure 4.11	Trailing edge of the airfoil.....	67
Figure 4.12	Outlet boundary in the C-Grid	68
Figure 4.13	Cell dimensions	69
Figure 4.14	O-Grid for airfoil	69
Figure 4.15	Enlarged view of O-Grid.....	70
Figure 4.16	O-Grid wake of an airfoil	70
Figure 5.1	Structured, 150x80 grid for the flat plate.....	72
Figure 5.2	Residual Drops versus iteration steps.....	73
Figure 5.3	Residual Drops of k versus Iteration steps	73
Figure 5.4	Residual Drops of ϵ & ω versus Iteration steps	73
Figure 5.5	Turbulent velocity profile results	75
Figure 5.6	Dimensionless turbulent kinetic energy versus y^+	76
Figure 5.7	Coefficient of Friction versus local Reynolds Number	77
Figure 5.8	(a) Laminar and (b) Turbulent velocity profiles	78
Figure 5.9	Turbulent viscosity contours	79
Figure 5.10	Turbulent viscosity contours	80
Figure 5.11	C_p distribution for different turbulence models	82
Figure 5.12	NACA0012, C-Grid overview	83
Figure 5.13	NACA0012, C-Grid closer view.....	83
Figure 5.14	Grid dependence results of C_p distribution	85
Figure 5.15	y^+ values for the first grid point from the wall	85
Figure 5.16	C_p distribution for different turbulence models	87
Figure 5.17	C_p distribution for different turbulence models	88
Figure 5.18	Laminar velocity profile at $x/c=0.319$	89

Figure 5.19	Turbulent velocity profile at $x/c=0.95$	90
Figure 5.20	Friction Coefficient	91
Figure 5.21	Turbulent Viscosity distribution on $x/c=0.9$	92
Figure 5.22	k^+ distribution on $x/c=0.9$	93
Figure 5.23	Turbulent Velocity Profiles on $x/c=0.9$	93
Figure 5.24	f_μ values for <i>Chien</i> and <i>Abid</i> $k-\epsilon$ on $x/c=0.9$	94
Figure 5.25	F_1 value transition for <i>Menter BSL</i> on $x/c=0.9$	95
Figure 5.26	C_l versus <i>AoA</i> graph	96
Figure 5.27	C_l versus <i>AoA</i> , Stall point detailed	97
Figure 5.28	C_d versus C_l graph	98
Figure 5.29	C_m versus <i>AoA</i> graph.....	98
Figure 5.30	C_p contours	99
Figure 5.31	C_p contours Left – Lower side, Right – Upper side.....	100
Figure 5.32	ONERA M6 WING, Turbulent Viscosity Contours.....	100
Figure 5.33	ONERA M6 WING, C_p distribution, $y/b=0.44$	101
Figure 5.34	ONERA M6 WING, C_p distribution, $y/b=0.65$	102
Figure 5.35	ONERA M6 WING, C_p distribution, $y/b=0.80$	102
Figure 5.36	ONERA M6 WING, C_p distribution, $y/b=0.90$	103
Figure 5.37	ONERA M6 WING, C_p distribution, $y/b=0.95$	103
Figure E.1	C_p contours, <i>Abid</i> $k-\epsilon$	140
Figure E.2	C_p contours, <i>Chien</i> $k-\epsilon$	141
Figure E.3	C_p contours, <i>Baldwin-Lomax</i>	141

Figure E.4	C_p contours, <i>Wilcox k-ω</i>	142
Figure E.5	C_p contours, <i>Menter BSL</i>	142
Figure E.6	μ_T contours, <i>Abid k-ϵ</i>	143
Figure E.7	μ_T contours, <i>Chien k-ϵ</i>	143
Figure E.8	μ_T contours, <i>Baldwin-Lomax</i>	144
Figure E.9	μ_T contours, <i>Wilcox k-ω</i>	144
Figure E.10	μ_T contours, <i>Menter BSL</i>	145
Figure E.11	k contours, <i>Abid k-ϵ</i>	145
Figure E.12	k contours, <i>Chien k-ϵ</i>	146
Figure E.13	k contours, <i>Wilcox k-ω</i>	146
Figure E.14	k contours, <i>Menter BSL</i>	147
Figure E.15	k production contours, <i>Abid k-ϵ</i>	147
Figure E.16	k production contours, <i>Chien k-ϵ</i>	148
Figure E.17	k production contours, <i>Wilcox k-ω</i>	148
Figure E.18	k production contours, <i>Menter BSL</i>	149
Figure E.19	k destruction contours, <i>Abid k-ϵ</i>	149
Figure E.20	k destruction contours, <i>Chien k-ϵ</i>	150
Figure E.21	k destruction contours, <i>Wilcox k-ω</i>	150
Figure E.22	k destruction contours, <i>Menter BSL</i>	151

LIST OF SYMBOLS

Latin Symbols

AoA	Angle of attack
$arg1$	Closure coefficient for two equation model
C_m	Moment coefficient
C_d	Drag coefficient
C_l	Lift coefficient
C_f	Friction Coefficient
C_p	Pressure Coefficient
$C_{\varepsilon 1}$	Closure coefficient for two equation models
$C_{\varepsilon 2}$	Closure coefficient for two equation models
C_{μ}	Closure coefficient for two equation models
$CD_{k\omega}$	Closure coefficient for two equation model
d	Wall distance from first grid point
D_k	Destruction term for turbulent kinetic energy
D_{ω}	Destruction term for specific dissipation rate
D_{ε}	Destruction term for dissipation per unit mass
D	Additional term for $k-\varepsilon$ models
$deln$	First grid point distance from the wall
E	Additional term for $k-\varepsilon$ models
f_{μ}	Closure coefficient for two equation models
f_1	Closure coefficient for two equation models
f_2	Closure coefficient for two equation models
F_1	Closure coefficient for two equation model
J	Jacobian

k	Turbulent kinetic energy
k^+	Dimensionless, sub-layer scaled, turbulent kinetic energy
M	Mach number
P	Static pressure
P_k	Production term for turbulent kinetic energy
P_ω	Production term for specific dissipation rate
P_ε	Production term for dissipation per unit mass
Re	Reynolds number
Re_k	Reynolds number based on turbulent kinetic energy
Re_τ	Reynolds number based on turbulent viscosity
Δt	Time step
TMU	Turbulent Viscosity (used in figures)
$u'(x, t)$	Fluctuating velocity
$U(x)$	Time averaged velocity
u^+	Dimensionless, sub-layer scaled, velocity
x	Spatial variable in physical domain
y	Spatial variable in physical domain
y^+	Dimensionless, sub-layer scaled, distance
z	Spatial variable in physical domain

Greek Symbols

Ω	Vorticity vector
β	Closure coefficient for two equation models
ε	Dissipation per unit mass
ζ	Spatial variable in computational domain
η	Spatial variable in computational domain
κ	Karman constant
μ	Laminar viscosity
μ_τ	Turbulent viscosity
μ_{total}	Viscosity combination of laminar and turbulent viscosities

ν	Laminar kinematic viscosity
ν_T	Turbulent kinematic viscosity
ξ	Spatial variable in computational domain
ρ	Density
σ_k	Closure coefficient for two equation models
σ_ω	Closure coefficient for two equation models
σ_ε	Closure coefficient for two equation models
τ_{xy}	Specific Reynolds stress
ω	Specific dissipation rate
Γ	Part of diffusion terms
ϕ	Closure coefficient for two equation model

Superscripts

<i>upwind</i>	Upwind differencing application
*	Conservative vector multiplied with M/Re
<i>n</i>	Time level
\sim	Dimensional values

Subscripts

∞ or <i>inf</i>	Free stream
<i>wall</i>	Wall value
<i>l</i>	Laminar
<i>T</i> or <i>t</i>	Turbulent
<i>corr</i>	Corrected Value

Operators

Δ^f	Forward differencing
∇^b	Backward differencing
Δ	Change representation for solution vectors
∂	Derivation

- Multiplication
- Distribution into derivative terms

CHAPTER 1

INTRODUCTION

One of the most important tasks in the discipline of engineering is the optimization of the designs according to certain variables. Since the population of our earth is growing faster than the growth of resources, one optimization parameter appears as the need to serve many people in the shortest time and the most cost effective way. Also during these services, companies are trying to profit from the products they sell. As a consequence, new designs are obliged to compensate the capital that is spent on the design and production stages, in a short time. Today, mankind is continuously developing high technologies in all aspects of engineering. The results of these developments allow engineers to design products that are huge in size and beneficial in use which provides the necessary compensation of money. A good example for this situation is the design of passenger and cargo planes which should be planned such that they would have as many passengers and carriages as possible, with which the safety constraints should not be violated. Then, any tiny modification that would result in a useful way is important for the manufacturer. To obtain these modifications, the designers are trying many different configurations of different sizes. The design steps are perhaps repeated many times to have these different configurations. The design procedures, of course, possess a very important step of testing the built prototype which would be very expensive for such a machine. As a result the need of a decrease in the number of test cases shows up as a great demand by the manufacturers. The decrease could not be a result of an arbitrary decision; on the contrary, it must be an educated determination. The function of CFD (Computational

Fluid Dynamics) could be seen more clearly in that step that which basically serves in different manners; as an analysis tool that is done on the early design stage, an elimination mechanism of different configurations on the test stage or an information provider for cases which are nearly impossible to test.

Developments in computer technology have led to many drastic changes in computation times and memory capabilities. These changes enabled the engineers to refer to CFD more frequently than before. Also the types of problems increased; turbulent flows, heat transfer and icing problems, particle tracing and direct numeric simulation applications appeared to be solved. By the help of parallel computing the computation loads could be shared into several different CPU's. Computer capabilities as such give us to solve two more equations for the turbulence models.

Turbulence, of which theory will be briefly examined in the oncoming chapters, could be defined as a flow phenomenon basically caused by a presence of a wall or a shear layer between two flows in which diffusion of every property of a fluid is tremendously enhanced. Statistical methods could be applied to simulate turbulence however; the computation capabilities are not so developed to solve a direct numerical simulation solution of a half wing of an airplane. Then the need for modeling this chaotic phenomenon appears. Although it is illogical to represent a case like turbulence in two partial differential equations but for a finite space based problem description, it appears to be quite accurate for a prediction of a "turbulent viscosity".

Implementation of several two-equation turbulence models to a finite difference based Navier-Stokes solver is the main motivation for this thesis

work. Two-equation turbulence models based on $k-\omega$ and $k-\varepsilon$ with different constants, correlations and boundary conditions are investigated.

Base solver named as LANS2D that will be introduced briefly in the following sections, is searched through the documents of TAI library and papers regarding the LU-ADI algorithm written by the authors of the base solver. Since turbulence models to be implemented are treated isolated from the progress of the base solver during a computation step, research for numerical scheme to construct a self working turbulence model solver is appeared to be the challenge. Literature survey regarding the turbulence models are accomplished by taking the needs for limitations and corrections into consideration. Many different references are searched and the ones that are directly used in this work are included in the references.

Definitions of turbulence and properties are introduced in the following section with giving the basic differences between turbulence models. This section searches for an answer to the need for turbulence modeling. Then the properties of the base solver are presented. Brief history of turbulence modeling is also included in this chapter. Numerical framework that the base of the coding steps appears in the sequent chapters involves non-dimensionalization, numerical scheme, discretization, boundary and initial conditions with some limitations. Complete implementation steps are given in this section with showing the intermediate steps in the appendix sections in detail. The results of the test cases for flat plate, free shear, cylinder and airfoil applications are also given with an additional wing computation.

CHAPTER 2

THEORY AND TURBULENCE MODELING

2.1 Turbulence, Definition and Properties

For ages, mankind tried to understand the natural events around and tried to find an explanation for them. When it is insufficient to clarify, these events were referred to as god given. Today many natural phenomena could be represented by scientific methods through cause and effect relationships. On the other hand most of them are still not "defined" and "understood" completely. One of the most important undefined cases is the turbulence. Today scientists are trying to develop equations of turbulence flow with the help of experimental techniques to solve this problem. Although this phenomenon is not completely solved and mentioning about its theory is certainly some kind of a dilemma, there are certain explanations of turbulence that are given by the pioneers of this subject. About five hundred years ago, Leonardo da Vinci (1452 – 1519) described turbulence and told his first observations as,

Observe the motion of the surface of the water, which resembles that of hair, which has two motions, of which one is caused by the weight of the hair, the other by the direction of the curls; thus the water has eddying motions, one part of which is due to the principal current, the other to random and reverse motion. [1]

Another description of Da Vinci gives a remarkably modern description with a sketch of turbulent flow,

...the smallest eddies are almost numberless, and large things are rotated only by large eddies and not by small ones, and small things are turned by small eddies and large. [2]



Figure 2.1 Leonardo da Vinci Sketch of turbulence

Von Karman quotes G. I. Taylor in 1937 by defining turbulence as;

an irregular motion which in general makes its appearance in fluids, gaseous or liquid, when they flow past solid surfaces or even when neighboring streams of the same fluid flow past or over one another.[3]

A more precise definition of turbulence has been made by Hinze that gives the basic characteristics in words as follows;

Turbulent fluid motion is an irregular condition of the flow in which the various quantities show a random variation with time and space

coordinates, so that statistically distinct average values can be discerned. [4]

Bradshaw adds the statement that turbulence has wide range of scales. More recent explanations of turbulence include several definitions that are describing turbulence in a more deterministic way such as

Turbulence is any chaotic solution to the 3-D Navier-Stokes equations that is sensitive to initial data and which occurs as a result of successive instabilities of laminar flows as a bifurcation parameter is increased through a succession of values. [5]

All of these definitions are quite successful in describing the turbulent flow but they are not sufficient to define the turbulence phenomena with all its characteristics. As mentioned before, defining all the characteristics of turbulent flow is still not possible though; some fundamental properties could be listed. The following particularities of turbulent flow are the blending of references [6] and [7].

Turbulence definitions address to an irregular motion which in general makes its appearance in fluids when they flow past solid surfaces or even when neighboring streams of the same fluid past or over one another. Therefore, the **instabilities** occurring in the flow cause laminar flow to turn into turbulent flow. Any solid surface projecting towards the flow streamlines is a source of disturbance for the turbulent flow to initiate. If a flow past over a flat plate is investigated, the fully turbulent region does not appear directly after the laminar part. There always appears a transition section which is the region where instabilities in laminar flow start. The flow in this region could be described neither as laminar, nor as turbulent. These instabilities occur

due to highly complex fluid-fluid and fluid-solid interactions. If one looks into this phenomenon from partial differential equations point of view, Navier-Stokes equations that are representing the viscous fluid flow produce instabilities due to the non-linear viscous and inertial terms in these equations.

The most frequently word group used in defining turbulence is “random fluctuations” that is referred to fluctuations of all variables transported within the flow namely, density, velocity, energy, pressure and so forth. When the randomness of a variable appears in a definition, **statistical methods** should be involved in. The values of variables within a turbulent flow could be interpreted by averaging them by several means such as in time and in space.

Turbulence is a **continuum** process. When it comes to a point to measure turbulence elements, length scale appears as a dimensional property. The length scales of eddies which will be explained in the following paragraphs, emerges much larger than the molecular length scale. This enables one to treat turbulence as a continuum phenomenon. Then, one can conclude that Navier-Stokes equations have all the physics of turbulence.

There are primarily two parts for the mechanism of turbulence. One is the small eddies and the other is the large eddies. If it is appropriate to say that the “responsibilities” of these two eddies are different such that as turbulence decays it transfers kinetic energy from large eddies to smaller ones. This could be referred to as a **cascade process**. The large eddies transport turbulence form one location to another, in other words the large eddies direct the turbulent flow depending upon the upstream history. This is the main reason why the turbulent flow is considered to be smarter than the

laminar flow because it remembers from where it comes and decides where to go.

The turbulence mechanism ***decays without an energy input***. In other words, a turbulent flow must be driven by the presence of a wall or any other disturbance present in the flow domain; otherwise, turbulent flow turns into laminar. The large eddies should be fed by a mechanism of mechanical energy input to gain kinetic energy to continue turbulence process. As large eddies grow, small eddies dissipate this kinetic energy to thermal energy. This is the dissipation mechanism of turbulent flow named as, turbulent viscosity.

Here appears another frequently used term, viscosity, in other words momentum diffusion. The latter word is the one that describes the viscosity better. In turbulent flow, diffusion of the momentum and other properties of flow increase tremendously. ***Enhanced diffusivity*** is another property, probably the most important, of turbulent flow. Diffusion of every property is increased in several orders of magnitude than the one in laminar flow.

2.2 Turbulence Modeling

It is convenient to start with asking the famous question of “why do we need turbulence modeling?” Two different approaches to the answer of this question could be of concern. One includes the physical answer, whereas the other looks into the problem in a more mathematical manner.

A fluid flow could be described in several ways. It could be either, compressible or incompressible, viscous or inviscid, in the same manner, either laminar or turbulent. If the last two definitions of flow are investigated in detail, certain parameters to decide on the type of flow whether it is laminar or turbulent could be found. Perhaps one of the most important parameter is the **Reynolds number**. For different types of flow (namely, flow in a pipe, flow over a flat plate etc.) different Reynolds numbers of transition from laminar to turbulent flow are defined. Another important parameter is the **roughness**. Through a pipe with a rough surface, it is detected that the flow gets turbulent in a shorter distance where as this length is larger in a smoother pipe. Such observations show that the descriptions of laminar or turbulent cases are types of a **flow**, not a **fluid**. If they were a property of a fluid, it is possible to measure the quantities of them; “how turbulent or how laminar a fluid is?” So here comes the answer to the question about the reason for modeling turbulence; since the presence of a turbulent media is a property flow, it should be modeled.

On the other hand, from a mathematical point of view, the turbulent motion could be included into the Navier-Stokes equations. It is mentioned that, statistical methods are used to average the fluctuating properties of flow in the turbulent case. Certain averaging techniques such as time, spatial and ensemble averaging are used to obtain the mean values of these properties. Homogenous turbulence, that is the averaged turbulent flow uniform in all

directions, spatial averaging is used where as, for stationary turbulence which, on the average, does not vary with time, time averaging is used. But ensemble averaging is the most suitable averaging for flows decaying in time [6]. For the flows that engineers mostly deal with, time averaging is used. Time averaging yields an average and a fluctuating part for a certain variable. These parts could be represented as the part of the instantaneous parameter, say velocity.

$$u_i(x,t) = U_i(x) + u'_i(x,t) \quad (2.1)$$

Here $u_i(x,t)$ is expressed as the instantaneous velocity with, $U_i(x)$; average and $u'_i(x,t)$ fluctuating part.

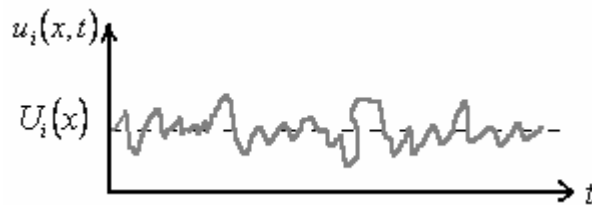


Figure 2.2 Time averaging

If this instantaneous velocity term given in Equation (2.1) is added into the Navier-Stokes equations so called **Reynolds Averaged Navier-Stokes (RANS)** equations are obtained.

$$\rho \cdot \frac{\partial U_i}{\partial t} + \rho \cdot U_j \cdot \frac{\partial U_i}{\partial x_j} = -\frac{\partial P}{\partial x_i} + \frac{\partial}{\partial x_j} \left(2 \cdot \mu \cdot S_{ji} - \rho \cdot \overline{u'_j \cdot u'_i} \right) \quad (2.2)$$

The quantity $-\rho \overline{u_j' \cdot u_i'}$ is known as the **Reynolds-stress tensor**. There arises the problem of finding the value of Reynolds stress tensor in order to determine the mean-flow properties of the turbulent flow. The mean flow variables could be solved (or computed) in the same manner as Navier-Stokes equations but the last term of RANS must be modeled.

2.3 Brief History of Turbulence Modeling and Turbulence Models

As already have mentioned, turbulence phenomenon starts to being investigated since Leonardo da Vinci. But until year 1877, any significant progress on neither theory nor modeling had occurred. At that year Boussinesq proposed an idea on the theory of turbulence that, turbulent stresses are linearly proportional to mean strain rates. Following Boussinesq's proposal, in 1894 Osborne Reynolds conducted the first notable experiments on turbulence and transition events. The experiments had resulted in that only physical parameter for a smooth and incompressible flow appears to be the Reynolds number. Reynolds stated turbulence as a highly random phenomenon that no movement of any particle could be determined previously. By these years, deterministic (referring to events that have no random or probabilistic aspects but proceed in a fixed predictable fashion) approaches to turbulence started to emerge.

Further progress was obtained by Prandtl's discovery of boundary layer in 1904. In 1925, "mixing length theory" has been evolved suggesting the computation of eddy viscosity by means of mixing lengths which is analogue to mean free path of a gas. Further researches like von Karman and Taylor had contributed to turbulence studies. This mixing length theory which was first appeared as an idea of Prandtl, became the basic turbulence models

named as **algebraic** or **zero-equation turbulence models**. The following correlations are the relations for algebraic models.

$$\tau_{xy} = \mu_T \cdot \frac{dU}{dy} = \frac{1}{2} \cdot \rho \cdot V_{mix} \cdot l_{mix} \cdot \frac{dU}{dy}$$

$$V_{mix} \approx cons \cdot l_{mix} \cdot \frac{dU}{dy} \quad (2.3)$$

$$\nu_T = l_{mix}^2 \cdot \frac{dU}{dy}$$

(Most popular algebraic models of turbulence are **Cebeci-Smith** [22] and **Baldwin-Lomax** [21] turbulence models.)

After these improvements on turbulence and turbulence modeling, Prandtl, postulated a model for the eddy viscosity in which the eddy viscosity is dependent on the kinetic energy of turbulent fluctuations, k . It was the first introduction of **one-equation turbulence model**.

Kinetic energy per unit mass is described and related to the Reynolds stress tensor as,

$$k = \frac{1}{2} \cdot \left(\overline{u'^2} + \overline{v'^2} + \overline{w'^2} \right) \quad (2.4)$$

$$\tau_{ii} = -\overline{u_i' \cdot u_i'} = -2 \cdot k$$

Implementation of this relation into Reynolds Stress Tensor Equation (this work is shown in detail and explained in [6, page 36-39]) resulted in a transport equation for the turbulent kinetic energy,

$$\underbrace{\frac{\partial k}{\partial t} + U_j \cdot \frac{\partial k}{\partial x_j}}_{\text{SUBSTANTIAL DERIVATIVE}} = \underbrace{\tau_{ij} \cdot \frac{\partial U_i}{\partial x_j}}_{\text{PRODUCTION}} - \underbrace{\varepsilon}_{\text{DISSIPATION}} + \frac{\partial}{\partial x_j} \cdot \left(\underbrace{\nu \cdot \frac{\partial k}{\partial x_j}}_{\text{MOLECULAR DIFFUSION}} - \underbrace{\frac{1}{2} \cdot \overline{(u_i' \cdot u_i' \cdot u_j')}}_{\text{TURBULENCE TRANSPORT}} - \underbrace{\frac{1}{\rho} \cdot \overline{(P' \cdot u_j')}}_{\text{PRESSURE DIFFUSION}} \right) \quad (2.5)$$

Each term has a different meaning regarding the turbulent flow. *Production term* could be regarded as the mechanism of kinetic energy of the mean flow turning into turbulent kinetic energy where as *Dissipation* appears to be the term describing the turbulent kinetic energy dissipated as thermal energy. Last three diffusion terms could be explained as the turbulent energy diffusion by fluid's natural molecular transport, diffusion by turbulent fluctuations and turbulent transport from pressure and velocity fluctuations in the order of appearance. The recent results of Direct Numerical Simulation (DNS) enables the diffusion terms to be treated as $\frac{\partial}{\partial x_j} \cdot \left(\left(\nu + \nu_T / \sigma_k \right) \cdot \frac{\partial k}{\partial x_j} \right)$.

(Most popular one equation turbulence models could be listed as, **Baldwin-Barth** [23] and **Spalart-Almaras** models [13])

The turbulence models listed up to here do not involve a length scale. Since the turbulent viscosity includes a velocity and a length scale (on dimensional grounds, the kinematic viscosity ν appears to be in m^2/s that is the product of a velocity and a length scale), the models without involving a length scale are regarded as incomplete.

Kolmogorov introduced the first complete turbulence model by presenting a time scale known as the rate of dissipation of energy in unit volume and time and represented as “ ω ”. The absent length scale is provided by $k^{1/2} / \omega$ where $k \cdot \omega$ is analogue to the dissipation rate “ ε ”. This success of additional equation showed up as the introduction of **two-equation turbulence**

models. Since the dissipation term in the “*k*” equation is evaluated by another transport for “ ω ”, the model is complete. Second equation appears as,

$$\frac{\partial \omega}{\partial t} + U_j \cdot \frac{\partial \omega}{\partial x_j} = -\beta \cdot \omega^2 + \frac{\partial}{\partial x_j} \cdot \left(\sigma \cdot \nu_T \cdot \frac{\partial \omega}{\partial x_j} \right) \quad (2.6)$$

Later Wilcox had modified the Kolmogorov’s ω equation and formed new correlations [6]

Today ***k*- ω** and ***k*- ϵ turbulence models** gained a great success in engineering applications of internal and external flows. The rest of the thesis will be about several two equation models and applications of them.

Other studies of turbulence modeling became very popular since the computational capabilities of computers have been continuously increasing in the recent years are being developed in great amounts. **DNS** applications are not only being studied extensively in universities but also provide important data and knowledge on turbulent flows. **LES** studies are also very popular for simulating large scales of turbulence where meteorology science uses.

The movements in the study of turbulence are described by Chapman and Tobak [5] in Figure 2.3.

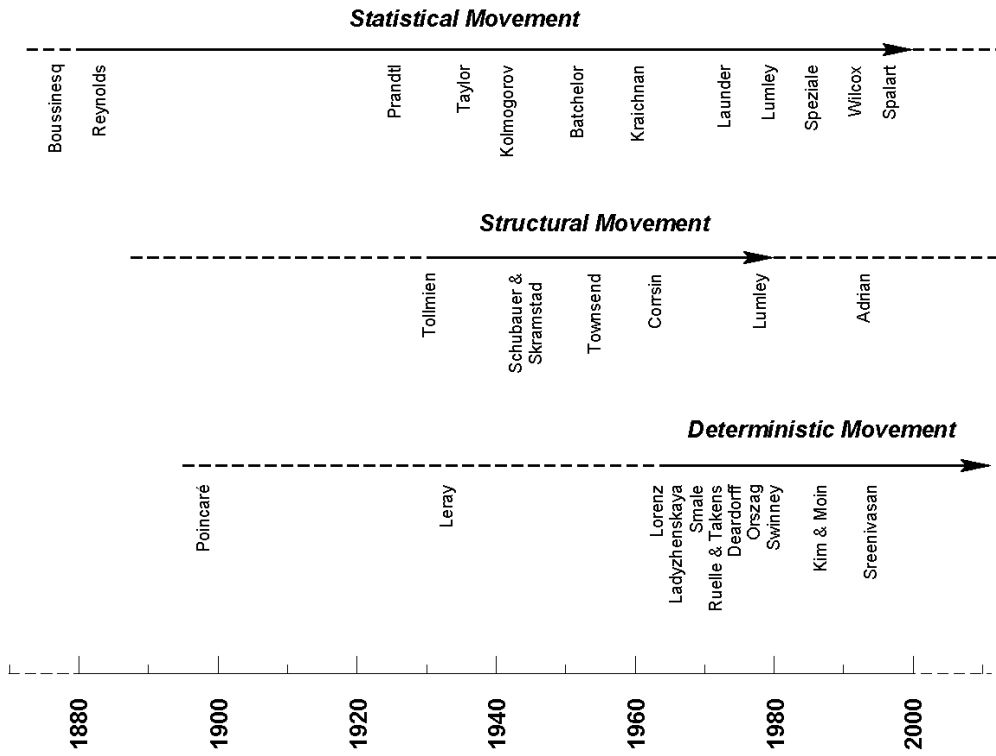


Figure 2.3 Movements of turbulence modeling [5]

CHAPTER 3

BASE SOLVER

In this study, several turbulence models are adapted to a thin layer Navier-Stokes code which was developed by Kozo Fujii and Shigeru Obayashi. The results of this code were published in [24]. The original solver uses a Lower Upper – Alternating Directions Implicit (LU-ADI) solver and an algebraic turbulence model of Baldwin-Lomax. The original code has two versions for 2D and 3D problems named as LANS2D and LANS3D. **LANS** is an acronym for **LU-ADI Navier-Stokes**.

Many different versions of LANS is present in certain forms. The present version includes convergence acceleration with variable time stepping and contains several upwind schemes. LANS2D and LANS3D are finite difference based codes which are designed to solve transonic flow over an airfoil and a wing. The governing equations regarding LANS2D will be investigated.

Turbulence models are added into these codes as separate modules by implementing initial and boundary conditions in appropriate subroutines. The turbulent viscosity is introduced into the code at each computational step by simply adding it to laminar viscosity.

$$\mu_{total} = \mu + \mu_T \quad (3.1)$$

3.1 Governing Equations

Navier-Stokes equations of conservative and vectorized form appear as follows:

$$\frac{\partial Q}{\partial t} + \frac{\partial E}{\partial x} + \frac{\partial F}{\partial y} = \frac{\partial E_v}{\partial x} + \frac{\partial F_v}{\partial y} \quad (3.2)$$

The left hand side of this equation represents the explicit form of the substantial derivative of variable Q while the right hand side stands for the diffusion terms. These vectors can be given as;

$$Q = \begin{bmatrix} \rho \\ \rho \cdot u \\ \rho \cdot v \\ e \end{bmatrix}, F = \begin{bmatrix} \rho \cdot v \\ \rho \cdot u \cdot v \\ \rho \cdot v^2 + p \\ v \cdot (e + p) \end{bmatrix}, E = \begin{bmatrix} \rho \cdot u \\ \rho \cdot u^2 + p \\ \rho \cdot u \cdot v \\ u \cdot (e + p) \end{bmatrix}$$

$$E_v = \begin{bmatrix} 0 \\ \tau_{xx} \\ \tau_{xy} \\ u \cdot \tau_{xx} + v \cdot \tau_{xy} + \mu \cdot \left(\frac{k}{k-1} \right) \cdot \frac{\partial}{\partial x} \left(\frac{P}{\rho} \right) \end{bmatrix} \quad (3.3)$$

$$F_v = \begin{bmatrix} 0 \\ \tau_{xy} \\ \tau_{yy} \\ u \cdot \tau_{xy} + v \cdot \tau_{yy} + \mu \cdot \left(\frac{k}{k-1} \right) \cdot \frac{\partial}{\partial y} \left(\frac{P}{\rho} \right) \end{bmatrix}$$

In Cartesian coordinates, it would be quite difficult to discretize the equations in a finite difference scheme due to the complexity of the geometry of the computational domain. Therefore, generalized coordinates are used to transform equations into the computational domain as shown in Figure 3.1.

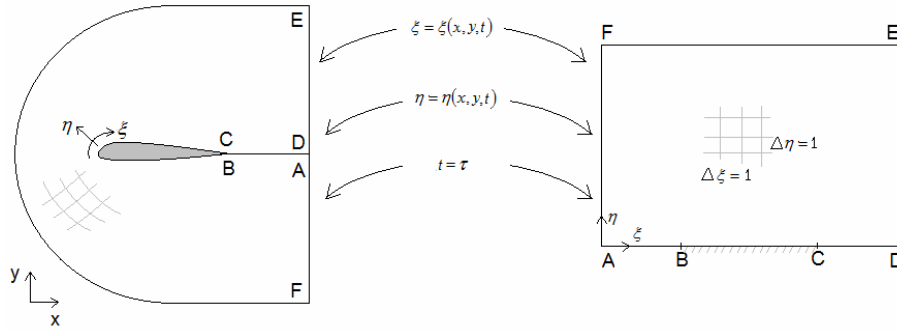


Figure 3.1 Coordinate transformation for finite difference scheme

After this transformation, Equations (3.2) and (3.3) become,

$$\frac{\partial \hat{Q}}{\partial \tau} + \frac{\partial \hat{E}}{\partial \xi} + \frac{\partial \hat{F}}{\partial \eta} = \frac{\partial \hat{E}_v}{\partial \xi} + \frac{\partial \hat{F}_v}{\partial \eta}$$

$$\hat{Q} = \frac{1}{J} \cdot \begin{bmatrix} \rho \\ \rho \cdot u \\ \rho \cdot v \\ e \end{bmatrix}, \hat{E} = \frac{1}{J} \cdot \begin{bmatrix} \rho \cdot U \\ \rho \cdot u \cdot U + \xi_x \cdot p \\ \rho \cdot v \cdot U + \xi_y \cdot p \\ U \cdot (e + p) - \xi_t \cdot p \end{bmatrix}, \hat{F} = \frac{1}{J} \cdot \begin{bmatrix} \rho \cdot V \\ \rho \cdot u \cdot V + \eta_x \cdot p \\ \rho \cdot v \cdot V + \eta_y \cdot p \\ V \cdot (e + p) - \eta_t \cdot p \end{bmatrix} \quad (3.4)$$

$$\hat{E}_v = \frac{1}{J} \cdot (\xi_x \cdot E_v + \xi_y \cdot F_v), \hat{F}_v = \frac{1}{J} \cdot (\eta_x \cdot E_v + \eta_y \cdot F_v)$$

3.2 Input and Output Files

Mach number, Reynolds number and angle of attack which represent the flow conditions are the basic input parameters and the solution method is selected in the input file. Central differencing upwind biased schemes with determination of turbulence models are available for selection in the input section. The smoothing parameters and secondary inputs such as number of iterations, time step values, smoothing steps are also included. During the implementation of turbulence models, several input parameters are added to the original input file such as, a parameter for the selection of spatial discretization scheme to be used in turbulence models, limitation activation, initial distribution flag and a transition point if necessary.

A structured C-Grid for airfoil geometry must be introduced by specifying the dimensions of the grid and the start and end points of body geometry.

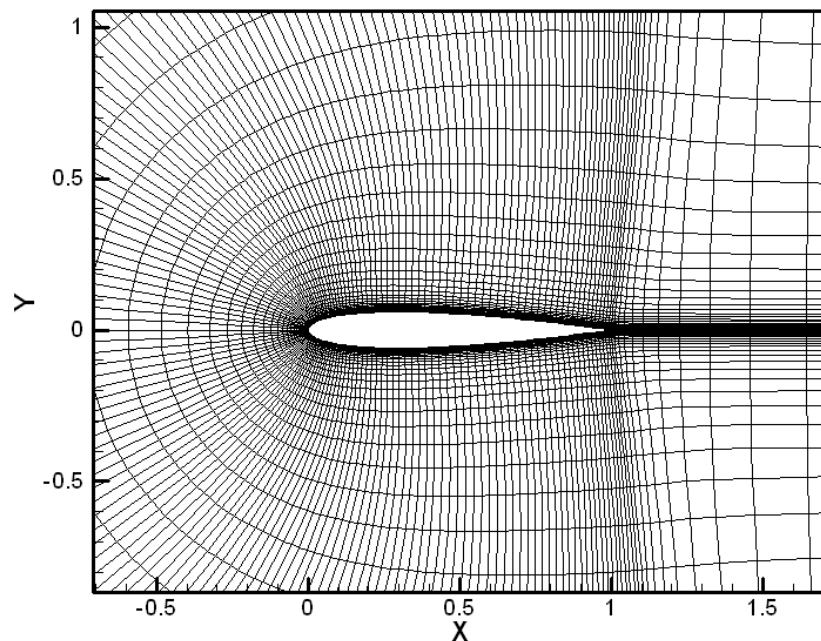


Figure 3.2 C-Grid for airfoil input for LANS2D

Output files regarding the converged solution are the residual graphs of flow variables including turbulence model quantities, field variable outputs, C_l , C_d and C_m values with C_p versus x/c values. Flow over a NACA0012 profile having properties of Mach number of 0.5 with 2.0 angle of attack degrees and $9 \cdot 10^6$ Reynolds number is analyzed. Residuals of flow variables and load coefficient values are given in Figures 3.3 and 3.4. Coefficient of pressure distribution along the surface of the airfoil is given in Figure 3.5. Contours of pressure and mach number is visualized in Figures 3.6 and 3.7.

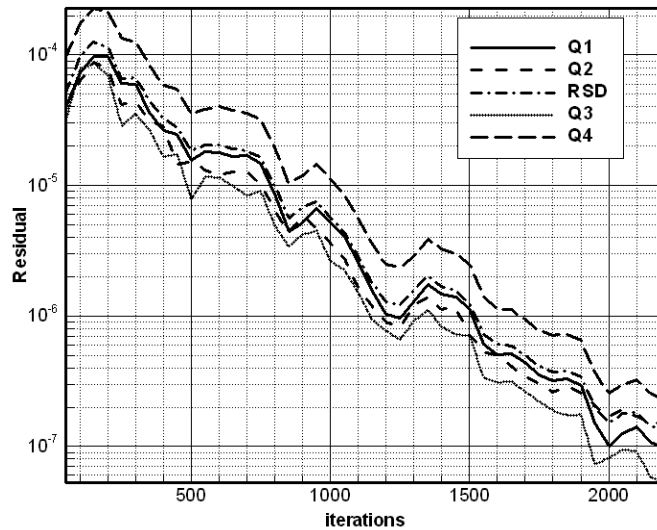


Figure 3.3 Residual graph of conservative flow variables

The execution of the modified code can be terminated when C_l , C_d and C_m convergence is achieved. User can either input a convergence criterion or simply follow residual drops in the residual graphs of C_l , C_d and C_m .

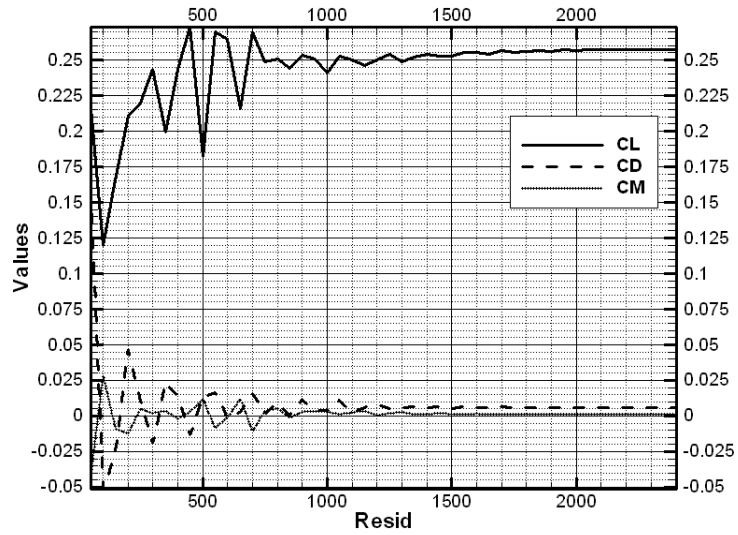


Figure 3.4 Residual graph of C_l , C_d and C_m variables

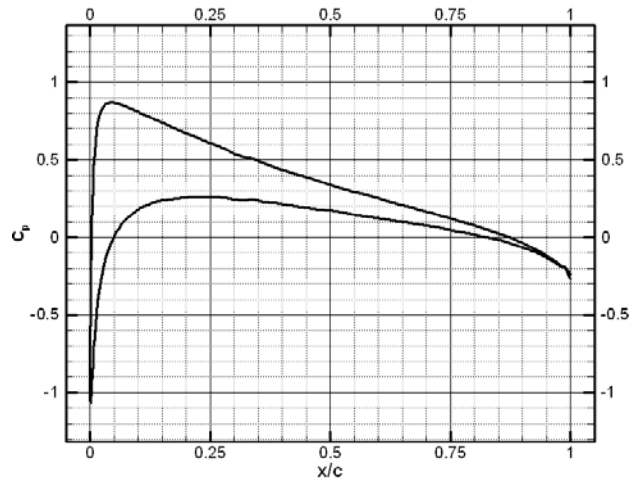


Figure 3.5 C_p versus x/c graph

Distribution of flow variables could be obtained such as density, velocity, local Mach number, energy, pressure, turbulent kinetic energy, dissipation, viscosity and so forth.

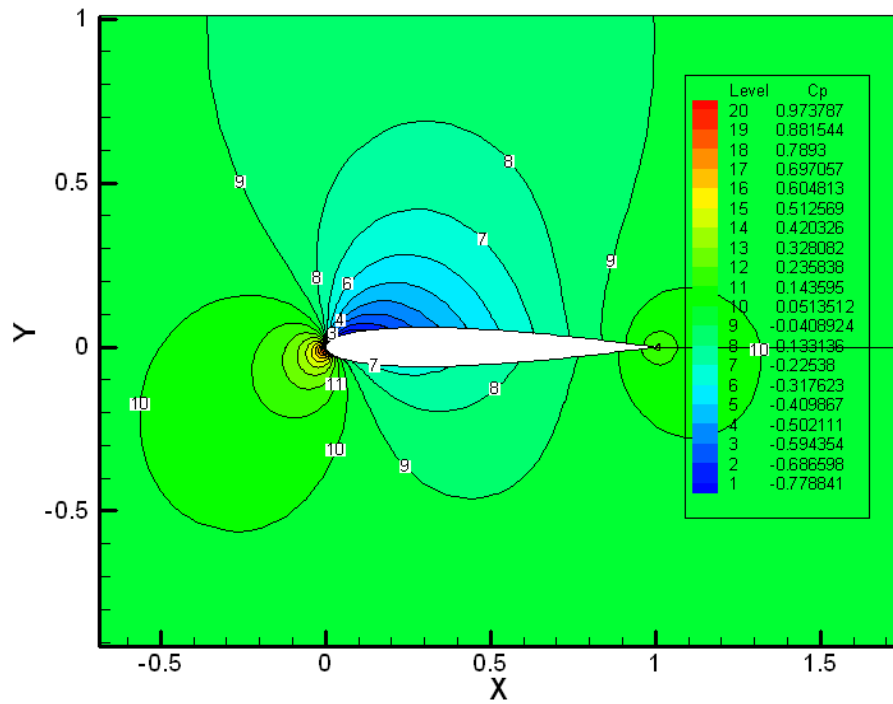


Figure 3.6 Contours of C_p

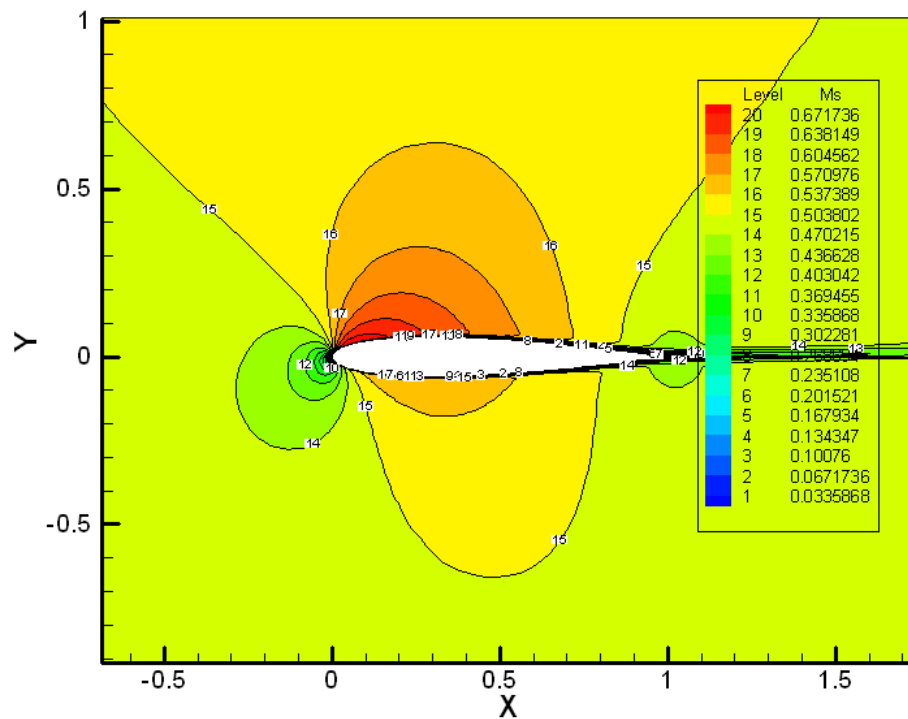


Figure 3.7 Contours of Mach number

CHAPTER 4

MODEL IMPLEMENTATION

The base solver which is mentioned in Chapter 3, included an algebraic turbulence model. This turbulence model was quite effective for the engineering problems concerning with the flow over an airfoil. However, there were several complications regarding this turbulence model. The mixing length and outer-inner region definitions are not well defined in junctions of two solid walls or not efficient for the free shear problems as in the wake of an airfoil. For this reason a turbulence model which solves transport equations was emerged.

Wilcox $k-\omega$ turbulence model was the first two equation turbulence model to be introduced to the code. After this turbulence model is implemented into the code, the others can be easily implemented since only model constants and correlations are to be changed. However, for Menter BSL method this situation is a little bit different

Following sections include the model equations, constants and correlations with the numerical framework, which includes all the steps of implementation from non-dimensionalization to limitations of turbulence model variables.

4.1 Model Equations and Correlations

The model equations and correlations, implemented to the base solver are introduced in this section. The general form of model equations will be in the form of,

$$\frac{\partial X}{\partial t} + U_j \cdot \frac{\partial X}{\partial x_j} = P(X) - D(X) + \frac{\partial}{\partial x_j} \cdot \left(\left(\nu + \sigma^* \cdot \nu_T \right) \cdot \frac{\partial X}{\partial x_j} \right) \quad (4.1)$$

To be consistent with general CFD applications, the conservative form of the variables are used. The conservative form brings many advantages for shock capturing [8] and definitions of momentum in the Navier-Stokes equations.

4.1.1 Wilcox k - ω turbulence model

After Kolmogorov's proposal of second equation for dissipation, turbulence model of k - ω has been modified many times by several researchers. From the results of DNS solutions, certain correlations and definitions are found. However the most robust turbulence model for eddy viscosity with two-equations appears to be the k - ω model. After the works of F.R. Menter, implementation of boundary conditions became much more simple and suitable also for the unstructured finite volume computations.

The following formulation with correlations and constants is named as Wilcox k - ω after D.C. Wilcox. [8]

Conservative form of the model equations can be given as,

$$\begin{aligned} \frac{\partial(\rho \cdot k)}{\partial t} + \frac{\partial(\rho \cdot u \cdot k)}{\partial x} + \frac{\partial(\rho \cdot v \cdot k)}{\partial y} &= P_k - D_k + \frac{\partial}{\partial x} \cdot \left(\left(\mu + \frac{\mu_T}{\sigma_k} \right) \cdot \frac{\partial k}{\partial x} \right) + \frac{\partial}{\partial y} \cdot \left(\left(\mu + \frac{\mu_T}{\sigma_k} \right) \cdot \frac{\partial k}{\partial y} \right) \\ \frac{\partial(\rho \cdot \omega)}{\partial t} + \frac{\partial(\rho \cdot u \cdot \omega)}{\partial x} + \frac{\partial(\rho \cdot v \cdot \omega)}{\partial y} &= P_\omega - D_\omega + \frac{\partial}{\partial x} \cdot \left(\left(\mu + \frac{\mu_T}{\sigma_\omega} \right) \cdot \frac{\partial \omega}{\partial x} \right) + \frac{\partial}{\partial y} \cdot \left(\left(\mu + \frac{\mu_T}{\sigma_\omega} \right) \cdot \frac{\partial \omega}{\partial y} \right) \end{aligned} \quad (4.2)$$

where turbulent viscosity is defined as,

$$\mu_T = \rho \cdot \frac{k}{\omega} \quad (4.3)$$

The production and dissipation terms are introduced in form of,

$$\begin{aligned} P_k &= \mu_T \cdot \Omega^2, \quad D_k = \beta' \cdot \rho \cdot k \cdot \omega, \\ P_\omega &= \zeta \cdot \rho \cdot \Omega^2, \quad D_\omega = \beta \cdot \rho \cdot \omega^2 \end{aligned} \quad (4.4)$$

Here, Ω is the magnitude of vorticity which is defined as $\Omega = \left(\frac{\partial u}{\partial y} - \frac{\partial v}{\partial x} \right)$. The

constants applied to this formulation could be listed as follows:

$$\begin{aligned} \beta &= 0.075, \quad \beta' = C_\mu = 0.09, \quad \sigma_k = 2.0, \quad \sigma_\omega = 2.0 \\ \zeta &= \frac{\beta}{C_\mu} - \frac{\kappa^2}{\sigma_\omega \cdot \sqrt{C_\mu}}, \quad \kappa = 0.41 \end{aligned} \quad (4.5)$$

4.1.2 Chien k - ε turbulence model

The present model appears as a low Reynolds number model, so that no effort is required for implementing the wall functions. Only simple boundary conditions for k and ε are specified. This model can be given as [10].

$$\begin{aligned} \frac{\partial(\rho \cdot k)}{\partial t} + \frac{\partial(\rho \cdot u \cdot k)}{\partial x} + \frac{\partial(\rho \cdot v \cdot k)}{\partial y} &= P_k - D_k + \frac{\partial}{\partial x} \cdot \left(\left(\mu + \frac{\mu_T}{\sigma_k} \right) \cdot \frac{\partial k}{\partial x} \right) + \frac{\partial}{\partial y} \cdot \left(\left(\mu + \frac{\mu_T}{\sigma_k} \right) \cdot \frac{\partial k}{\partial y} \right) \\ \frac{\partial(\rho \cdot \varepsilon)}{\partial t} + \frac{\partial(\rho \cdot u \cdot \varepsilon)}{\partial x} + \frac{\partial(\rho \cdot v \cdot \varepsilon)}{\partial y} &= P_\varepsilon - D_\varepsilon + \frac{\partial}{\partial x} \cdot \left(\left(\mu + \frac{\mu_T}{\sigma_\varepsilon} \right) \cdot \frac{\partial \varepsilon}{\partial x} \right) + \frac{\partial}{\partial y} \cdot \left(\left(\mu + \frac{\mu_T}{\sigma_\varepsilon} \right) \cdot \frac{\partial \varepsilon}{\partial y} \right) \end{aligned} \quad (4.6)$$

Turbulent viscosity is defined as,

$$\mu_T = C_\mu \cdot f_\mu \cdot \frac{k^2}{\varepsilon} \quad (4.7)$$

The production and dissipation terms are implemented by using,

$$\begin{aligned} P_k &= \mu_T \cdot \Omega^2, \quad D_k = \rho \cdot \varepsilon + D, \\ P_\varepsilon &= C_{\varepsilon 1} \cdot f_1 \cdot \Omega^2 \cdot \mu_T \cdot \frac{\varepsilon}{k}, \quad D_\varepsilon = C_{\varepsilon 2} \cdot f_2 \cdot \rho \cdot \frac{\varepsilon^2}{k} + E \end{aligned} \quad (4.8)$$

The D and E terms appearing in the destruction terms of k and ε are in modifications due to changes in boundary conditions of ε . Details of these

boundary conditions are given in Section 4.2.5. D and E for Chien k - ε turbulence model are as follows:

$$D = -2.0 \cdot \mu \cdot \frac{k}{y^2}$$

$$E = -2.0 \cdot \mu \cdot \frac{\varepsilon}{y^2} \cdot \exp\left(-\frac{y^+}{2.0}\right)$$
(4.9)

As it is seen in Equation (4.9) the E term includes the definition of y^+ . This definition is valid only for wall bounded flows since the wall shear stress is used to calculate this term. The model is not applied in the wake region of a C-Grid for an airfoil.

The model constants appear as,

$$f_1 = 1.0, f_2 = 1.0 - 0.22 \cdot \exp\left(-\left(\frac{\text{Re}_t}{6.0}\right)^2\right), f_\mu = 1.0 - \exp(-0.0115 \cdot y^+)$$
(4.10)

$$C_\mu = 0.09, C_{\varepsilon 1} = 1.35, C_{\varepsilon 2} = 1.80, \sigma_k = 1.0, \sigma_\varepsilon = 1.3, \text{Re}_t = \frac{\rho \cdot k^2}{\mu \varepsilon}$$

4.1.3 Abid k - ε turbulence model

Another k - ε turbulence model is implemented to eliminate y^+ term in the auxiliary terms. However, if the other k - ε turbulence models are investigated, it can be seen that, there is a wall distance dependence for every k - ε

turbulence model. Defining a wall distance for the wake side is much more applicable than correlating a y^+ value. The model is implemented in the following form [8].

$$\begin{aligned} \frac{\partial(\rho \cdot k)}{\partial t} + \frac{\partial(\rho \cdot u \cdot k)}{\partial x} + \frac{\partial(\rho \cdot v \cdot k)}{\partial y} &= P_k - D_k + \frac{\partial}{\partial x} \cdot \left(\left(\mu + \frac{\mu_T}{\sigma_k} \right) \cdot \frac{\partial k}{\partial x} \right) + \frac{\partial}{\partial y} \cdot \left(\left(\mu + \frac{\mu_T}{\sigma_k} \right) \cdot \frac{\partial k}{\partial y} \right) \\ \frac{\partial(\rho \cdot \varepsilon)}{\partial t} + \frac{\partial(\rho \cdot u \cdot \varepsilon)}{\partial x} + \frac{\partial(\rho \cdot v \cdot \varepsilon)}{\partial y} &= P_\varepsilon - D_\varepsilon + \frac{\partial}{\partial x} \cdot \left(\left(\mu + \frac{\mu_T}{\sigma_\varepsilon} \right) \cdot \frac{\partial \varepsilon}{\partial x} \right) + \frac{\partial}{\partial y} \cdot \left(\left(\mu + \frac{\mu_T}{\sigma_\varepsilon} \right) \cdot \frac{\partial \varepsilon}{\partial y} \right) \end{aligned} \quad (4.11)$$

Defining turbulent viscosity by,

$$\mu_T = C_\mu \cdot f_\mu \cdot \frac{k^2}{\varepsilon} \quad (4.12)$$

The production and destruction terms can be given as follows:

$$\begin{aligned} P_k &= \mu_T \cdot \Omega^2, \quad D_k = \rho \cdot \varepsilon + D, \\ P_\varepsilon &= C_{\varepsilon 1} \cdot f_1 \cdot \Omega^2 \cdot \mu_T \cdot \frac{\varepsilon}{k}, \quad D_\varepsilon = C_{\varepsilon 2} \cdot f_2 \cdot \rho \cdot \frac{\varepsilon^2}{k} + E \end{aligned} \quad (4.13)$$

Due to the boundary condition for ε , D and E terms appear to be zero.

$$\begin{aligned} D &= 0 \\ E &= 0 \end{aligned} \quad (4.14)$$

Constants and correlations for this model are as,

$$f_1 = 1.0, f_2 = \left[1.0 - \exp\left(-\frac{\text{Re}_k}{12}\right) \right],$$

$$f_\mu = \left[1 + 4 \cdot (\text{Re}_t^{-0.75}) \right] \cdot \tanh(0.008 \cdot \text{Re}_k), \text{Re}_k = \frac{\rho \cdot \sqrt{k} \cdot d}{\mu} \quad (4.15)$$

$$C_\mu = 0.09, C_{\varepsilon 1} = 1.45, C_{\varepsilon 2} = 1.83, \sigma_k = 1.0, \sigma_\varepsilon = 1.4, \text{Re}_t = \frac{\rho \cdot k^2}{\mu \varepsilon}$$

4.1.4 Menter Baseline (BSL) turbulence model

Menter's works [16] have shown that for turbulent flow calculations accomplished by standard $k-\omega$ models, the turbulent viscosity values differ in a great amount due to the changing values of free stream values of k and ω . For $k-\varepsilon$ models this dependence removes.

F.R. Menter modified the standard $k-\omega$ and $k-\varepsilon$ models and correlated them in a single formulation by a blending function where the $k-\omega$ model is activated near the solid wall surfaces while $k-\varepsilon$ is activated for the free shear and free stream regions.

The formulation appears with a blending function of F_1 as,

$$\frac{\partial(\rho \cdot k)}{\partial t} + \frac{\partial(\rho \cdot u \cdot k)}{\partial x} + \frac{\partial(\rho \cdot v \cdot k)}{\partial y} = P_k - D_k + \frac{\partial}{\partial x} \cdot \left(\left(\mu + \frac{\mu_T}{\sigma_k} \right) \cdot \frac{\partial k}{\partial x} \right) + \frac{\partial}{\partial y} \cdot \left(\left(\mu + \frac{\mu_T}{\sigma_k} \right) \cdot \frac{\partial k}{\partial y} \right) \quad (4.16)$$

$$\frac{\partial(\rho \cdot \omega)}{\partial t} + \frac{\partial(\rho \cdot u \cdot \omega)}{\partial x} + \frac{\partial(\rho \cdot v \cdot \omega)}{\partial y} = P_\omega - D_\omega + \frac{\partial}{\partial x} \cdot \left(\left(\mu + \frac{\mu_T}{\sigma_\omega} \right) \cdot \frac{\partial \omega}{\partial x} \right) + \frac{\partial}{\partial y} \cdot \left(\left(\mu + \frac{\mu_T}{\sigma_\omega} \right) \cdot \frac{\partial \omega}{\partial y} \right) + 2.0 \cdot \rho \cdot (1.0 - F_1) \cdot \sigma_{\omega_2} \cdot \frac{1.0}{\omega} \cdot \left(\frac{\partial k}{\partial x} \cdot \frac{\partial \omega}{\partial x} + \frac{\partial k}{\partial y} \cdot \frac{\partial \omega}{\partial y} \right)$$

The last term for the ω equation is the cross diffusion term which is frequently neglected by the modelers since its effect is not so significant. It is provided here in order to complete the transfer from $k-\omega$ to $k-\varepsilon$ model.

Definition of turbulent viscosity is the same as Wilcox $k-\omega$ model,

$$\mu_T = \rho \cdot \frac{k}{\omega} \quad (4.17)$$

and production and destruction terms appear as,

$$P_k = \mu_T \cdot \Omega^2, \quad D_k = \beta' \cdot \rho \cdot k \cdot \omega, \quad (4.18)$$

$$P_\omega = \zeta \cdot \rho \cdot \Omega^2, \quad D_\omega = \beta \cdot \rho \cdot \omega^2$$

Definitions of constants have to be modified since different turbulence models are applied for different regions in Menter BSL model. The manipulation of these constants are given in [11] with other zonal two equation turbulence models of Menter.

Here the blending function of F_1 plays an important role for the definition of model constants. For this constant, the following pattern is used,

$$\phi = F_1 \cdot \phi_1 + (1.0 - F_1) \cdot \phi_2 \quad (4.19)$$

While ϕ_1 and ϕ_2 in the above equation represents $k-\omega$ and $k-\varepsilon$ models, respectively. Then for standard $k-\omega$ model,

$$\begin{aligned} \beta_1 = 0.075, \beta^* = 0.09, \sigma_{k1} = 0.5, \sigma_{\omega1} = 0.5, \\ \kappa = 0.41, \zeta_1 = \frac{\beta_1}{\beta'} - \sigma_{\omega1} \cdot \frac{\kappa^2}{\sqrt{\beta'}} \end{aligned} \quad (4.20)$$

whereas for standard $k-\varepsilon$ model,

$$\begin{aligned} \beta_2 = 0.0828, \beta^* = 0.09, \sigma_{k2} = 1.0, \sigma_{\omega2} = 0.856, \\ \kappa = 0.41, \zeta_2 = \frac{\beta_2}{\beta'} - \sigma_{\omega2} \cdot \frac{\kappa^2}{\sqrt{\beta'}}; \end{aligned} \quad (4.21)$$

At this point, the reader should be careful about the definitions of σ 's. At the blending stage by using Equation (4.19), the values of σ given by Equations (4.20) and (4.21) should be used whereas, reciprocals of this blended values should be implemented to model equations (4.16).

In order to demonstrate this, assume that the value of F_1 is calculated as 0.6. Then for that value of F_1 , β is calculated as,

$$\beta = F_1 \cdot \beta_1 + (1.0 - F_1) \cdot \beta_2 = 0.6 \cdot 0.075 + (1.0 - 0.6) \cdot 0.0828 = 0.07812$$

The other constants could be calculated in a similar manner.

$$\begin{aligned} \beta &= F_1 \cdot \beta_1 + (1.0 - F_1) \cdot \beta_2 \\ \zeta &= F_1 \cdot \zeta_1 + (1.0 - F_1) \cdot \zeta_2 \\ \sigma_k &= \frac{1}{(F_1 \cdot \sigma_{k1} + (1.0 - F_1) \cdot \sigma_{k2})} \\ \sigma_\omega &= \frac{1}{(F_1 \cdot \sigma_{\omega1} + (1.0 - F_1) \cdot \sigma_{\omega2})} \end{aligned} \quad (4.22)$$

Calculation of blending function F_1 appears to be a little challenging; however modification from the Wilcox $k-\omega$ model to Menter BSL model simply includes implementing the blending function definition to model constants. Once F_1 is defined, enforcing this term to zero or one, transforms model directly to $k-\epsilon$ or $k-\omega$ models.

$$\begin{aligned} \arg 1 &= \min \left(\max \left(\frac{\sqrt{k}}{0.09 \cdot \omega \cdot y}; \frac{500 \cdot \mu}{\rho \cdot y^2 \cdot \omega} \right); \frac{4 \cdot \rho \cdot \sigma_{\omega 2} \cdot k}{CD_{k\omega} \cdot y^2} \right) \\ F_1 &= \tanh(\arg 1^4) \\ CD_{k\omega} &= \max \left(2 \cdot \rho \cdot \sigma_{\omega 2} \cdot \frac{1}{\omega} \cdot \left(\frac{\partial k}{\partial x} \cdot \frac{\partial \omega}{\partial x} + \frac{\partial k}{\partial y} \cdot \frac{\partial \omega}{\partial y} \right); 10^{-20} \right) \end{aligned} \quad (4.23)$$

4.2 Numerical Framework

Computation based operations for physical problems are quite challenging since the partial differential equations of type hyperbolic, elliptic and

parabolic types to be discretized spatially and temporarily. It is expected to get more accurate results as the computational grid describing physical domain gets finer but numerical problems occur with the difficulty of precision and memory levels. For this reason an attentive numerical framework must be accomplished.

Numerical framework includes; a non-dimensionalization study that turns the variables into variables with normalized values, a generalized coordinate transformation which makes it possible to evaluate derivatives with respect to the physical space coordinate axes, description of a numerical scheme to solve the governing partial differential equations iteratively, a discretization method to interpret the matrix formation for the solution bands, implementation of boundary and initial conditions and, at last, a limitation section that appears as the most tricky part of the model implementations in.

4.2.1 Non-Dimensionalization

In the field of computational engineering dealing with thermo fluid sciences, problems have to be classified properly in order to implement a solution technique. Classifications such as incompressible, compressible, turbulent, laminar etc. flow require a common property which shows its character properly. There are certain dimensionless numbers that represent the flow field and enable one to define the problem type some of which are *Reynolds Number (Re)* and *Mach Number (M)* that enable one to evaluate the flow characteristics. Due to these facts, in CFD applications the derivations of the equations start with a non-dimensionalization. The non-dimensionalization decrease the numerical errors since the variables are generally normalized by their corresponding free stream values. The non-dimensionalized

variables are given in [8]. These non-dimensionalized variables can be given as,

$$\begin{aligned}
 k &= \frac{\tilde{k}}{\tilde{a}_\infty^2}, & \omega &= \frac{\tilde{\omega} \cdot \tilde{\mu}_\infty}{\tilde{\rho}_\infty \cdot \tilde{a}_\infty^2}, & \varepsilon &= \frac{\tilde{\varepsilon} \cdot \tilde{\mu}_\infty}{\tilde{\rho}_\infty \cdot \tilde{a}_\infty^4}, & \rho &= \frac{\tilde{\rho}}{\tilde{\rho}_\infty}, & u &= \frac{\tilde{u}}{\tilde{a}_\infty} \\
 P &= \frac{\tilde{P}}{\tilde{\rho}_\infty \cdot \tilde{a}_\infty^2}, & x &= \frac{\tilde{x}}{\tilde{L}_R}, & \mu &= \frac{\tilde{\mu}}{\tilde{\mu}_\infty}, & t &= \frac{\tilde{t} \cdot \tilde{a}_\infty}{\tilde{L}_R}, & \Omega &= \frac{\tilde{\Omega} \cdot \tilde{L}_R}{\tilde{a}_\infty}
 \end{aligned} \tag{4.24}$$

k - ω turbulence models that are investigated in this study, namely, *Wilcox k - ω* and *Menter BSL Models*, possess same kind of k equation description. The results of the following non-dimensionalization work are given in [8]. The terms given in tilde (\sim), are the dimensional values while the others represent the non-dimensional forms given in Equation (4.24). The non-dimensionalization for the models and constants are represented in Appendix A.

The non-dimensionalized k equation for models of *Wilcox k - ω* and *Menter BSL Models*, appears as,

$$\begin{aligned}
 &\left(\frac{\partial(\rho \cdot k)}{\partial t} + \frac{\partial(\rho \cdot u \cdot k)}{\partial x} + \frac{\partial(\rho \cdot v \cdot k)}{\partial y} \right) = \\
 &\left[\mu_T \cdot \Omega^2 - \beta \cdot \rho \cdot k \cdot \omega \cdot \left(\frac{\text{Re}}{M_\infty} \right)^2 + \left(\frac{\partial}{\partial x} \cdot \left(\left(\mu + \frac{\mu_T}{\sigma_k} \right) \cdot \frac{\partial k}{\partial x} \right) + \frac{\partial}{\partial y} \cdot \left(\left(\mu + \frac{\mu_T}{\sigma_k} \right) \cdot \frac{\partial k}{\partial y} \right) \right) \right] \cdot \left[\frac{M_\infty}{\text{Re}} \right]
 \end{aligned} \tag{4.25}$$

k - ω turbulence models mentioned in the previous section differ only in ω equation. The difference occurs because of the *Cross Diffusion* term in the *Menter BSL Model*.

For *Wilcox k- ω turbulence model*, non-dimensionalized ω equation appears as,

$$\begin{aligned} & \left(\frac{\partial(\rho \cdot \omega)}{\partial t} + \frac{\partial(\rho \cdot u \cdot \omega)}{\partial x} + \frac{\partial(\rho \cdot v \cdot \omega)}{\partial y} \right) \\ & = \left[\zeta \cdot \rho \cdot \Omega^2 - \beta \cdot \rho \cdot \omega^2 \cdot \left(\frac{\text{Re}}{M_\infty} \right)^2 + \left(\frac{\partial}{\partial x} \cdot \left(\left(\mu + \frac{\mu_T}{\sigma_k} \right) \cdot \frac{\partial \omega}{\partial x} \right) + \frac{\partial}{\partial y} \cdot \left(\left(\mu + \frac{\mu_T}{\sigma_k} \right) \cdot \frac{\partial \omega}{\partial y} \right) \right) \right] \cdot \left[\frac{M_\infty}{\text{Re}} \right] \end{aligned} \quad (4.26)$$

For *Menter BSL turbulence model* with an addition of the cross diffusion term, this equation becomes,

$$\begin{aligned} & \left(\frac{\partial(\rho \cdot \omega)}{\partial t} + \frac{\partial(\rho \cdot u \cdot \omega)}{\partial x} + \frac{\partial(\rho \cdot v \cdot \omega)}{\partial y} \right) \\ & = \left[\zeta \cdot \rho \cdot \Omega^2 - \beta \cdot \rho \cdot \omega^2 \cdot \left(\frac{\text{Re}}{M_\infty} \right)^2 + \left(\frac{\partial}{\partial x} \cdot \left(\left(\mu + \frac{\mu_T}{\sigma_k} \right) \cdot \frac{\partial \omega}{\partial x} \right) + \frac{\partial}{\partial y} \cdot \left(\left(\mu + \frac{\mu_T}{\sigma_k} \right) \cdot \frac{\partial \omega}{\partial y} \right) \right) \right] \cdot \left[\frac{M_\infty}{\text{Re}} \right] \\ & \quad + 2 \cdot \rho \cdot (1 - F_1) \cdot \sigma_{\omega 2} \cdot \frac{1}{\omega} \cdot \left(\frac{\partial k}{\partial x} \cdot \frac{\partial \omega}{\partial x} + \frac{\partial k}{\partial y} \cdot \frac{\partial \omega}{\partial y} \right) \end{aligned} \quad (4.27)$$

Similar work could be applied to *k- ϵ* turbulence models. The results of non-dimensionalizations are given directly without presenting the intermediate steps in Appendix A.

For *Chien k- ϵ turbulence model* and *Abid k- ϵ turbulence model*, the *k* equation becomes;

$$\begin{aligned} & \left(\frac{\partial(\rho \cdot k)}{\partial t} + \frac{\partial(\rho \cdot u \cdot k)}{\partial x} + \frac{\partial(\rho \cdot v \cdot k)}{\partial y} \right) \\ & = \left[\mu_T \cdot \Omega^2 - \rho \cdot \epsilon \cdot \left(\frac{\text{Re}}{M_\infty} \right)^2 - D + \left(\frac{\partial}{\partial x} \cdot \left(\left(\mu + \frac{\mu_T}{\sigma_k} \right) \cdot \frac{\partial k}{\partial x} \right) + \frac{\partial}{\partial y} \cdot \left(\left(\mu + \frac{\mu_T}{\sigma_k} \right) \cdot \frac{\partial k}{\partial y} \right) \right) \right] \cdot \left[\frac{M_\infty}{\text{Re}} \right] \end{aligned} \quad (4.28)$$

The term D given by Equations (4.9) and (4.13) for *Chien k-ε turbulence model* and *Abid k-ε turbulence model*, becomes

$$D = 2.0 \cdot \mu \cdot \frac{k}{y^2}, \quad D = 0.0$$

The non-dimensional ε equation of appears as;

$$\left(\frac{\partial(\rho \cdot \varepsilon)}{\partial t} + \frac{\partial(\rho \cdot u \cdot \varepsilon)}{\partial x} + \frac{\partial(\rho \cdot v \cdot \varepsilon)}{\partial y} \right) = \left[C_{\varepsilon 1} \cdot f_1 \cdot \Omega^2 \cdot \mu_T \cdot \frac{\varepsilon}{k} - C_{\varepsilon 2} \cdot f_2 \cdot \rho \cdot \frac{\varepsilon^2}{k} \cdot \left(\frac{\text{Re}}{M_\infty} \right)^2 + E + \left(\frac{\partial}{\partial x} \cdot \left(\left(\mu + \frac{\mu_T}{\sigma_\varepsilon} \right) \cdot \frac{\partial \varepsilon}{\partial x} \right) + \frac{\partial}{\partial y} \cdot \left(\left(\mu + \frac{\mu_T}{\sigma_\varepsilon} \right) \cdot \frac{\partial \varepsilon}{\partial y} \right) \right) \right] \cdot \left[\frac{M_\infty}{\text{Re}} \right] \quad (4.29)$$

With 'E' terms of are given as follows

$$E = -2.0 \cdot \mu \cdot \frac{\varepsilon}{y^2} \cdot \exp\left(-\frac{y^+}{2.0}\right), \quad E = 0.0$$

for Chien *k-ε* and Abid *k-ε* models, respectively.

As described before, there are auxiliary parameters either used in the turbulence model equations or used as an output. Computation of these parameters is being done once in each iteration step. Non-dimensionalization regarding the variables used is presented in the Appendix A.

4.2.2 Transformation to Generalized Coordinate System

Finite difference applications require the representation of space derivatives by Taylor series expansion in terms of the values in the neighboring nodes. However these spatial derivatives are with respect to the independent variables of space coordinates x and y . The solution line directions are not always perpendicular or parallel to these coordinates. As a result, a coordinate transformation is required.

The following relations are used to transform the derivatives of time and space.

$$\begin{aligned}
 \tau &= t, \quad \xi = \xi(x, y, t), \quad \eta = \eta(x, y, t) \\
 \partial_t &= \partial_\tau + \xi_\tau \cdot \partial_\xi + \eta_\tau \cdot \partial_\eta \\
 \partial_x &= \xi_x \cdot \partial_\xi + \eta_x \cdot \partial_\eta \\
 \partial_y &= \xi_y \cdot \partial_\xi + \eta_y \cdot \partial_\eta
 \end{aligned} \tag{4.30}$$

The relation between metrics of the transformation appears to be [9]

$$\begin{aligned}
 \xi_x &= J \cdot y_\eta, \quad \xi_y = -J \cdot x_\eta, \quad \xi_t = -x_\tau \cdot \xi_x - y_\tau \cdot \xi_y \\
 \eta_x &= -J \cdot y_\xi, \quad \eta_y = J \cdot x_\xi, \quad \eta_t = -x_\tau \cdot \eta_x - y_\tau \cdot \eta_y \\
 J^{-1} &= \frac{1}{J} = x_\xi \cdot y_\eta - y_\xi \cdot x_\eta
 \end{aligned} \tag{4.31}$$

The transformation of equations into generalized coordinates is given in Appendix B. The results of transformation are presented here:

Main Solution Equation

$$\frac{\partial Q}{\partial \tau} + \frac{\partial F}{\partial \xi} + \frac{\partial G}{\partial \eta} = \frac{M_\infty}{\text{Re}} \left(\frac{\partial H}{\partial \xi} + \frac{\partial K}{\partial \eta} + M \right) \quad (4.32)$$

k- ω Turbulence Models

$$Q = \frac{1}{J} \cdot \begin{bmatrix} \rho \cdot k \\ \rho \cdot \omega \end{bmatrix} \quad F = \frac{1}{J} \cdot \begin{bmatrix} \rho \cdot U \cdot k \\ \rho \cdot U \cdot \omega \end{bmatrix} \quad G = \frac{1}{J} \cdot \begin{bmatrix} \rho \cdot V \cdot k \\ \rho \cdot V \cdot \omega \end{bmatrix}$$

$$H = \frac{1}{J} \cdot \begin{bmatrix} (\xi_x^2 + \xi_y^2) \cdot \left(\mu + \frac{\mu_T}{\sigma_k} \right) \cdot \frac{\partial k}{\partial \xi} \\ (\xi_x^2 + \xi_y^2) \cdot \left(\mu + \frac{\mu_T}{\sigma_\omega} \right) \cdot \frac{\partial \omega}{\partial \xi} \end{bmatrix}$$

$$K = \frac{1}{J} \cdot \begin{bmatrix} (\eta_x^2 + \eta_y^2) \cdot \left(\mu + \frac{\mu_T}{\sigma_k} \right) \cdot \frac{\partial k}{\partial \eta} \\ (\eta_x^2 + \eta_y^2) \cdot \left(\mu + \frac{\mu_T}{\sigma_\omega} \right) \cdot \frac{\partial \omega}{\partial \eta} \end{bmatrix} \quad (4.33)$$

$$M = \frac{1}{J} \cdot \begin{bmatrix} \mu_T \cdot \Omega^2 - \beta' \cdot \rho \cdot k \cdot \omega \cdot \left(\frac{\text{Re}}{M_\infty} \right)^2 \\ \zeta \cdot \rho \cdot \Omega^2 - \beta \cdot \rho \cdot \omega^2 \cdot \left(\frac{\text{Re}}{M_\infty} \right)^2 \end{bmatrix} \text{ for Wilcox } k\text{-}\omega \text{ formulation}$$

$$M = \frac{1}{J} \cdot \begin{bmatrix} \mu_T \cdot \Omega^2 - \beta' \cdot \rho \cdot k \cdot \omega \cdot \left(\frac{\text{Re}}{M_\infty} \right)^2 \\ \zeta \cdot \rho \cdot \Omega^2 - \beta \cdot \rho \cdot \omega^2 \cdot \left(\frac{\text{Re}}{M_\infty} \right)^2 + 2 \cdot \rho \cdot (1 - F_1) \cdot \sigma_{\omega 2} \cdot \frac{1}{\omega} \cdot \left(\frac{\partial k}{\partial x} \cdot \frac{\partial \omega}{\partial x} + \frac{\partial k}{\partial y} \cdot \frac{\partial \omega}{\partial y} \right) \end{bmatrix}$$

for Menter BSL formulation

k-ε Turbulence Models

$$\begin{aligned}
 Q &= \frac{1}{J} \cdot \begin{bmatrix} \rho \cdot k \\ \rho \cdot \varepsilon \end{bmatrix} & F &= \frac{1}{J} \cdot \begin{bmatrix} \rho \cdot U \cdot k \\ \rho \cdot U \cdot \varepsilon \end{bmatrix} & G &= \frac{1}{J} \cdot \begin{bmatrix} \rho \cdot V \cdot k \\ \rho \cdot V \cdot \varepsilon \end{bmatrix} \\
 H &= \frac{1}{J} \cdot \begin{bmatrix} (\xi_x^2 + \xi_y^2) \cdot \left(\mu + \frac{\mu_T}{\sigma_k} \right) \cdot \frac{\partial k}{\partial \xi} \\ (\xi_x^2 + \xi_y^2) \cdot \left(\mu + \frac{\mu_T}{\sigma_\varepsilon} \right) \cdot \frac{\partial \varepsilon}{\partial \xi} \end{bmatrix} \\
 K &= \frac{1}{J} \cdot \begin{bmatrix} (\eta_x^2 + \eta_y^2) \cdot \left(\mu + \frac{\mu_T}{\sigma_k} \right) \cdot \frac{\partial k}{\partial \eta} \\ (\eta_x^2 + \eta_y^2) \cdot \left(\mu + \frac{\mu_T}{\sigma_\varepsilon} \right) \cdot \frac{\partial \varepsilon}{\partial \eta} \end{bmatrix} \\
 M &= \frac{1}{J} \cdot \begin{bmatrix} \mu_T \cdot \Omega^2 - \rho \cdot \varepsilon \cdot \left(\frac{\text{Re}}{M_\infty} \right)^2 - 2.0 \cdot \mu \cdot \frac{k}{y^2} \\ C_{\varepsilon 1} \cdot f_1 \cdot \Omega^2 \cdot \mu_T \cdot \frac{\varepsilon}{k} - C_{\varepsilon 2} \cdot f_2 \cdot \rho \cdot \frac{\varepsilon^2}{k} \cdot \left(\frac{\text{Re}}{M_\infty} \right)^2 \\ -2.0 \cdot \mu \cdot \frac{\varepsilon}{y^2} \cdot \exp\left(-\frac{y^+}{2.0}\right) \end{bmatrix} \quad (4.34)
 \end{aligned}$$

for Chien *k-ε* formulation

$$M = \frac{1}{J} \cdot \begin{bmatrix} \mu_T \cdot \Omega^2 - \rho \cdot \varepsilon \cdot \left(\frac{\text{Re}}{M_\infty} \right)^2 \\ C_{\varepsilon 1} \cdot f_1 \cdot \Omega^2 \cdot \mu_T \cdot \frac{\varepsilon}{k} - C_{\varepsilon 2} \cdot f_2 \cdot \rho \cdot \frac{\varepsilon^2}{k} \cdot \left(\frac{\text{Re}}{M_\infty} \right)^2 \end{bmatrix}$$

for Abid *k-ε* formulation

4.2.3 Numerical Scheme

The numerical computations of compressible Navier-Stokes equations are improved with the introduction of many finite difference schemes among

which the most successful ones appeared to be ADI and Approximate Factorization. The equations of turbulence models are similar to the Navier-Stokes equations in terms of the nature of variables such as convection, diffusion, production and destruction with their representation of derivatives. Since these equations have similar representations, the numerical scheme and solution procedures that are used for Navier-Stokes calculations could also be used for turbulence model equations as suggested by *Beam and Warming* [12].

In the two-dimensional turbulence models, the main solution equations could be represented as follows, including second derivatives of diffusion terms K and H ;

$$\frac{\partial Q}{\partial \tau} + \frac{\partial F(Q)}{\partial \xi} + \frac{\partial G(Q)}{\partial \eta} = \frac{M_\infty}{\text{Re}} \left(\frac{\partial H(Q, Q_\xi)}{\partial \xi} + \frac{\partial K(Q, Q_\eta)}{\partial \eta} + M(Q) \right) \quad (4.35)$$

The time differencing formula appears as;

$$\Delta Q^n = \frac{\theta \cdot \Delta t}{1 + \phi} \cdot \frac{\partial}{\partial t} \Delta Q^n + \frac{\Delta t}{1 + \phi} \cdot \frac{\partial}{\partial t} Q^n + \frac{\phi}{1 + \phi} \cdot \Delta Q^{n-1} \quad (4.36)$$

with the definitions of time discretization given by

$$Q^n = Q(n \cdot \Delta t), \quad \Delta Q^n = Q^{n+1} - Q^n \quad (4.37)$$

The constants ϕ in the time differencing formula (4.36), appears as control parameters of the numerical scheme. The degree of error and the implicit / explicit behavior of the scheme is controlled by these constants.

Table 4.1 Partial List of Schemes [3]

θ	ϕ	Scheme	Degree of Error
0	0	Euler, explicit	$O(\Delta t^2)$
0	-0.5	Leapfrog, implicit	$O(\Delta t^3)$
0.5	0	Trapezoidal, implicit	$O(\Delta t^3)$
1	0	Euler, implicit	$O(\Delta t^2)$
1	0.5	3 point backward, implicit	$O(\Delta t^3)$

Before expanding the main solution equation (4.35) the following representations for non-dimensional variables can be introduced to simplify the notation.

$$H^* = H \cdot \frac{M_\infty}{Re}, \quad K^* = K \cdot \frac{M_\infty}{Re}, \quad M^* = M \cdot \frac{M_\infty}{Re}$$

The scheme given in Equation (4.36) will be studied in parts as,

$$\Delta Q^n = \frac{\theta \cdot \Delta \tau}{1 + \phi} \cdot \underbrace{\frac{\partial}{\partial \tau} \Delta Q^n}_I + \frac{\Delta \tau}{1 + \phi} \cdot \underbrace{\frac{\partial}{\partial \tau} Q^n}_II + \frac{\phi}{1 + \phi} \cdot \Delta Q^{n-1}$$

Term 1 in the above equation can be expanded as

$$\frac{\partial}{\partial \tau} \Delta Q^n = \frac{\partial}{\partial \xi} \left(-\Delta F^n + \Delta H^{*n} \right) + \frac{\partial}{\partial \eta} \left(-\Delta G^n + \Delta K^{*n} \right) + \Delta M^{*n} \quad (4.38)$$

while term 2 can be given as

$$\frac{\partial}{\partial \tau} Q^n = \frac{\partial}{\partial \xi} \left(-F^n + H^{*n} \right) + \frac{\partial}{\partial \eta} \left(-G^n + K^{*n} \right) + M^{*n} \quad (4.39)$$

If Equations (4.38) and (4.39) are added to Equation (4.36), the following form can be obtained.

$$\begin{aligned} \Delta Q^n &= \frac{\theta \cdot \Delta \tau}{1 + \phi} \cdot \left(\frac{\partial}{\partial \xi} \left(-\Delta F^n + \Delta H^{*n} \right) + \frac{\partial}{\partial \eta} \left(-\Delta G^n + \Delta K^{*n} \right) + \Delta M^{*n} \right) \\ &+ \frac{\Delta \tau}{1 + \phi} \cdot \left(\frac{\partial}{\partial \xi} \left(-F^n + H^{*n} \right) + \frac{\partial}{\partial \eta} \left(-G^n + K^{*n} \right) + M^{*n} \right) + \frac{\phi}{1 + \phi} \cdot \Delta Q^{n-1} \end{aligned} \quad (4.40)$$

Variables described in the n^{th} time level are known and the values at the time level $n+1$ are desired. As described in Equation (4.40) ΔQ^n is to be found in order to find $(n+1)^{th}$ value of Q, which is given by Equation (4.37).

The variables that are represented with a change (Δ -delta) operator in front of them are dependent on the changes in Q. These change variables are formed as;

$$F^{n+1} = F^n + \left(\frac{\partial F}{\partial Q} \right)^n \cdot (Q^{n+1} - Q^n)$$

$$\Delta F^n = \left(\frac{\partial F}{\partial Q} \right)^n \cdot \Delta Q^n$$

The term representing the derivative of F with respect to Q is known as the Jacobian term. All of these change terms could be found by using this representation as:

$$\Delta F^n = \left(\frac{\partial F}{\partial Q} \right)^n \cdot \Delta Q^n = A^n \cdot \Delta Q^n$$

$$\Delta G^n = \left(\frac{\partial G}{\partial Q} \right)^n \cdot \Delta Q^n = B^n \cdot \Delta Q^n$$

$$\Delta H^{*n} = \left(\frac{\partial H^*}{\partial Q} \right)^n \cdot \Delta Q^n + \left(\frac{\partial H^*}{\partial Q_\xi} \right)^n \cdot \Delta Q_\xi^n = U^n \cdot \Delta Q^n + R^n \cdot \Delta Q_\xi^n = (U - R_\xi)^n \cdot \Delta Q^n + \frac{\partial}{\partial \xi} (R \cdot \Delta Q)^n$$

$$\Delta K^{*n} = \left(\frac{\partial K^*}{\partial Q} \right)^n \cdot \Delta Q^n + \left(\frac{\partial K^*}{\partial Q_\eta} \right)^n \cdot \Delta Q_\eta^n = V^n \cdot \Delta Q^n + S^n \cdot \Delta Q_\eta^n = (V - S_\eta)^n \cdot \Delta Q^n + \frac{\partial}{\partial \eta} (S \cdot \Delta Q)^n$$

$$\Delta M^{*n} = \left(\frac{\partial M^*}{\partial Q} \right)^n \cdot \Delta Q^n = C^n \cdot \Delta Q^n$$

After derivations of these Jacobian terms, Equation (4.40) becomes;

$$\Delta Q^n = \frac{\theta \cdot \Delta \tau}{1 + \phi} \cdot \left[\begin{aligned} & \left[\left(\frac{\partial}{\partial \xi} (-A + U - R_\xi)^n + \frac{\partial^2}{\partial \xi^2} R^n \right) \cdot \Delta Q^n \right. \\ & \left. + \left(\frac{\partial}{\partial \eta} (-B + V - S_\eta)^n + \frac{\partial^2}{\partial \eta^2} S^n \right) \cdot \Delta Q^n + C^n \cdot \Delta Q^n \right] \end{aligned} \right] \quad (4.41)$$

$$+ \frac{\Delta \tau}{1 + \phi} \cdot \left(\frac{\partial}{\partial \xi} (-F^n + H^{*n}) + \frac{\partial}{\partial \eta} (-G^n + K^{*n}) + M^{*n} \right) + \frac{\phi}{1 + \phi} \cdot \Delta Q^{n-1}$$

If Jacobian terms are separated and collected in left hand side of the equation the following equation is obtained. The “•” operator in this expression has a function of distribution ΔQ^n term into the spatial derivatives.

$$\left\{ 1 + \frac{\theta \cdot \Delta \tau}{1 + \phi} \cdot \left[\left(\frac{\partial}{\partial \xi} (A - U + R_\xi)^n - \frac{\partial^2}{\partial \xi^2} R^n \right) + \left(\frac{\partial}{\partial \eta} (B - V + S_\eta)^n - \frac{\partial^2}{\partial \eta^2} S^n \right) - C^n \right] \right\} \bullet \Delta Q^n = \frac{\Delta \tau}{1 + \phi} \cdot \left(\frac{\partial}{\partial \xi} (-F^n + H^{*n}) + \frac{\partial}{\partial \eta} (-G^n + K^{*n}) + M^{*n} \right) + \frac{\phi}{1 + \phi} \cdot \Delta Q^{n-1}$$

The above equation could be approximately factored by neglecting the cross derivatives as

$$\left[1 + \frac{\theta \cdot \Delta \tau}{1 + \phi} \cdot \left(\frac{\partial}{\partial \eta} (B - V + S_\eta)^n - \frac{\partial^2}{\partial \eta^2} S^n - C^n \right) \right] \cdot \left[1 + \frac{\theta \cdot \Delta \tau}{1 + \phi} \cdot \left(\frac{\partial}{\partial \xi} (A - U + R_\xi)^n - \frac{\partial^2}{\partial \xi^2} R^n \right) \right] \bullet \Delta Q^n = \frac{\Delta \tau}{1 + \phi} \cdot \left(\frac{\partial}{\partial \xi} (-F^n + H^{*n}) + \frac{\partial}{\partial \eta} (-G^n + K^{*n}) + M^{*n} \right) + \frac{\phi}{1 + \phi} \cdot \Delta Q^{n-1} \quad (4.42)$$

By this factorization, the equation could be solved in two steps. The main difference between approximate factorization and ADI could be explained such that the former one solves an equation in two steps where the latter solves an equation twice in alternating directions.

$$\begin{aligned}
& \left[1 + \frac{\theta \cdot \Delta \tau}{1 + \phi} \cdot \left(\frac{\partial}{\partial \eta} (B - V + S_\eta)^n - \frac{\partial^2}{\partial \eta^2} S^n - C^n \right) \right] \bullet \Delta Q^{n \otimes} = RHS^n \\
& \left[1 + \frac{\theta \cdot \Delta \tau}{1 + \phi} \cdot \left(\frac{\partial}{\partial \xi} (A - U + R_\xi)^n - \frac{\partial^2}{\partial \xi^2} R^n \right) \right] \bullet \Delta Q^n = \Delta Q^{n \otimes} \\
& RHS^n = \frac{\Delta \tau}{1 + \phi} \cdot \left(\frac{\partial}{\partial \xi} (-F^n + H^{*n}) + \frac{\partial}{\partial \eta} (-G^n + K^{*n}) + M^{*n} \right) + \frac{\phi}{1 + \phi} \cdot \Delta Q^{n-1}
\end{aligned} \tag{4.43}$$

Jacobian calculations for $k-\omega$ models of Wilcox and Menter and $k-\varepsilon$ models are given in Appendix C. The resultant form of iterative schemes with corresponding matrices is given in the next three pages as a compact set of equations.

$$\left[1 + \frac{\theta \cdot \Delta \tau}{1 + \phi} \cdot \left(\frac{\partial}{\partial \eta} (B - V + S_\eta)^n - \frac{\partial^2}{\partial \eta^2} S^n - C^n \right) \right] \cdot \Delta Q^{n^\otimes} = RHS^n$$

$$\left[1 + \frac{\theta \cdot \Delta \tau}{1 + \phi} \cdot \left(\frac{\partial}{\partial \xi} (A - U + R_\xi)^n - \frac{\partial^2}{\partial \xi^2} R^n \right) \right] \cdot \Delta Q^n = \Delta Q^{n^\otimes}$$

$$RHS^n = \frac{\Delta \tau}{1 + \phi} \cdot \left(\frac{\partial}{\partial \xi} (-F^n + H^{*n}) + \frac{\partial}{\partial \eta} (-G^n + K^{*n}) + M^{*n} \right) + \frac{\phi}{1 + \phi} \cdot \Delta Q^{n-1}$$

k- ω Models

$$Q = \frac{1}{J} \cdot \begin{bmatrix} \rho \cdot k \\ \rho \cdot \omega \end{bmatrix} \quad F = \frac{1}{J} \cdot \begin{bmatrix} \rho \cdot U \cdot k \\ \rho \cdot U \cdot \omega \end{bmatrix} \quad G = \frac{1}{J} \cdot \begin{bmatrix} \rho \cdot V \cdot k \\ \rho \cdot V \cdot \omega \end{bmatrix}$$

$$H^* = \frac{M_\infty}{\text{Re}} \cdot \frac{1}{J} \cdot \begin{bmatrix} (\xi_x^2 + \xi_y^2) \cdot \left(\mu + \frac{\mu_T}{\sigma_k} \right) \cdot \frac{\partial k}{\partial \xi} \\ (\xi_x^2 + \xi_y^2) \cdot \left(\mu + \frac{\mu_T}{\sigma_\omega} \right) \cdot \frac{\partial \omega}{\partial \xi} \end{bmatrix} \quad K^* = \frac{M_\infty}{\text{Re}} \cdot \frac{1}{J} \cdot \begin{bmatrix} (\eta_x^2 + \eta_y^2) \cdot \left(\mu + \frac{\mu_T}{\sigma_k} \right) \cdot \frac{\partial k}{\partial \eta} \\ (\eta_x^2 + \eta_y^2) \cdot \left(\mu + \frac{\mu_T}{\sigma_\omega} \right) \cdot \frac{\partial \omega}{\partial \eta} \end{bmatrix}$$

$$M^* = \frac{M_\infty}{\text{Re}} \cdot \frac{1}{J} \cdot \begin{bmatrix} \mu_T \cdot \Omega^2 - \beta' \cdot \rho \cdot k \cdot \omega \cdot \left(\frac{\text{Re}}{M_\infty} \right)^2 \\ \zeta \cdot \rho \cdot \Omega^2 - \beta \cdot \rho \cdot \omega^2 \cdot \left(\frac{\text{Re}}{M_\infty} \right)^2 \end{bmatrix}$$

Equation set (4.44)

(Wilcox k- ω)

$$M^* = \frac{M_\infty}{\text{Re} J} \cdot \begin{bmatrix} \mu_T \cdot \Omega^2 - \beta \cdot \rho \cdot k \cdot \omega \cdot \left(\frac{\text{Re}}{M_\infty} \right)^2 \\ \zeta \cdot \rho \cdot \Omega^2 - \beta \cdot \rho \cdot \omega^2 \cdot \left(\frac{\text{Re}}{M_\infty} \right)^2 + 2 \cdot \rho \cdot (1 - F_1) \cdot \sigma_\omega \cdot \frac{1}{\omega} \cdot \left(\frac{\partial k}{\partial x} \cdot \frac{\partial \omega}{\partial x} + \frac{\partial k}{\partial y} \cdot \frac{\partial \omega}{\partial y} \right) \end{bmatrix} \quad (\text{Menter BSL})$$

$$A = \begin{bmatrix} U & 0 \\ 0 & U \end{bmatrix} \quad B = \begin{bmatrix} V & 0 \\ 0 & V \end{bmatrix}$$

$$U = \frac{M_\infty}{\text{Re}} \cdot \begin{bmatrix} \frac{\Gamma_k}{J} \cdot \frac{\partial \left(\frac{J}{\rho} \right)}{\partial \xi} & 0 \\ 0 & \frac{\Gamma_\omega}{J} \cdot \frac{\partial \left(\frac{J}{\rho} \right)}{\partial \xi} \end{bmatrix} \quad R = \frac{M_\infty}{\text{Re}} \cdot \begin{bmatrix} \Gamma_k \cdot \frac{1}{\rho} & 0 \\ 0 & \Gamma_\omega \cdot \frac{1}{\rho} \end{bmatrix} \quad R_\xi = \frac{\partial R}{\partial \xi}$$

$$V^n = \frac{M_\infty}{\text{Re}} \cdot \begin{bmatrix} \frac{\Gamma'_k}{J} \cdot \frac{\partial(J/\rho)}{\partial\eta} & 0 \\ 0 & \frac{\Gamma'_\omega}{J} \cdot \frac{\partial(J/\rho)}{\partial\eta} \end{bmatrix} \quad S = \frac{M_\infty}{\text{Re}} \cdot \begin{bmatrix} \Gamma'_k \cdot 1/\rho & 0 \\ 0 & \Gamma'_\omega \cdot 1/\rho \end{bmatrix} \quad S_\eta = \frac{\partial S}{\partial\eta}$$

$$C^n = \frac{M_\infty}{\text{Re}} \cdot \begin{bmatrix} \frac{\Omega^2}{\omega} - \beta' \cdot \omega \cdot \left(\frac{\text{Re}}{M_\infty}\right)^2 & -\frac{k}{\omega^2} \cdot \Omega^2 - \beta' \cdot k \cdot \left(\frac{\text{Re}}{M_\infty}\right)^2 \\ 0 & -2.0 \cdot \beta \cdot \omega \cdot \left(\frac{\text{Re}}{M_\infty}\right)^2 \end{bmatrix} \quad (\text{Wilcox } k-\omega)$$

$$C' = \frac{M_\infty}{\text{Re}} \cdot \begin{bmatrix} -\beta \cdot \omega \cdot \left(\frac{\text{Re}}{M_\infty}\right)^2 & 0 \\ 0 & -2 \cdot \rho \cdot (1-F_1) \cdot \sigma_{\omega 2} \cdot \frac{1}{\omega^2} \cdot \left(\frac{\partial k}{\partial x} \cdot \frac{\partial \omega}{\partial x} + \frac{\partial k}{\partial y} \cdot \frac{\partial \omega}{\partial y}\right) - 2.0 \cdot \beta \cdot \omega \cdot \left(\frac{\text{Re}}{M_\infty}\right)^2 \end{bmatrix} \quad (\text{Menter BSL})$$

k-ε Models

$$Q = \frac{1}{J} \cdot \begin{bmatrix} \rho \cdot k \\ \rho \cdot \varepsilon \end{bmatrix} \quad F = \frac{1}{J} \cdot \begin{bmatrix} \rho \cdot U \cdot k \\ \rho \cdot U \cdot \varepsilon \end{bmatrix} \quad G = \frac{1}{J} \cdot \begin{bmatrix} \rho \cdot V \cdot k \\ \rho \cdot V \cdot \varepsilon \end{bmatrix}$$

$$H^* = \frac{M_\infty}{\text{Re}} \cdot \frac{1}{J} \cdot \begin{bmatrix} (\xi_x^2 + \xi_y^2) \cdot \left(\mu + \frac{\mu_T}{\sigma_k}\right) \cdot \frac{\partial k}{\partial \xi} \\ (\xi_x^2 + \xi_y^2) \cdot \left(\mu + \frac{\mu_T}{\sigma_\varepsilon}\right) \cdot \frac{\partial \varepsilon}{\partial \xi} \end{bmatrix} \quad K^* = \frac{M_\infty}{\text{Re}} \cdot \frac{1}{J} \cdot \begin{bmatrix} (\eta_x^2 + \eta_y^2) \cdot \left(\mu + \frac{\mu_T}{\sigma_k}\right) \cdot \frac{\partial k}{\partial \eta} \\ (\eta_x^2 + \eta_y^2) \cdot \left(\mu + \frac{\mu_T}{\sigma_\varepsilon}\right) \cdot \frac{\partial \varepsilon}{\partial \eta} \end{bmatrix}$$

$$M^* = \frac{M_\infty}{\text{Re}} \cdot \frac{1}{J} \cdot \begin{bmatrix} \mu_T \cdot \Omega^2 - \rho \cdot \varepsilon \cdot \left(\frac{\text{Re}}{M_\infty}\right)^2 - 2.0 \cdot \mu \cdot \frac{k}{y^2} \\ C_{\varepsilon 1} \cdot f_1 \cdot \Omega^2 \cdot \mu_T \cdot \frac{\varepsilon}{k} - C_{\varepsilon 2} \cdot f_2 \cdot \rho \cdot \frac{\varepsilon^2}{k} \cdot \left(\frac{\text{Re}}{M_\infty}\right)^2 - 2.0 \cdot \mu \cdot \frac{\varepsilon}{y^2} \cdot \exp\left(-\frac{y^+}{2.0}\right) \end{bmatrix} \quad (\text{Chien } k-\varepsilon)$$

$$M^* = \frac{M_\infty}{\text{Re}} \cdot \frac{1}{J} \cdot \begin{bmatrix} \mu_T \cdot \Omega^2 - \rho \cdot \varepsilon \cdot \left(\frac{\text{Re}}{M_\infty}\right)^2 \\ C_{\varepsilon 1} \cdot f_1 \cdot \Omega^2 \cdot \mu_T \cdot \frac{\varepsilon}{k} - C_{\varepsilon 2} \cdot f_2 \cdot \rho \cdot \frac{\varepsilon^2}{k} \cdot \left(\frac{\text{Re}}{M_\infty}\right)^2 \end{bmatrix} \quad (\text{Abid } k-\varepsilon)$$

Equation set (4.45)

$$A = \begin{bmatrix} U & 0 \\ 0 & U \end{bmatrix} \quad B = \begin{bmatrix} V & 0 \\ 0 & V \end{bmatrix}$$

$$U = \frac{M_\infty}{\text{Re}} \cdot \begin{bmatrix} \frac{\Gamma_k}{J} \cdot \frac{\partial(J/\rho)}{\partial\xi} & 0 \\ 0 & \frac{\Gamma_\varepsilon}{J} \cdot \frac{\partial(J/\rho)}{\partial\xi} \end{bmatrix} \quad R = \frac{M_\infty}{\text{Re}} \cdot \begin{bmatrix} \Gamma_k \cdot 1/\rho & 0 \\ 0 & \Gamma_\varepsilon \cdot 1/\rho \end{bmatrix} \quad R_\xi = \frac{\partial R}{\partial\xi}$$

$$V^n = \frac{M_\infty}{\text{Re}} \cdot \begin{bmatrix} \frac{\Gamma'_k}{J} \cdot \frac{\partial(J/\rho)}{\partial\eta} & 0 \\ 0 & \frac{\Gamma'_\varepsilon}{J} \cdot \frac{\partial(J/\rho)}{\partial\eta} \end{bmatrix} \quad S = \frac{M_\infty}{\text{Re}} \cdot \begin{bmatrix} \Gamma'_k \cdot 1/\rho & 0 \\ 0 & \Gamma'_\varepsilon \cdot 1/\rho \end{bmatrix} \quad S_\eta = \frac{\partial S}{\partial\eta}$$

$$C^n = \frac{M_\infty}{\text{Re}} \cdot \begin{bmatrix} C_\mu \cdot f_\mu \cdot 20 \cdot \frac{k}{\varepsilon} \cdot \Omega^2 - 20 \cdot \frac{\mu}{\rho \cdot y^2} & -C_\mu \cdot f_\mu \cdot \frac{k^2}{\varepsilon^2} \cdot \Omega^2 - \left(\frac{\text{Re}}{M_\infty}\right)^2 \\ C_{\varepsilon 1} \cdot f_1 \cdot \Omega^2 \cdot C_\mu \cdot f_\mu + C_{\varepsilon 2} \cdot f_2 \cdot \frac{\varepsilon^2}{k^2} \cdot \left(\frac{\text{Re}}{M_\infty}\right)^2 & -20 \cdot C_{\varepsilon 2} \cdot f_2 \cdot \frac{\varepsilon}{k} \cdot \left(\frac{\text{Re}}{M_\infty}\right)^2 - 20 \cdot \frac{\mu}{\rho \cdot y^2} \cdot \exp\left(-\frac{y^+}{20}\right) \end{bmatrix} \quad (\text{Chien } k-\varepsilon)$$

$$C^n = \frac{M_\infty}{\text{Re}} \cdot \begin{bmatrix} C_\mu \cdot f_\mu \cdot 20 \cdot \frac{k}{\varepsilon} \cdot \Omega^2 - 20 \cdot \frac{\mu}{\rho \cdot y^2} & -C_\mu \cdot f_\mu \cdot \frac{k^2}{\varepsilon^2} \cdot \Omega^2 - \left(\frac{\text{Re}}{M_\infty}\right)^2 \\ C_{\varepsilon 1} \cdot f_1 \cdot \Omega^2 \cdot C_\mu \cdot f_\mu + C_{\varepsilon 2} \cdot f_2 \cdot \frac{\varepsilon^2}{k^2} \cdot \left(\frac{\text{Re}}{M_\infty}\right)^2 & -20 \cdot C_{\varepsilon 2} \cdot f_2 \cdot \frac{\varepsilon}{k} \cdot \left(\frac{\text{Re}}{M_\infty}\right)^2 \end{bmatrix} \quad (\text{Abid } k-\varepsilon)$$

4.2.4 Spatial Discretization

The effort presented up to this point is the steps of numerical framework to have the solution equations ready for the spatial discretization. As described before it is necessary to discretize the derivatives of governing equations need to be discretized with respect to solution points. The discretization of equations with respect to the solution nodes of the computational domain is presented in this section. At first, it would be better to give the domain representation.

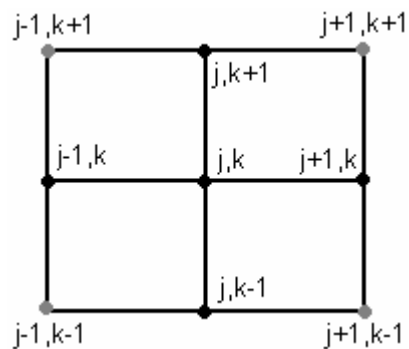


Figure 4.1 Domain representation for a solution node

Primary solution point is the node having index of (j,k) . Neighboring nodes could be listed as, $(j+1,k)$, $(j-1,k)$, $(j,k+1)$ and $(j,k-1)$ which are used to evaluate derivative terms. The other nodes given in Figure 4.2 but not listed here are the secondary neighboring nodes that are used in computation of second derivatives which are generally appearing in the boundary conditions or cross derivative terms of approximate factorization.

There are certain aspects of discretization that must be carefully investigated such as the discretization of convection terms. The convection terms in the model equations should be evaluated using the “upwind” schemes. Another important concept is the discretization of the diffusion terms. These terms occupy second derivatives of variables and inclusion of secondary neighboring grid points is necessary for an ordinary discretization. Certain solution methods could be applied to avoid these problems.

Discretization of the convection terms is carried out by adding a second order dissipation into central differencing. This is equivalent to a first order upwind scheme is shown in [14].

Plus-minus flux splitting method of Steger-Warming is used for the representation of the dissipative property of upwind schemes.

$$A = T_{\xi} \Lambda_A T_{\xi}^{-1} = T_{\xi} (\Lambda_A^+ + \Lambda_A^-) T_{\xi}^{-1} = A^+ + A^- \quad (4.46)$$

$$\Lambda_A^{\pm} = \frac{\Lambda_A \pm |\Lambda_A|}{2}$$

The vectors of convective terms could be represented as:

$$F = A \cdot \Delta Q = (A^+ + A^-) \cdot \Delta Q = F^+ + F^- \quad (4.47)$$

$$G = B \cdot \Delta Q = (B^+ + B^-) \cdot \Delta Q = G^+ + G^-$$

Defining the backward and forward difference operators as such,

$$\nabla_{\xi}^b u_{j,k} = \frac{u_{j,k} - u_{j-1,k}}{\Delta \xi} \quad (4.48)$$

$$\Delta_{\xi}^f u_{j,k} = \frac{u_{j+1,k} - u_{j,k}}{\Delta \xi}$$

Steger-Warming plus-minus flux splitting vector represented as,

$$F^{\pm} = A^{\pm} \cdot \Delta Q = \frac{A}{2} \cdot \Delta Q \pm \frac{|A|}{2} \cdot \Delta Q = \frac{F}{2} \cdot \Delta Q \pm \frac{|A|}{2} \cdot \Delta Q$$

By rewriting the flux derivatives using the first order differencing operators of backward and forward differencing the following derivation for convective term discretization is achieved.

$$\begin{aligned} & \nabla_{\xi}^b F^+ + \Delta_{\xi}^f F^- \\ & \nabla_{\xi}^b \left(\frac{F}{2} \cdot \Delta Q + \frac{|A|}{2} \cdot \Delta Q \right) + \Delta_{\xi}^f \left(\frac{F}{2} \cdot \Delta Q - \frac{|A|}{2} \cdot \Delta Q \right) \\ & \frac{1}{2} \cdot \left[(\nabla_{\xi}^b + \Delta_{\xi}^f) \cdot F + (\nabla_{\xi}^b - \Delta_{\xi}^f) \cdot |A| \cdot \Delta Q \right] \\ & \left[\delta_{\xi} \cdot F - \frac{1}{2 \cdot \Delta \xi} \cdot (\Delta_{\xi} \nabla_{\xi}) \cdot |A| \cdot \Delta Q \right] \\ & \left[\delta_{\xi} \cdot F - \frac{1}{2 \cdot \Delta \xi} \cdot (\Delta_{\xi} \nabla_{\xi}) \cdot |F| \right] \end{aligned}$$

It can be seen that the upwind scheme could be written in the form of central difference term, $(\delta_{\xi} \cdot F)$, with an added dissipation term $(-\frac{1}{2 \cdot \Delta \xi} \cdot (\Delta_{\xi} \nabla_{\xi}) \cdot |F|)$ into it. The detailed work for this approach is given in [14]. It is advised that this kind of upwind discretization should be applied for subsonic regimes. For supersonic regimes, standard upwind schemes of Steger-Warming, Roe or van Leer could be applied.

When it comes for the diffusion discretization, a standard application would result in,

$$\delta_{\xi} \cdot (\Gamma \cdot \delta_{\xi} \cdot \phi)_i = \frac{(\Gamma \cdot \delta_{\xi} \cdot \phi)_{i+1} - (\Gamma \cdot \delta_{\xi} \cdot \phi)_{i-1}}{(\xi_{i+1} - \xi_{i-1})} = \frac{\Gamma_{i+1} \cdot \frac{\phi_{i+2} - \phi_i}{\xi_{i+2} - \xi_i} - \Gamma_{i-1} \cdot \frac{\phi_i - \phi_{i-2}}{\xi_i - \xi_{i-2}}}{(\xi_{i+1} - \xi_{i-1})}$$

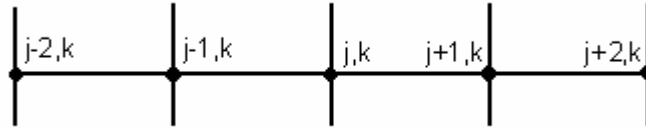


Figure 4.2 Standard diffusion discretization nodes

where δ_{ξ} represents the first derivative with respect to ξ , that is $\frac{\partial}{\partial \xi}$. It can easily be seen that for a standard application of the second derivative, the solution points included in the derivative term, extends up to two node neighborhood of the primary solution node.

If imaginary solution nodes between the primary nodes say, $i+1/2$ and $i-1/2$, are employed, the diffusion discretization can be represented so,

$$\delta_{\xi} \cdot (\Gamma \cdot \delta_{\xi} \cdot \phi)_i = \frac{(\Gamma \cdot \delta_{\xi} \cdot \phi)_{i+\frac{1}{2}} - (\Gamma \cdot \delta_{\xi} \cdot \phi)_{i-\frac{1}{2}}}{\frac{1}{2} \cdot (\xi_{i+1} - \xi_{i-1})} = \frac{\Gamma_{i+\frac{1}{2}} \cdot \frac{\phi_{i+1} - \phi_i}{\xi_{i+1} - \xi_i} - \Gamma_{i-\frac{1}{2}} \cdot \frac{\phi_i - \phi_{i-1}}{\xi_i - \xi_{i-1}}}{\frac{1}{2} \cdot (\xi_{i+1} - \xi_{i-1})} \quad (4.49)$$

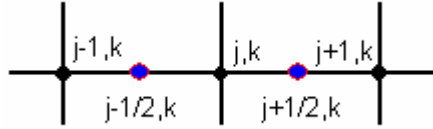


Figure 4.3 Diffusion discretization with imaginary solution nodes

The solution nodes then lay within the given primary solution node and its primary neighbors as shown in Figure 4.2.

The details of the discretization are presented in Appendix D in full detail. The discretized equations can be given as,

ξ sweep

$$\begin{aligned} & \left[-t^* \cdot \frac{B_{j,k-1}}{2} - t^* \cdot \frac{|B|_{j,k-1}}{2} - t^* \cdot V_{\eta KR} - t^* \cdot S_{\eta KR} - t^* \cdot S_{j,k-1} \right] \cdot \Delta Q_{j,k-1}^n \otimes \\ & + \left[I + t^* \cdot |B|_{j,k} + t^* \cdot V_{\eta K} + t^* \cdot S_{\eta K} + 2 \cdot t^* \cdot S_{j,k} - t^* \cdot C_{j,k} \right] \cdot \Delta Q_{j,k}^n \otimes \\ & \left[t^* \cdot \frac{B_{j,k+1}}{2} - t^* \cdot \frac{|B|_{j,k+1}}{2} - t^* \cdot V_{\eta KP} + t^* \cdot S_{\eta KP} - t^* \cdot S_{j,k+1} \right] \cdot \Delta Q_{j,k+1}^n \otimes \end{aligned}$$

= RHS

$$\begin{aligned} & = -t^{**} \cdot \frac{F_{j+1,k} - F_{j-1,k}}{2} + \left[\frac{|F|_{j+1,k} - 2 \cdot |F|_{j,k} - |F|_{j-1,k}}{2} \right] + t^{**} \cdot H \cdot \\ & - t^{**} \cdot \frac{G_{j,k+1} - G_{j,k-1}}{2} + \left[\frac{|G|_{j,k+1} - 2 \cdot |G|_{j,k} - |G|_{j,k-1}}{2} \right] + t^{**} \cdot K \cdot \\ & + t^{**} \cdot M_{j,k}^* + \frac{\phi}{1 + \phi} \cdot \Delta Q_{j,k}^{n-1} \end{aligned}$$

η sweep

$$\begin{aligned}
& \left[-t^* \cdot \frac{A_{j-1,k}}{2} - t^* \cdot \frac{|A|_{j-1,k}}{2} - t^* \cdot U_{\xi_{JR}} - t^* \cdot R_{\xi_{JR}} - t^* \cdot R_{j-1,k} \right] \cdot q_{j-1,k} \\
& + \left[I + t^* \cdot |A|_{j,k} + t^* \cdot U_{\xi_J} + t^* \cdot R_{\xi_J} + 2 \cdot t^* \cdot R_{j,k} \right] \cdot q_{j,k} \\
& \left[t^* \cdot \frac{A_{j+1,k}}{2} - t^* \cdot \frac{|A|_{j+1,k}}{2} - t^* \cdot U_{\xi_{JP}} + t^* \cdot R_{\xi_{JP}} - t^* \cdot R_{j+1,k} \right] \cdot q_{j+1,k} \\
& = \Delta Q_{j,k}^n \otimes
\end{aligned}$$

The vectors given in the previous set of equations are fully identified in Appendix D. For a certain solution band, the discretized equations form a block tri-diagonal matrix. The solution of such a system could be obtained by a tri-diagonal matrix solver. [15]

4.2.5 Boundary and Initial Conditions

During the computation of the discretized equations, certain conditions for the boundaries that are not included in the tri-diagonal matrix should be given explicitly at each iteration step. These boundary nodes are included in the solution as the boundary conditions. For the problems investigated by using turbulence models, there are certain correlations for different types of boundary types. The representations of physical domains with the boundaries are presented in Figures 4.4 to 4.7.

Boundary conditions are be tabulated as in Table 4.2

Table 4.2 List of Boundary Condition types

	Boundary Condition Types
S1	Wall type BC
S2	Wake type BC (upper surface)
S3	Wake type BC (lower surface)
S4	Outlet type BC (lower side)
S5	Outlet type BC (upper side)
S6	Symmetry type BC
I1	Initial Condition

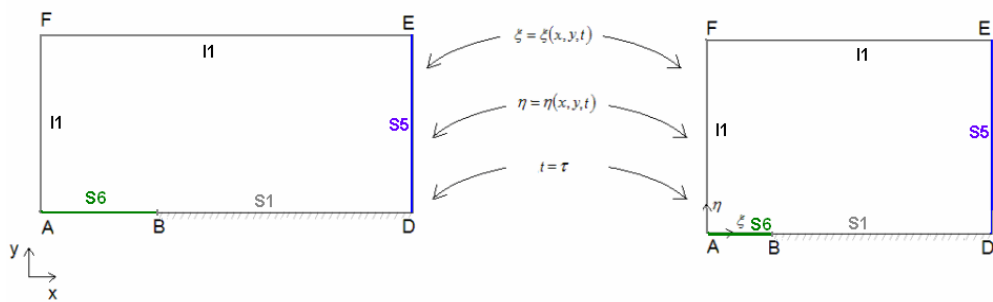


Figure 4.4 Boundary condition types for flat plate

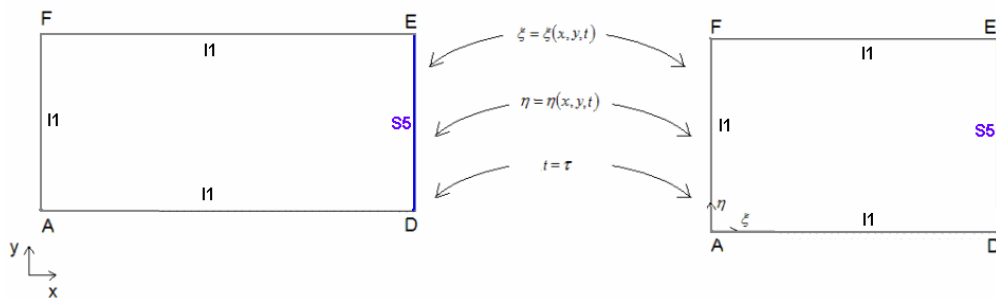


Figure 4.5 Boundary condition types for free shear

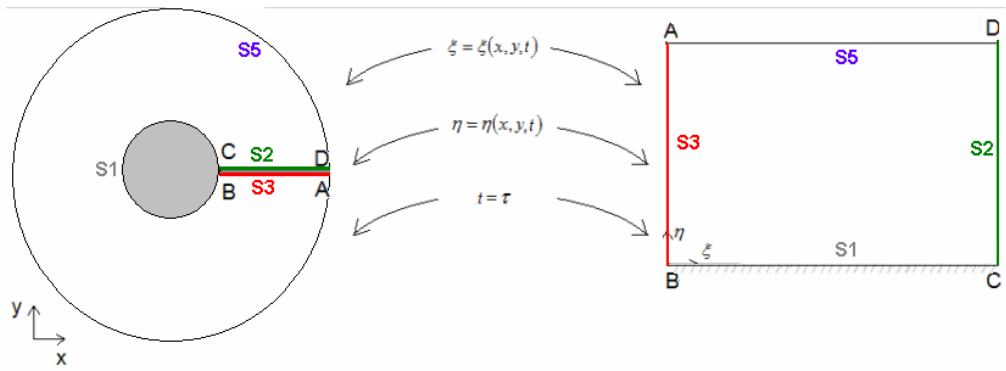


Figure 4.6 Boundary condition types for cylinder

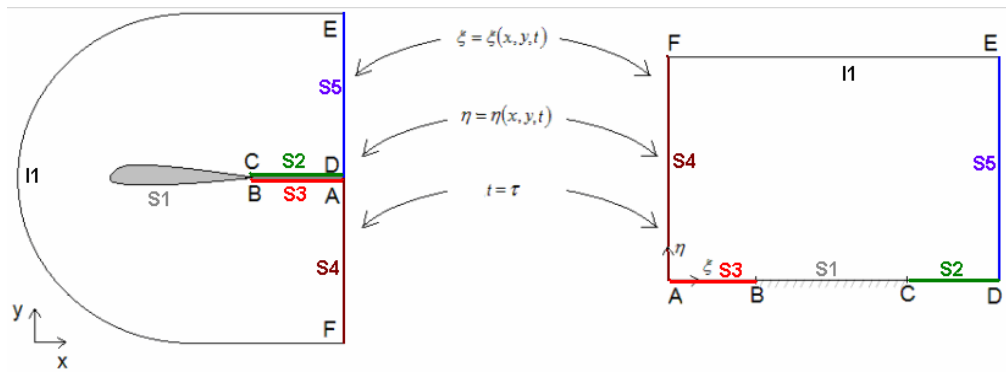


Figure 4.7 Boundary condition types for airfoil

The boundary condition types could be summarized as above. The labels starting with the character S denotes the boundary conditions whereas the ones starting with I is refers to initial conditions. Boundary conditions are updated at each step of the computation while the initial conditions of are introduced at the first iteration.

4.2.5.1 Wall boundary condition, S1

Wall boundary conditions for a Navier-Stokes solver would be easier to manipulate since no slip boundary conditions are applied. Since turbulent kinetic energy is defined as Equation (2.4), if no velocity appears on the wall surface, the fluctuations of its components will also be null. Then the wall boundary condition for k is simply zero. However it is not so easy to implement the boundary condition for ω on wall. There are many studies on different types of boundary conditions and the one, which is appeared to be more extensively used, is applied given in [8]. With these two boundary conditions for the turbulent variables, the resulting boundary condition for turbulent viscosity becomes,

$$\tilde{\mu}_{tj,1} = 0$$

with

(4.50)

$$\tilde{k}_{j,1} = 0$$

$$\tilde{\omega}_{j,1} = \frac{60 \cdot \tilde{\mu}_{j,2}}{\tilde{\rho}_{j,2} \cdot \beta \cdot \tilde{d}_{j,2}^2} = \frac{60 \cdot \mu_{j,2}}{\rho_{j,2} \cdot \beta \cdot d_{j,2}^2} \cdot \left(\frac{M_\infty}{\text{Re}} \right)^2$$

Menter's studies have shown that a boundary condition related to the magnitude of vorticity at the wall with multiplication of a constant gives results similar to the boundary condition given by the above equation.

$$\tilde{k}_{j,1} = 0$$

(4.51)

$$\tilde{\omega}_{j,1} = 1000 \cdot \Omega$$

This application makes the model more robust since it is not necessary to calculate the wall distance for the first grid point.

For $k-\omega$ models the wall boundary conditions are generally given in a form similar to the above equations. However, the implementation of Boundary Condition for ε is different for different $k-\varepsilon$ turbulence models. Two $k-\varepsilon$ models are investigated and the difference of these models appear at the very early stage of the model representations, in Equations (4.9) and (4.14). On the other hand the boundary condition for k , as expected, remains same as the boundary conditions in $k-\omega$ models since the definition of k is related to the velocity fluctuations.

$$\tilde{\mu}_{t,j,1} = 0$$

with

$$\begin{aligned} \tilde{k}_{j,1} &= 0 \\ \tilde{\varepsilon}_{j,1} &= 0 \quad \text{Chien } k - \varepsilon \end{aligned} \tag{ 4.52 }$$

$$\tilde{\varepsilon}_{j,1} = \frac{2 \cdot \tilde{\mu}_{j,2}}{\tilde{\rho}_{j,2}} \cdot \left(\frac{\partial \sqrt{\tilde{k}}}{\partial \tilde{n}} \right)_{j,1}^2 = \frac{2 \cdot \mu_{j,2}}{\rho_{j,2}} \cdot \left(\frac{\partial \sqrt{k}}{\partial n} \right)_{j,1}^2 \cdot \left(\frac{M_\infty}{\text{Re}} \right)^2 \quad \text{Abid } k - \varepsilon$$

The boundary condition for *Abid* $k-\varepsilon$ model is taken from reference [8]

4.2.5.2 Wake boundary conditions, S2, S3

Actually, a wake phenomenon is a free shear problem. However, due to the structure of the C-Grid, the wake regions appear as a boundary condition. This boundary condition is simply applied as a permeable boundary

condition which serves as a continuity region from upper side of the wake to lower side. The application of this boundary condition for a variable, say turbulent kinetic energy, appears as,

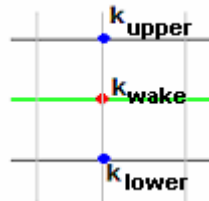


Figure 4.8 Representation of wake boundary

$$k_{wake} = \frac{k_{upper} + k_{lower}}{2}, \quad \omega_{wake} = \frac{\omega_{upper} + \omega_{lower}}{2}, \quad \varepsilon_{wake} = \frac{\varepsilon_{upper} + \varepsilon_{lower}}{2} \quad (4.53)$$

The implementation of wake boundary condition for ω and ε appeared to be insufficient to transport the strength of these parameters from the wall boundary to free shear regions as in the case of cylinder and airfoil problems. Some remedies for this problem is presented in Section 4.2.6.

4.2.5.3 Outlet boundary conditions, S4, S5

There are certain boundary condition types for outlet conditions. The most extensive used one for the turbulence models is the extrapolation boundary condition. This boundary condition stands for the situation where the outer boundaries of the domain are sufficiently far away that every variable for the boundary node is just the same as the variable at the node adjacent to the boundary.

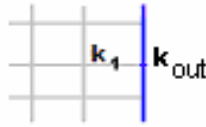


Figure 4.9 Representation of outlet boundary

$$k_{out} = k_1 \quad (4.54)$$

4.2.5.4 Symmetry boundary condition, S6

Since the flow approaches the flat plate with a zero angle of attack, the flow appears to be symmetric with respect to the first horizontal grid line. The symmetry condition can be implemented by setting the derivatives with respect to normal direction to zero. Hence,

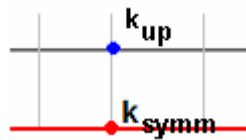


Figure 4.10 Symmetry boundary representation

$$k_{symm} = k_{up} \quad (4.55)$$

4.2.5.5 Initial Condition, I1

The initial conditions for the turbulence model variables are used as,

$$k_{\infty} = 9.0 \cdot 10^{-9}, \quad \omega_{\infty} = 1.0 \cdot 10^{-6}, \quad \varepsilon_{\infty} = 1.0 \cdot 10^{-17}, \quad \mu_{t\infty} = 9.0 \cdot 10^{-3}$$

The flow initialization could be applied in a different way to speed up the development of the boundary layer. However, this application of initial conditions was found to be unnecessary since initialization with free stream conditions is enough to develop a boundary layer. The artificial boundary layer correlations can be given as,

$$\begin{aligned}
 k_{IC} &= \max(k_{\infty}, -C_1 \cdot d^2 + C_2 \cdot d) \\
 \omega_{IC} &= \max\left(-12444d + 0.54 \frac{C_{\mu} \cdot k_{IC}}{\nu 3d}\right) \\
 C_{\mu} &= 1, \quad \nu 3d = \frac{100k_{IC}}{t_{\max}}, \quad t_{\max} = -C_1 \cdot S_{\max}^2 + C_2 \cdot S_{\max}, \quad S_{\max} = \frac{C_2}{2 \cdot C_1}, \quad C_1 = 458, \quad C_2 = 1.68
 \end{aligned} \tag{4.56}$$

For k - ω turbulence models the above correlations are applied where as for k - ε models,

$$\begin{aligned}
 k_{IC} &= \min(zk4, \max(zk1, \min(zk2, zk3))) \\
 \omega_{IC} &= \min(ep4, \max(ep1, \min(ep2, ep3))) \\
 zk1 &= k_{\infty}, & ep1 &= \varepsilon_{\infty} \\
 zk2 &= 10^{-471 \cdot d + 0.47}, & ep2 &= 10^{-555 \cdot d - 6} \\
 zk3 &= 10^{-37.5 \cdot d - 3.7}, & ep3 &= 10^{-280 \cdot d - 9.2} \\
 zk4 &= 6.7 \cdot d, & ep4 &= \min(1 \cdot 10^{20}, 10^{13333 \cdot d - 9.8})
 \end{aligned} \tag{4.57}$$

The correlations above are referenced from [8].

4.2.6 Limitations and Improvements

Limitations during the computation of turbulence models are employed to keep turbulence variables as positive and to contribute the progress of the computation steps. These limitations should not affect the general structure of the solution and should be applied in an accurate amount. Otherwise, limitations would yield incorrect solutions.

The limitations applied in this study could be summarized as follows,

- 1) *Production Limitation:* For the k - ω models, the production term of k variable, P_k , should not be greater than twenty times the destruction of the same variable, D_k . [11]

$$P_k \leq 20 \cdot D_k \quad (4.58)$$

- 2) *Destruction Positivity:* The destruction terms are included into the left side (Jacobian term) only if its contribution is positive. [8]

$$\begin{aligned} -t^* \cdot \left(-\beta' \cdot \omega \cdot \left(\frac{\text{Re}}{M_\infty} \right)^2 \right) \leq 0, & \quad \rightarrow \quad -t^* \cdot \left(-\beta' \cdot \omega \cdot \left(\frac{\text{Re}}{M_\infty} \right)^2 \right) = 0 \\ -t^* \cdot \left(-2.0 \cdot \beta \cdot \omega \cdot \left(\frac{\text{Re}}{M_\infty} \right)^2 \right) \leq 0, & \quad \rightarrow \quad -t^* \cdot \left(-2.0 \cdot \beta \cdot \omega \cdot \left(\frac{\text{Re}}{M_\infty} \right)^2 \right) = 0 \quad (4.59) \\ -t^* \cdot \left(-\beta' \cdot k \cdot \left(\frac{\text{Re}}{M_\infty} \right)^2 \right) \leq 0, & \quad \rightarrow \quad -t^* \cdot \left(-\beta' \cdot k \cdot \left(\frac{\text{Re}}{M_\infty} \right)^2 \right) = 0 \end{aligned}$$

3) *Turbulence Parameters Positivity*: k , ω , ε and μ_T values are not allowed to have negative values. Several applications for this limitation are tested. These applications could be listed as follows,

a) If any computed value appears to be negative, the computed values are assigned to their corresponding values at the last time step.

$$\begin{aligned}
 k^{n+1}_{corr} &= k^{n+1} - \Delta k^n \\
 \omega^{n+1}_{corr} &= \omega^{n+1} - \Delta \omega^n \\
 \varepsilon^{n+1}_{corr} &= \varepsilon^{n+1} - \Delta \varepsilon^n \\
 \mu_t^{n+1}_{corr} &= \mu_t^n
 \end{aligned}
 \tag{4.60}$$

When this approach is used, the replaced variables tend to get negative values continuously

b) The negative values can be replaced by the corresponding linearly interpolated value from the neighboring grid points

$$\begin{aligned}
 k_{j,k} &= \frac{k_{j+1,k} + k_{j-1,k}}{2} \\
 \omega_{j,k} &= \frac{\omega_{j+1,k} + \omega_{j-1,k}}{2} \\
 \varepsilon_{j,k} &= \frac{\varepsilon_{j+1,k} + \varepsilon_{j-1,k}}{2} \\
 \mu_{t,j,k} &= \frac{\mu_{t,j+1,k} + \mu_{t,j-1,k}}{2}
 \end{aligned}
 \tag{4.61}$$

The results of this application appeared to be significant and this strategy is used for limitation.

c) Assigning free stream values to the nodes having negative values appears to be a third approach for having positive turbulent variables.

$$\begin{aligned}
 k &= k_{\infty} \\
 \omega &= \omega_{\infty} \\
 \varepsilon &= \varepsilon_{\infty} \\
 \mu_t &= \mu_{t\infty}
 \end{aligned}
 \tag{ 4.62 }$$

Among the three approaches the latter one found to be the worst for negative values problem.. This limitation appeared to be insufficient and for some cases, it directs the computation to incorrect solutions.

4) *Turbulent Viscosity Limitation:* The non-dimensional turbulent viscosity is not allowed to take values larger than 100.000 [8].

$$\mu_t \leq 10^5
 \tag{ 4.63 }$$

5) *f_{μ} Limitation:* For k - ε models, the greatest value for f_{μ} is one [10], that is

$$f_{\mu} \leq 1
 \tag{ 4.64 }$$

6) *Cross Diffusion Improvement:* k - ω turbulence model equations are derived from k - ε turbulence model by primarily using a transformation of $\varepsilon = C_{\mu} \cdot k \cdot \omega$. This transformation brings a cross diffusion term into the ω equation. This term is not so significant for the near wall regions whereas it is appears significant for the wake, free shear and mixing flows. The effect of this term appears as an increase in the production term in the ω equation.

Model equation of ω sometimes referred as deficient without this cross diffusion term, however some scientists refer the cross term as insignificant term. In this study this term is included into the model just enable k - ω model to be more efficient.

$$\begin{aligned} \frac{\partial(\rho \cdot \omega)}{\partial t} + \frac{\partial(\rho \cdot u \cdot \omega)}{\partial x} + \frac{\partial(\rho \cdot v \cdot \omega)}{\partial y} = P_{\omega} - D_{\omega} + \frac{\partial}{\partial x} \cdot \left(\left(\mu + \frac{\mu_T}{\sigma_{\omega}} \right) \cdot \frac{\partial \omega}{\partial x} \right) + \frac{\partial}{\partial y} \cdot \left(\left(\mu + \frac{\mu_T}{\sigma_{\omega}} \right) \cdot \frac{\partial \omega}{\partial y} \right) \\ + 2 \cdot \frac{\left(\mu + \frac{\mu_T}{\sigma} \right)}{k} \cdot \left(\frac{\partial k}{\partial x} \cdot \frac{\partial \omega}{\partial x} + \frac{\partial k}{\partial y} \cdot \frac{\partial \omega}{\partial y} \right) + \frac{\omega}{k} \cdot \left((\sigma - \sigma^*) \cdot \mu_T \left(\frac{\partial k}{\partial x} + \frac{\partial k}{\partial y} \right) \right) \end{aligned}$$

$$\sigma = \sigma^*$$

$$\begin{aligned} \frac{\partial(\rho \cdot \omega)}{\partial t} + \frac{\partial(\rho \cdot u \cdot \omega)}{\partial x} + \frac{\partial(\rho \cdot v \cdot \omega)}{\partial y} = P_{\omega} - D_{\omega} + \frac{\partial}{\partial x} \cdot \left(\left(\mu + \frac{\mu_T}{\sigma_{\omega}} \right) \cdot \frac{\partial \omega}{\partial x} \right) + \frac{\partial}{\partial y} \cdot \left(\left(\mu + \frac{\mu_T}{\sigma_{\omega}} \right) \cdot \frac{\partial \omega}{\partial y} \right) \\ + 2 \cdot \frac{\left(\mu + \frac{\mu_T}{\sigma} \right)}{k} \cdot \underbrace{\left(\frac{\partial k}{\partial x} \cdot \frac{\partial \omega}{\partial x} + \frac{\partial k}{\partial y} \cdot \frac{\partial \omega}{\partial y} \right)}_{\text{CROSSDIFFUSION}} \end{aligned}$$

$$\sigma_k = \sigma_{\omega} = \sigma$$

There are certain methods to implement the cross diffusion term. These are as follows

a) This term could be included into the equations directly. Current application includes the insertion of the cross diffusion term into the destruction term of ω as,

$$-\beta \cdot \omega^2 + 2 \cdot \frac{\left(\mu + \frac{\mu_T}{\sigma} \right)}{k} \cdot \left(\frac{\partial k}{\partial x} \cdot \frac{\partial \omega}{\partial x} + \frac{\partial k}{\partial y} \cdot \frac{\partial \omega}{\partial y} \right)$$

$$\left[-\beta + 2 \cdot \frac{\left(\mu + \frac{\mu_T}{\sigma} \right)}{k \cdot \omega^2} \cdot \left(\frac{\partial k}{\partial x} \cdot \frac{\partial \omega}{\partial x} + \frac{\partial k}{\partial y} \cdot \frac{\partial \omega}{\partial y} \right) \right] \cdot \omega^2$$

After non-dimensionalization,

$$-\beta + 2 \cdot \frac{\left(\mu + \frac{\mu_T}{\sigma} \right)}{k \cdot \omega^2} \cdot \left(\frac{\partial k}{\partial x} \cdot \frac{\partial \omega}{\partial x} + \frac{\partial k}{\partial y} \cdot \frac{\partial \omega}{\partial y} \right) \cdot \left(\frac{M_\infty}{\text{Re}} \right)^2 \quad (4.65)$$

b) Cross diffusion term is applied to increase the production of ω term. Increasing the production term of ω means that the turbulent viscosity will decrease. Decreasing the k production is identical to increasing the destruction of k . This method accomplishes the implementation of cross diffusion effect by decreasing the k production term. [6].

$$D_k = -\beta' \cdot \omega \cdot \left(\frac{\text{Re}}{M_\infty} \right)^2$$

$$\beta' = \beta'_o \cdot f'_\beta$$

$$\beta'_o = 0.09 \quad (4.66)$$

$$f'_\beta = \begin{cases} 1, & \chi_k \leq 0 \\ 1 + 680 \cdot \chi_k^2, & \chi_k > 0 \end{cases} \quad \chi_k \equiv \frac{1}{\omega^3} \cdot \frac{\partial k}{\partial x_j} \cdot \frac{\partial \omega}{\partial x_j}$$

7) ω and ε , *Wake Transportation*: The above limitations are sufficient for the computations including a wall boundary. However, it is observed that for free shear applications such as the wake region of the airfoil problem, ω does not rise sufficiently so result in an increase in the turbulent viscosity.

This problem appears as errors due to negative pressure. Reason to this problem defined as the increase in ω parameter at the wall and deficiency in convecting this value towards the free shear regions. The aspect ratio of the cells at the very beginning of the wake section is not suitable for the solution of a free shear problem appearing in that region. This problem occurs due to the structure of the C-Grid.

In viscous flow solutions, boundary layer has a great importance in the solution. For turbulent flows y^+ at the first grid point from the wall boundary should not have a value greater than 1. That value is obtained by giving a first grid point distance of nearly $5 \cdot 10^{-6}$ units. This wall distance continues in the chord wise direction. At the trailing edge, the aspect ratio appears to be in the order of 100 (Figure 4.11) whereas near to the outlet boundary, the cell aspect ratios reach up to a million (Figure 4.12). This kind of grid distribution is not suitable for a solution of free shear flow.

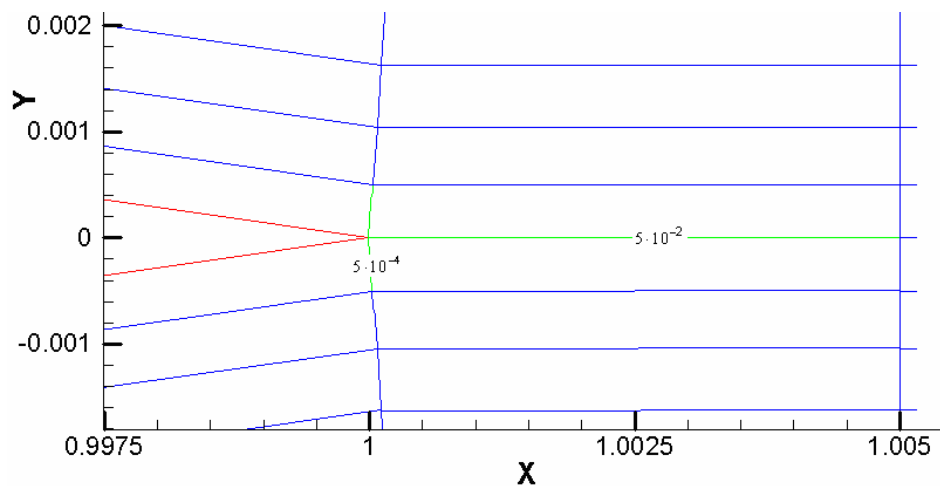


Figure 4.11 Trailing edge of the airfoil

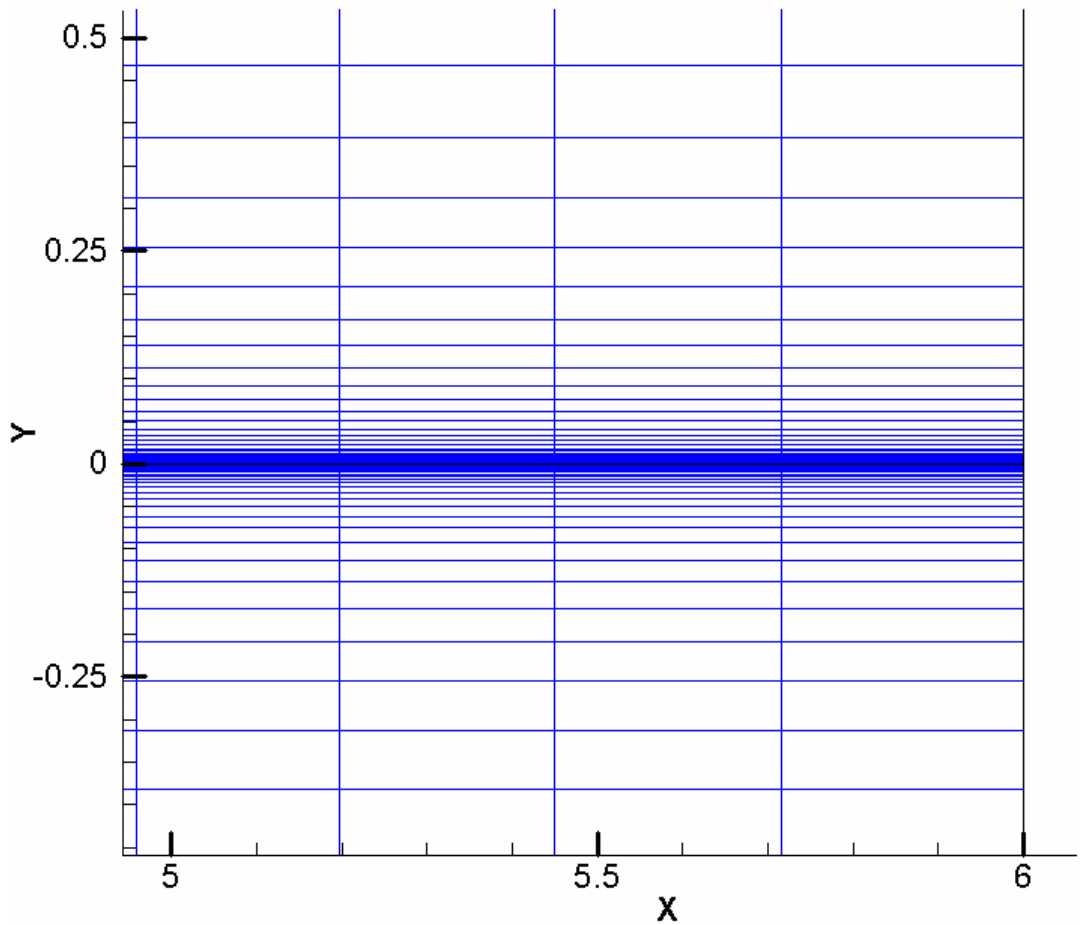


Figure 4.12 Outlet boundary in the C-Grid

Certain ideas to increase the production of ω appeared during this study. One of them is the derivation of a function which evaluates the cell aspect ratio and increases the production of ω .

$$P_{\omega} = f \cdot P_{\omega}$$

$$f = f(AR_{ave}, \omega)$$

$$AR_{ave} = \frac{AR_1 + AR_2}{2} = \frac{\frac{a}{b} + \frac{b}{a}}{2} = \frac{a^2 + b^2}{2 \cdot a \cdot b}$$

The AR term represents the aspect ratio of the cell. a and b shown in Figure 4.13.

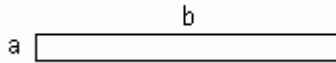


Figure 4.13 Cell dimensions

Similar problems are encountered with for the $k-\epsilon$ models.

During the computations of test cases, an easier method to overcome this problem is obtained. In this method, ω and ϵ values at the wake boundaries are simply being multiplied by a constant that can be adjusted by the user. This constant could vary between 5 to 100. This improvement is an artificial one with no logical contribution to the solution, whereas it provides a quick and easy solution for the wake transformation problem. However after this implementation, the C-Grid is converted to O-Grid which eliminates the aspect ratio problem so that no artificial increase in ω and ϵ is required. The grid properties is presented in Figures 4.14, 4.15 and 4.16.

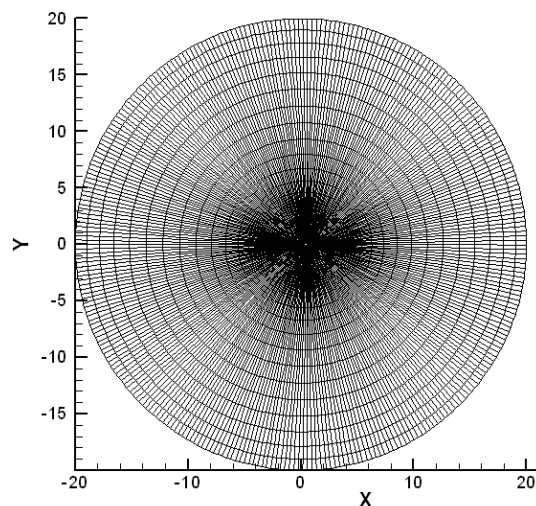


Figure 4.14 O-Grid for airfoil

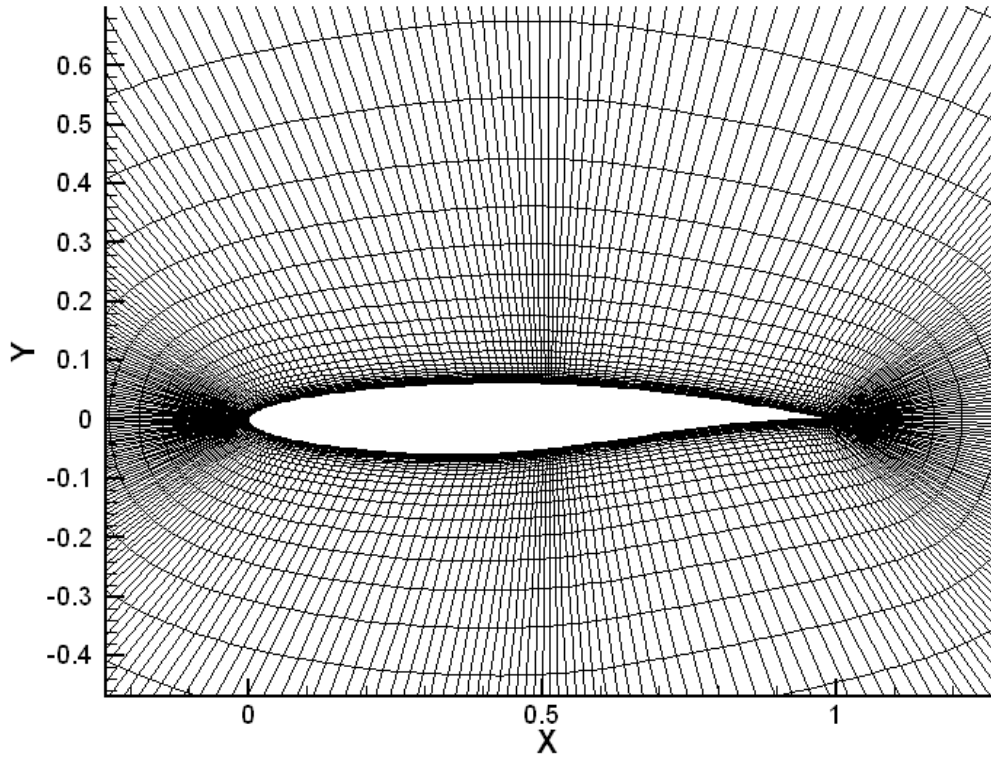


Figure 4.15 Enlarged view of O-Grid

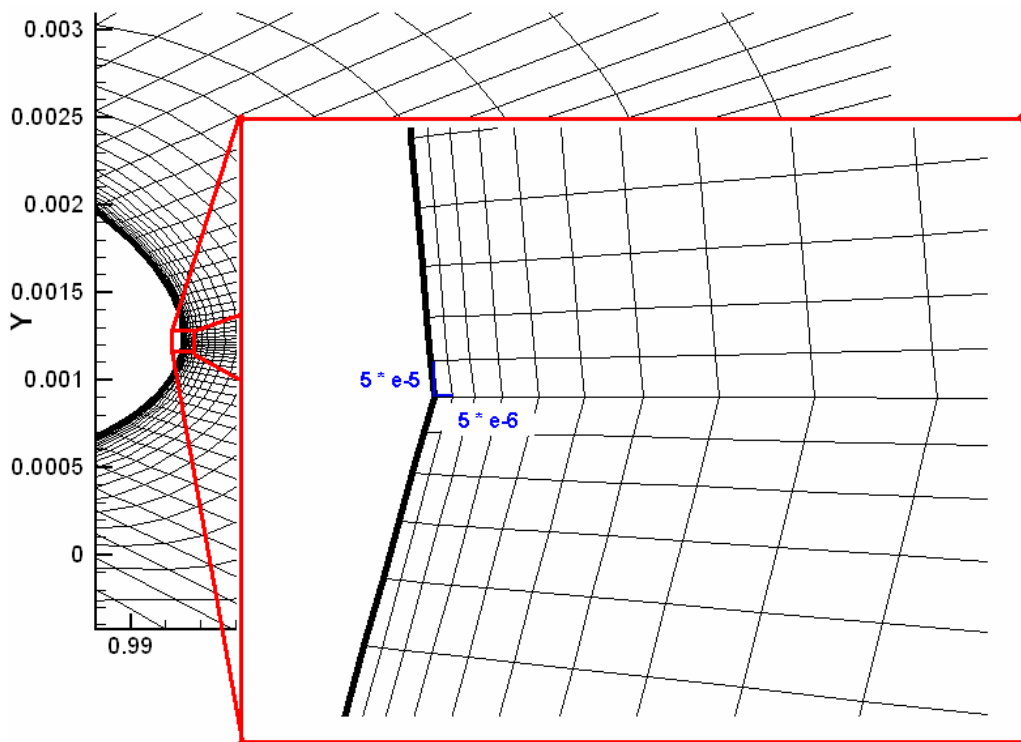


Figure 4.16 O-Grid wake of an airfoil

CHAPTER 5

RESULTS AND DISCUSSIONS

The implemented turbulence models are verified by using the flow over a flat plate and results are compared with the available experimental data. Later on, the computational capability of the code is tested by using the free shear flow, flow over a cylinder problems without comparing with the experimental data and numerical results.

The greatest motivation for the development of this code is to handle the airfoil test cases. Extensive validation of turbulence models with experimental data is presented in this section. A three-dimensional application for the flow over a ONERA M6 wing is also considered.

5.1 Flat Plate

Turbulence models of *Baldwin-Lomax*, *Wilcox $k-\omega$* , *Menter BSL* and *Chien $k-\varepsilon$* are tested for this case. The experimental data obtained from [10] although original work for data collection was carried out by Coles [17]. The test case a Mach number of 0.2 and a free stream Reynolds Number of 2.28×10^7 . As discussed in the Section 4.2.5 angle of attack is taken as zero degrees. The static pressure and temperature are taken as 1 atm. and 21.3 °C respectively.

A structured 150x80 grid with wall boundaries starting from 30th node is used in computations. First grid point distance of 10⁻⁶ and same distance from the beginning of the wall boundary is used. The structured grid for this test case is given in Figure 5.1.

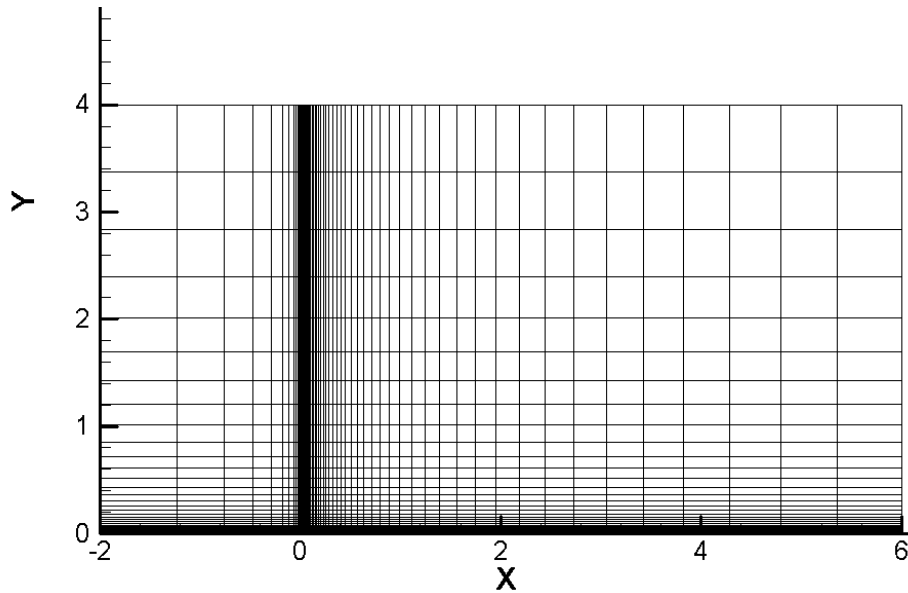


Figure 5.1 Structured, 150x80 grid for the flat plate

Residuals of variables are calculated by using;

$$RES = \frac{\sum_{n=1}^{n=node} |Q^{n+1} - Q^n|}{nnode}$$

where *nnode* stands for the number of nodes appear in the domain. *Wilcox k- ω* and *Menter BSL* turbulence models appeared to have the fastest convergence properties among the others which can be seen from Figures 5.2, 5.3 and 5.4. It is assumed that the convergence is achieved when the residual drops by 3 orders. Convergence is obtained for *Wilcox k- ω* and *Menter BSL* turbulence models after 6000 iterations while 6500 iterations

are required for *Baldwin-Lomax* turbulence model. The longest convergence period is obtained from *Chien k-ε* that has a value of 9500 iterations.

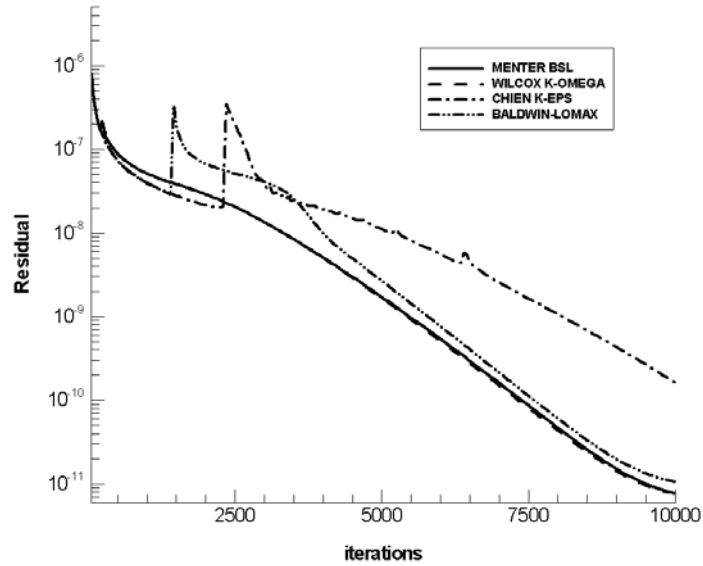


Figure 5.2 Residual Drops versus iteration steps.

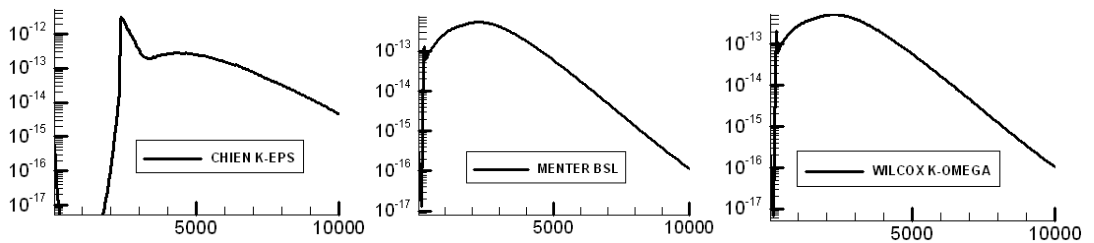


Figure 5.3 Residual Drops of k versus Iteration steps

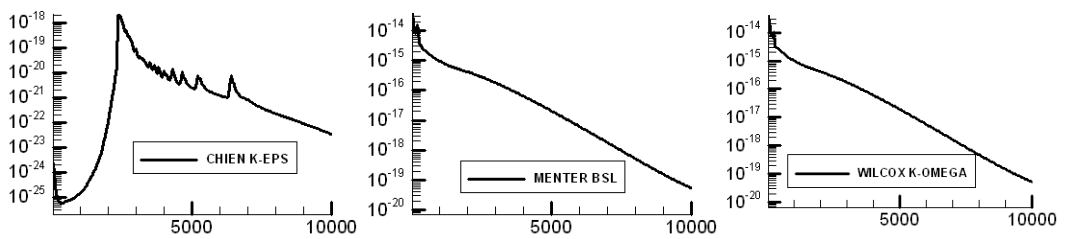


Figure 5.4 Residual Drops of ϵ & ω versus Iteration steps

Experimental data obtained from [10] represents the turbulent boundary layer characteristics by figuring out k^+ , u^+ versus y^+ graphics. Derivations of k^+ , u^+ and y^+ parameters are given in Appendix A, Auxiliary Definitions section.

For the u^+ versus y^+ graph, typical velocity profile for a turbulent boundary layer is compared with the computed values by plotting in Figure 5.5. The turbulent boundary layer profiles possess a viscous sub layer of profile that obeys to the correlation given in Equation 5.1. This viscous sub-layer is considered to be valid up to y^+ values of 10.

$$u^+ = y^+ \quad (5.1)$$

Log layer for which a correlation derived by von Karman is as follows:

$$u^+ = \frac{1}{\kappa} \ln(y^+) + C \quad (5.2)$$

$C \cong 5$ for smooth surfaces

$\kappa = 0.41$ Karman's constant

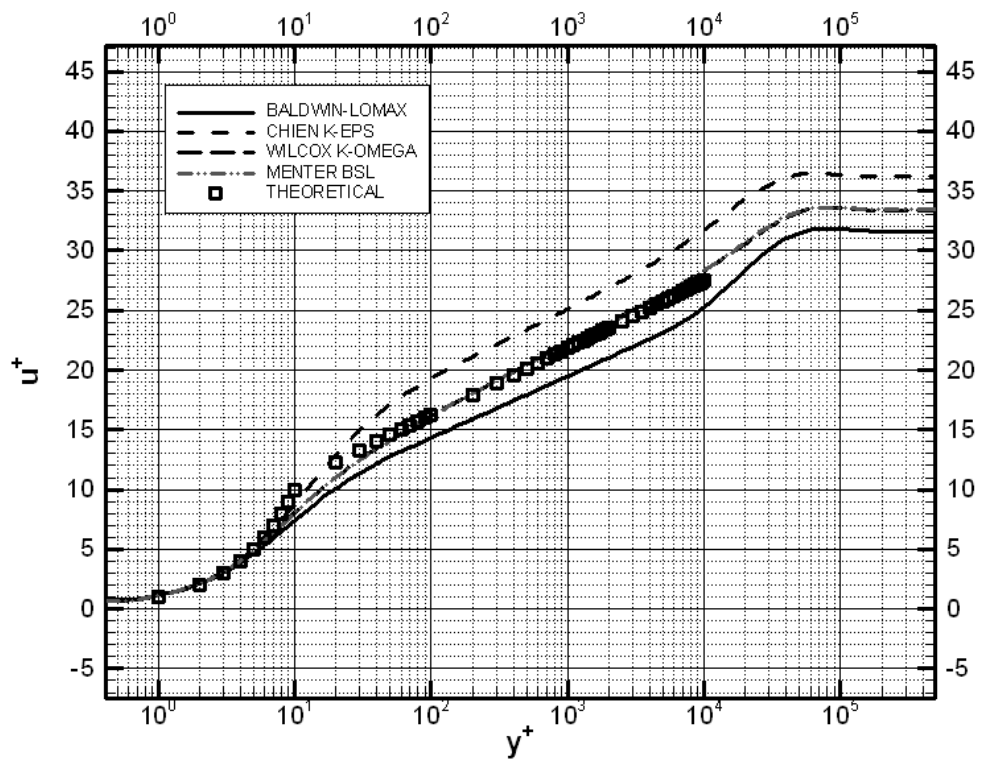


Figure 5.5 Turbulent velocity profile results

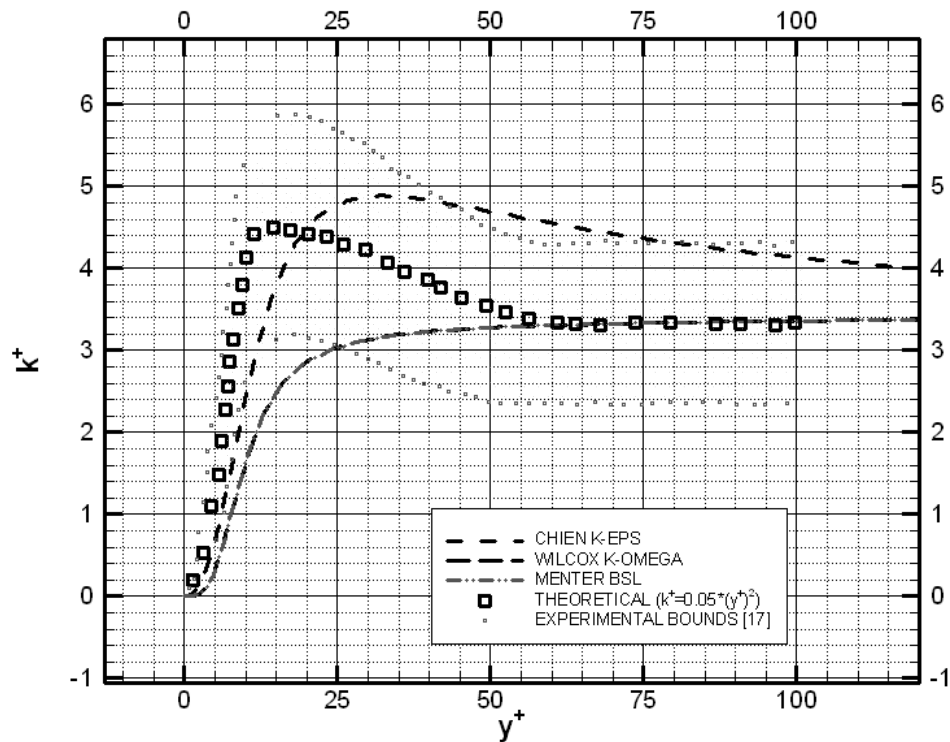


Figure 5.6 Dimensionless turbulent kinetic energy versus y^+

For the velocity profiles in turbulent boundary layer, the results of Wilcox $k-\omega$ and *Menter BSL* models appeared to be nearly the same. Since the flat plate problem is simply a wall bounded problem, it is expected to get the $k-\omega$ characteristics of *Menter BSL* model to be dominant. The results of these two models appeared to be the best among the other models that are plotted in Figure 5.5. In Figure 5.6, *Chien $k-\epsilon$* achieved the closest prediction for determining the peak point of the dimensionless turbulent kinetic energy. However, the free stream value of k^+ predicted by the *Wilcox $k-\omega$* and *Menter BSL* models appear to be the closest ones to the theoretical values. Among all of the turbulence models, the experimental bounds for k^+ values are almost never exceeded.

The transition location from laminar to turbulent region is the primary criteria for the coefficient of friction. In the application of the turbulence models, transition location is not introduced explicitly. In fact transition location is predicted by the solver. The calculation of coefficient of friction, C_f is given in Appendix A.

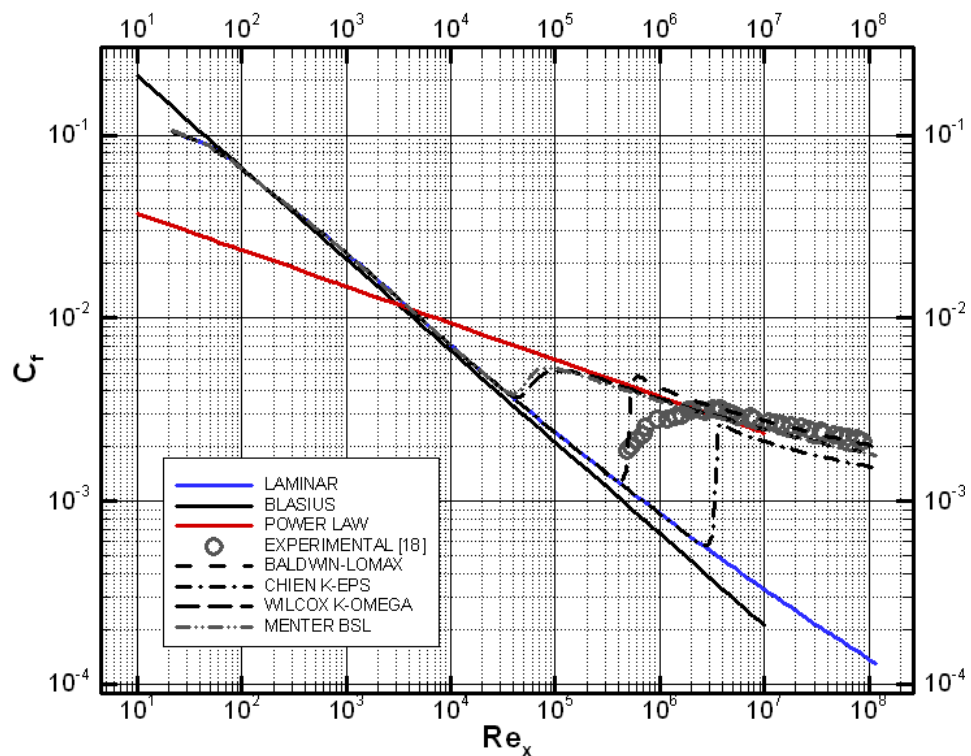


Figure 5.7 Coefficient of Friction versus local Reynolds Number

The experimental data is available in reference [18] and it is collected from the works of Wieselsberger, Gebers, Froude, Kempf, Schoenherr.

In Figure 5.7, friction coefficient is compared with theoretical and analytical solutions related to laminar and turbulent flows. The transition location is best captured by *Chien k-ε*, where as the transition style is not similar to the experimental transition regime. On the other hand, *k-ω* models determine

transition in a similar manner with experimental data but the location of transition could not be determined accurately. Experience on computation of turbulent models showed that the transition location could be tuned by adjusting the production term of turbulent kinetic energy. However this non-physical method is not applied in this study.

Two different locations of the domain are chosen for the comparison of the velocity profiles. One of the locations is close to the leading edge where turbulent viscosity assumes its freestream values and other one is the fully turbulent region.

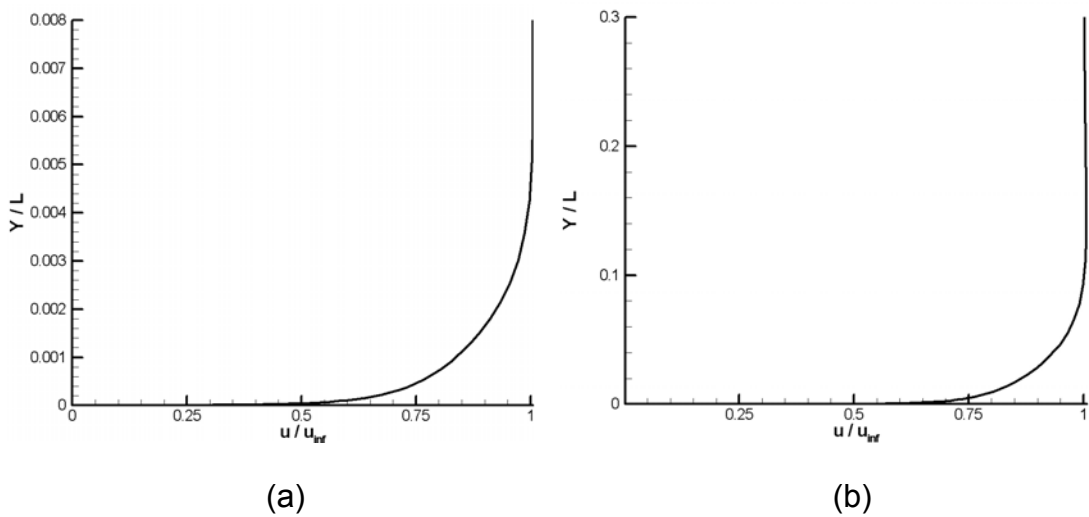


Figure 5.8 (a) Laminar and (b) Turbulent velocity profiles

5.2 Free Shear

The investigation of this test case is performed in order to see whether the wake resolution could be obtained by grid refinement in the solution domain. The grid dimensions are not so logically decided since this test case is a numerical experiment. A 1001x501 grid is used with the domain dimensions

of 5 units by 2.5 units. The grid sizes are equal in both directions of x and y with values of $1e-3$.

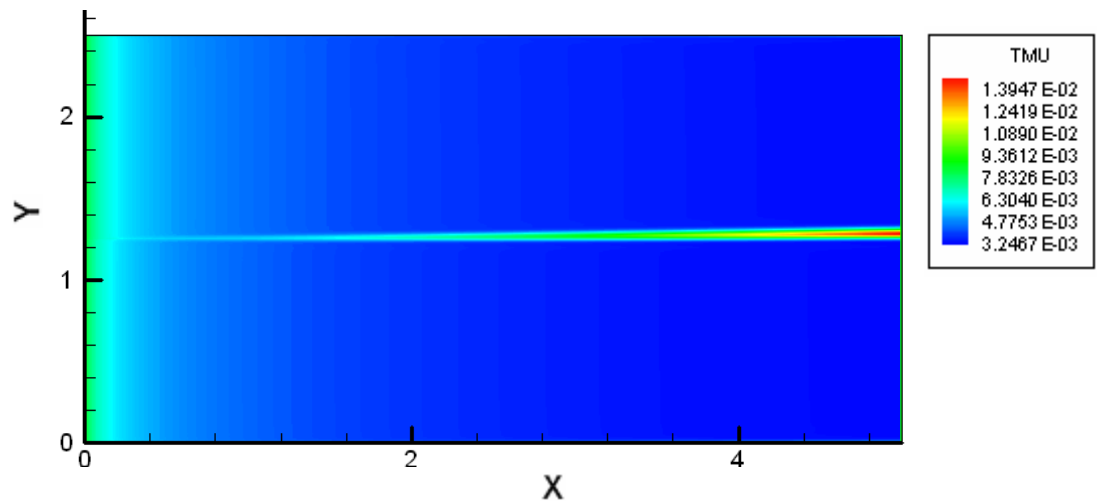


Figure 5.9 Turbulent viscosity contours

The free stream Mach numbers on the upper and lower sides are 0.24 and 0.2, respectively. These values correspond to pressure and suction sides of an airfoil at the trailing edge. The turbulent viscosity contours is shown from Figure 5.9.

5.3 Cylinder

C-Grid version of the original code is adapted to an O-Grid by changing some of the boundary conditions. The details of boundary conditions are given in Section 4.2.5.

Grid has 300 nodes around the cylinder and 40 nodes in normal direction. First grid distance of 5×10^{-6} units is used.

The first trial of this application is evaluated in flow having a Mach number 0.5 and a Reynolds number of 5×10^5 over a cylinder. The wake resolution for the O-Grid is accomplished which was not possible for the C-Grid.

Wake cut for the domain is remained at the right side of the cylinder that no important turbulent flow development occurs. The results showed that for a wake grid formation of acceptable aspect ratios for the grid cells, the computations do not need any limitations regarding the increase in ω values in the wake that is explained in Section 4.2.6.

The results are not compared with the available experimental data since the aim of this test case is to adapt the code to handle O-Grids and to investigate wake properties of the O-Grid.

Turbulent viscosity values increase in the regions of vortical flows as shown in Figure 5.10.

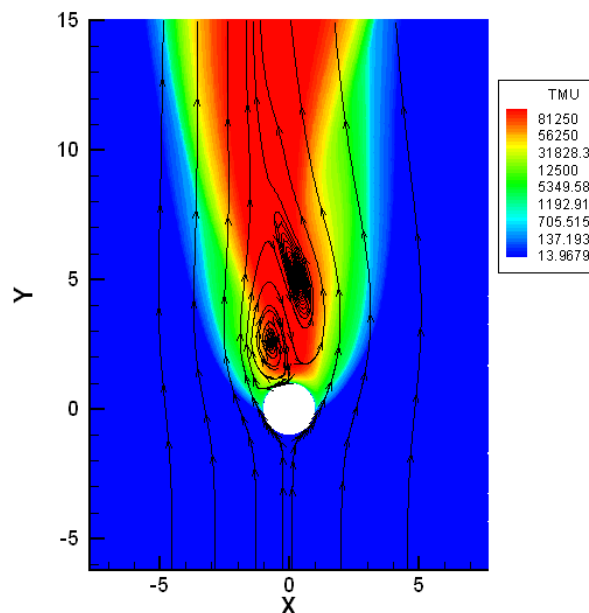


Figure 5.10 Turbulent viscosity contours

5.4 Airfoil

Extensive literature survey to obtain experimental data for this application was done and significant turbulent flow data to compare the accuracy of turbulence models were obtained.

Three distinct airfoil profiles of NACA0012, RAE2822 and NACA63-2-415 are tested with different flow conditions. A grid dependence test regarding the changes in the pressure coefficient distribution with refinement of grids in the boundary layer direction is presented. Visualization of laminar and turbulent velocity profiles with momentum thickness of the boundary layer is compared with the available data. Contours of turbulent kinetic energy, turbulent viscosity, production and destruction terms for k term are presented in Appendix E. Lift, drag and moment coefficients are compared with the experimental results for the NACA63-2-415 test case.

The results for NACA0012 and RAE2822 have taken from Maksymiuk and Pulliam's work [19]. The data for lift, drag, moment coefficients of NACA63-2-415 obtained from Abbott and Doenhoff [20].

5.4.1 NACA0012

First test case for the flow over airfoil posses the properties of 0.7 Mach number with 1.86 degrees of Angle of attach and a Reynolds number of 9.0×10^6

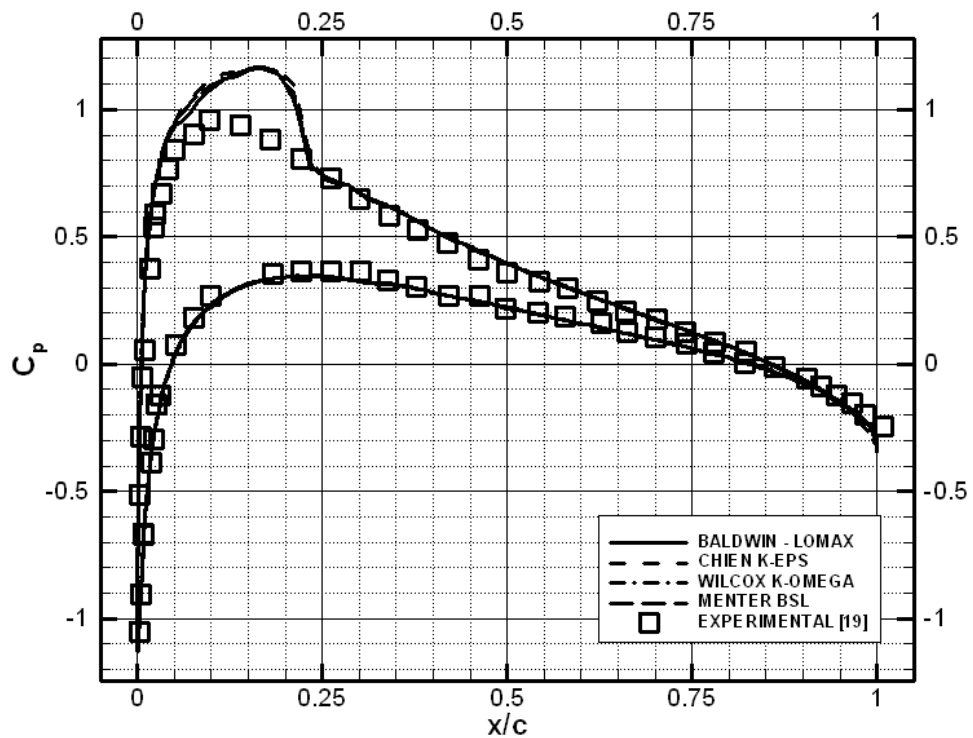


Figure 5.11 C_p distribution for different turbulence models

Computations with all of the turbulence models gave approximately the same results as shown in Figure 5.11. The jump in the leading edge suction side is investigated in detail. Grids used in computation have dimensions of 219×65 and initial grid node distance from the wall is 5×10^{-6} units.

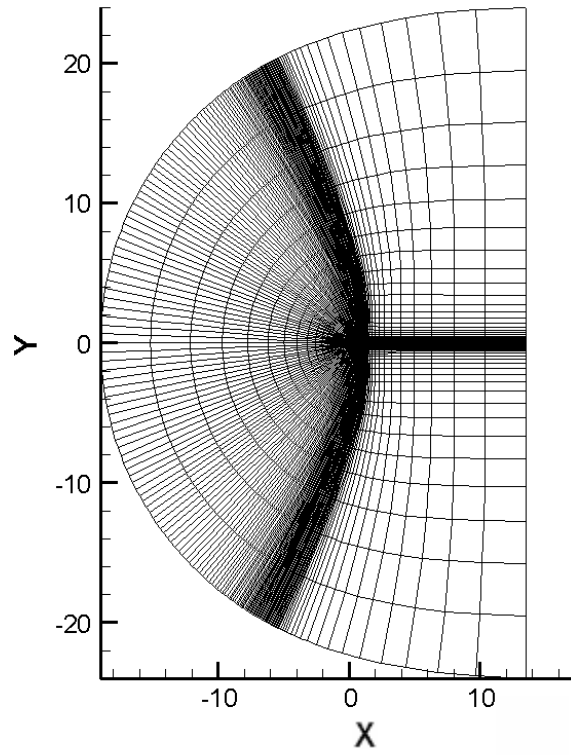


Figure 5.12 NACA0012, C-Grid overview

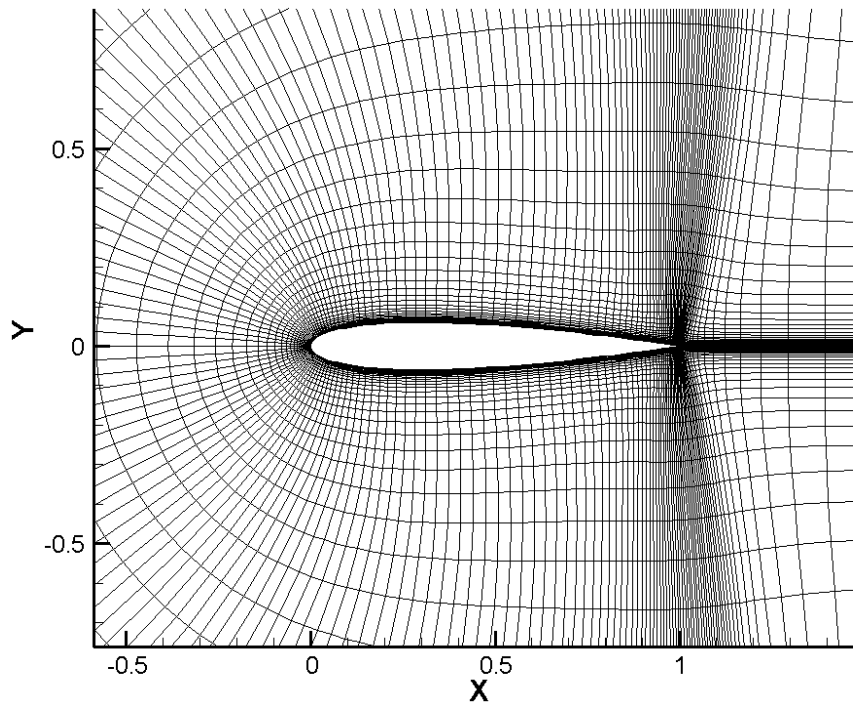


Figure 5.13 NACA0012, C-Grid closer view

The raise in coefficient of pressure could be a result of the decrease in the velocity in that region. The decrease in the velocity is because of excess total viscosity. Viscosity damps the velocity field so that the resultant velocity decreases. This kind of damping could be removed only if correct transition locations from laminar to turbulent can be given.

Adjustment of initial grid spacing from the wall has an important effect on the turbulent viscosity contours. The finer grid spacing results in a larger turbulent boundary layer and early transition. Several grids with different initial grid spacing are tried and the results are shown in Figure 5.14. As the grid is refined near the solid boundary, turbulent viscosity production is increased. This production of viscosity enables the accurate determination of the pressure distribution in turbulent regions at the trailing edge. However, the prediction of pressure distribution at the suction surface of the leading edge, where laminar boundary layer is expected, appears to be poor. The computation of coarsened grid near the solid boundary will result in a better pressure coefficient prediction of leading edge and a worse one in trailing edge. The y^+ values are given in Figure 5.15, which shows that primary rule for turbulence model calculations that the first grid point should have a y^+ value of nearly 1, is violated in the coarsened grid.

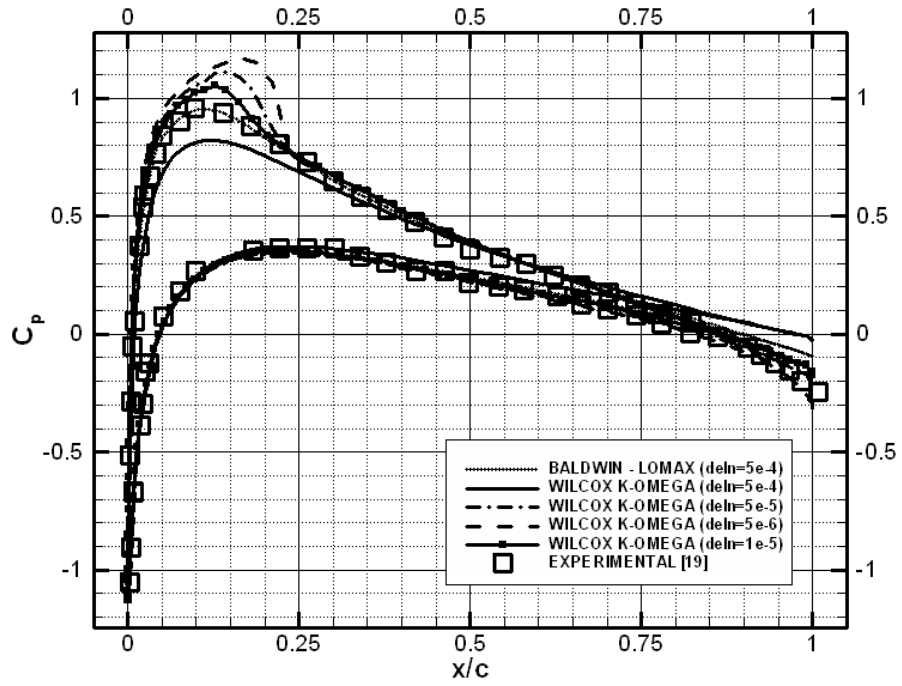


Figure 5.14 Grid dependence results of C_p distribution

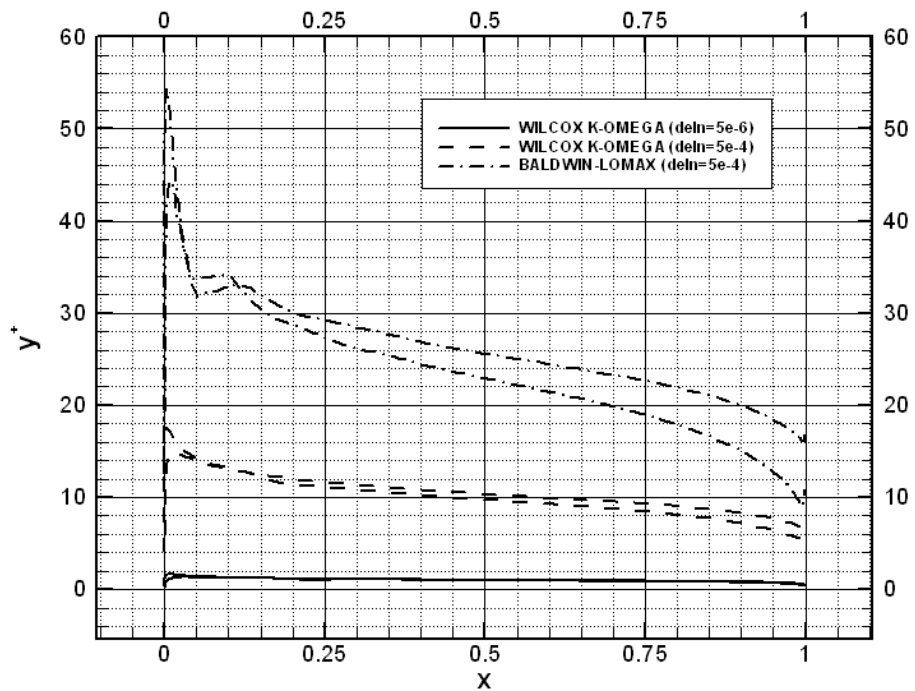


Figure 5.15 y^+ values for the first grid point from the wall

The results for C_l and C_d compared to the experimental values are tabulated against the experimental values in Table 5.1.

Table 5.1 C_l , C_d results for different turbulence models

	C_l	C_d
Experimental	0.254	0.0083
Baldwin-Lomax	0.303	0.0081
Chien k-eps	0.309	0.0052
Wilcox k-omega	0.305	0.0077
Wilcox k-omega (deln=1e-5)	0.309	0.0073
Menter BSL	0.300	0.0074

The best prediction of lift coefficient is obtained by *Menter BSL*. However the other results for lift coefficient are also in a good agreement with the experimental data. Drag coefficient prediction is obtained most accurately by *Baldwin-Lomax* model.

Second test case for the flow over the NACA0012 airfoil has 0.55 Mach number with 9.86 degrees of Angle of attach and a Reynolds number of 9.0×10^6

Figure 5.16 represents the comparison of pressure coefficient computations in which the best solution is obtained from $k-\omega$ based models of *Menter* and *Wilcox* where *Chien k- ϵ* is failed to predict the pressure coefficients accurately.

For the load computations, in Table 5.2, *Menter BSL* model takes the lead to detect the coefficients of lift and drag most accurately.

Table 5.2 C_l , C_d results for different turbulence models

	C_l	C_d
Experimental	0.988	0.0362
Baldwin-Lomax	1.0427	0.0613
Chien k-eps	1.047	0.0561
Wilcox k-omega	1.0459	0.0616
Menter BSL	0.961	0.0580

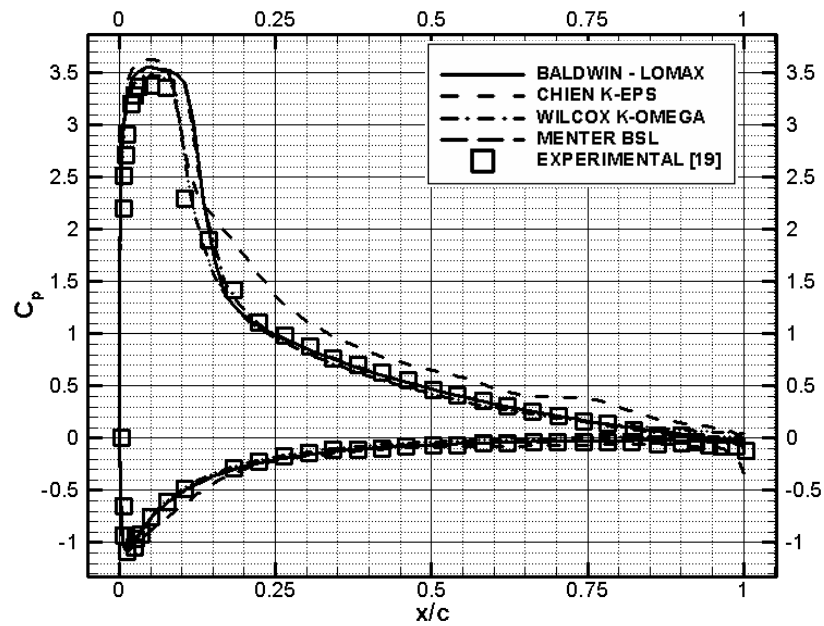


Figure 5.16 C_p distribution for different turbulence models

5.4.2 RAE2822

Transonic airfoil case of RAE2822 is carried out to compare the pressure coefficients. Velocity distributions in laminar and turbulent regions are another comparison data for turbulence models.

RAE2822 test case is carried out with the properties of 0.725 Mach number with 2.92 degrees of Angle of attach and a Reynolds number of 9.0×10^6

Table 5.3 C_l , C_d results for different turbulence models

	C_l	C_d
Experimental	0.747	0.0123
Baldwin-Lomax	0.822	0.0163
Chien k-eps	0.849	
Wilcox k-omega	0.841	0.0168
Menter BSL	0.814	0.0155
Abid k-eps	0.790	0.0151

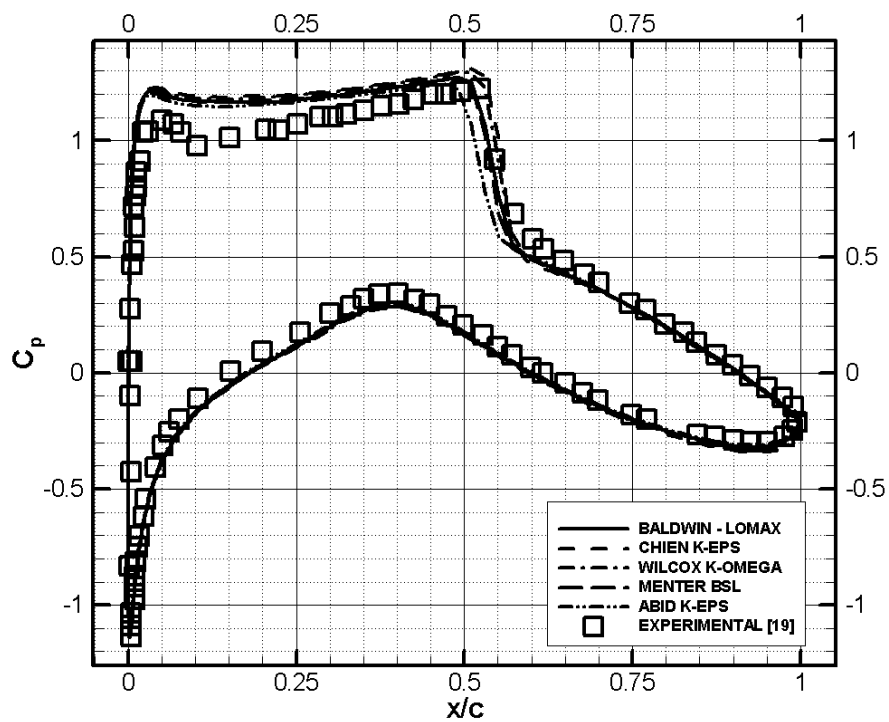


Figure 5.17 C_p distribution for different turbulence models

From Figure 5.17, the shock location is accurately determined by *Wilcox k- ω* since the peak point is captured and a steep decrease in pressure is detected in a good agreement with the experimental data. The over estimation of pressure coefficient in the leading edge regions of suction side is due to the excess increase in the turbulent viscosity. This problem could be solved by inputting the transition location explicitly or having a mechanism of obtaining transition location accurately.

The laminar and turbulent velocity profiles are compared with experimental data in Figures 5.18 and 5.19. For turbulent velocity profile *Abid k- ϵ* is the turbulence model that has good results whereas for laminar one, *Baldwin-Lomax* appeared to be successful.

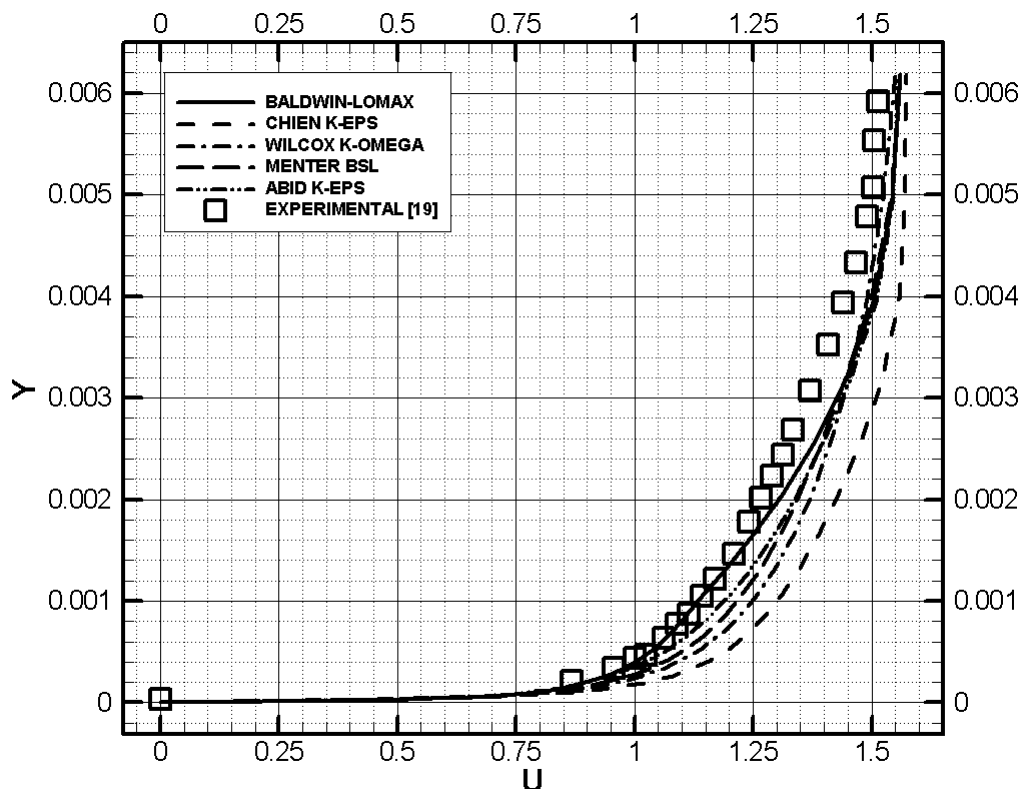


Figure 5.18 Laminar velocity profile at $x/c=0.319$

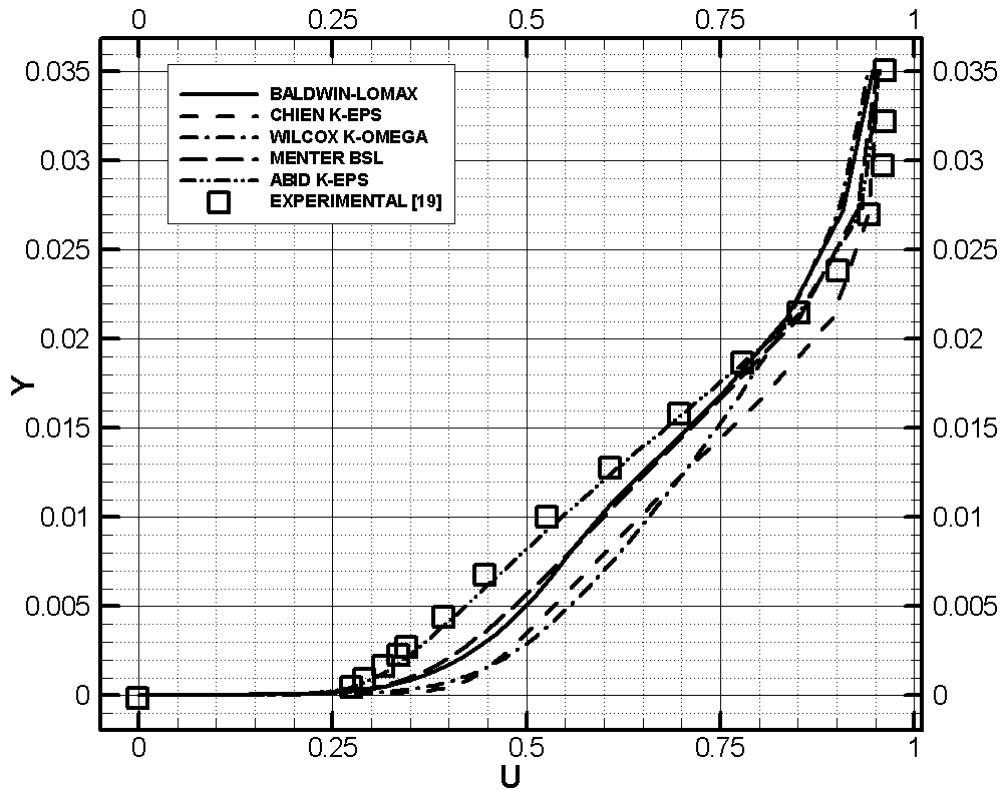


Figure 5.19 Turbulent velocity profile at $x/c=0.95$

The best friction coefficient detection is achieved by *Chien k- ϵ* turbulence model before the shock region while the worst prediction is obtained by the *Baldwin-Lomax* model. The sudden drop of friction coefficient due to shock presence is seen in Figure 5.20 near the x/c location of 0.5 on the suction side.

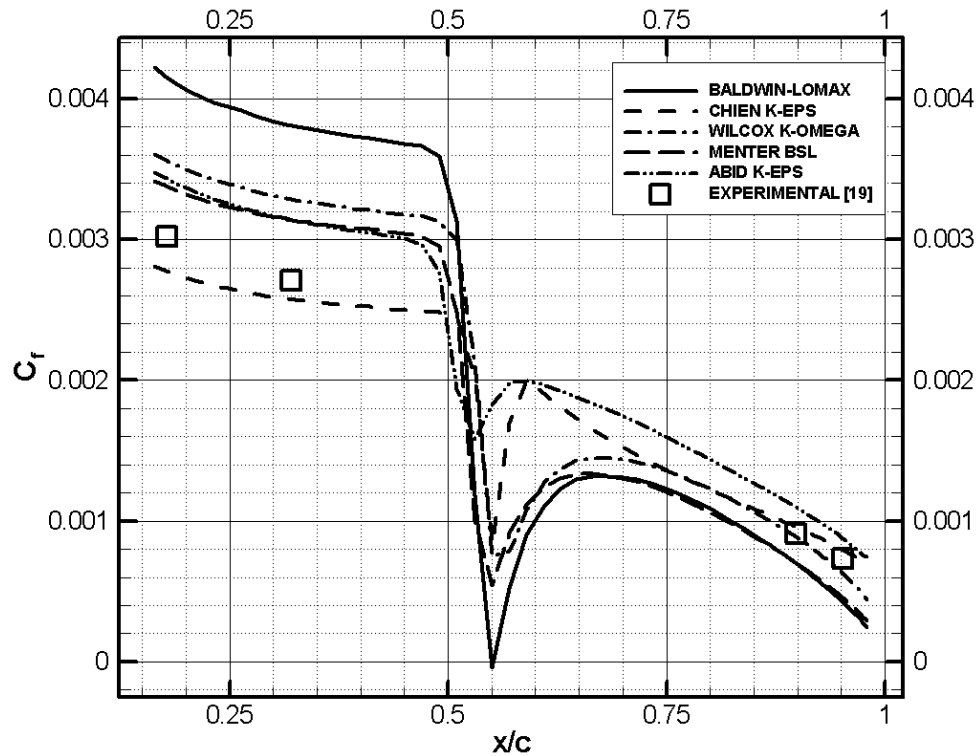


Figure 5.20 Friction Coefficient

Outputs of turbulent viscosity and dimensionless turbulent kinetic energy are observed in Figures 5.21 and 5.22. *Wilcox k- ω* appeared to produce highest turbulent viscosity. The other models except *Baldwin-Lomax* behave in a similar manner near to the peak points of turbulent viscosity values which are obtained at y^+ having a value of 2×10^3 .

An interesting discussion could be the difference between the turbulent viscosity values of *Menter BSL* and *Wilcox k- ω* models. Actually, they both involve the same equations with the same constants and correlations near the boundary. But due to the transition from *k- ω* to standard *k- ϵ* model, the peak values of the turbulent viscosities differ from non-dimensional value of 1300 to 1850. Figure 5.25 represents the transition of the two models in *Menter BSL*. It is important to note that transition occurs close to a y^+ value where highest turbulent viscosity is achieved.

Baldwin-Lomax algebraic turbulence model produces negative turbulent viscosity values that have no physical meaning.

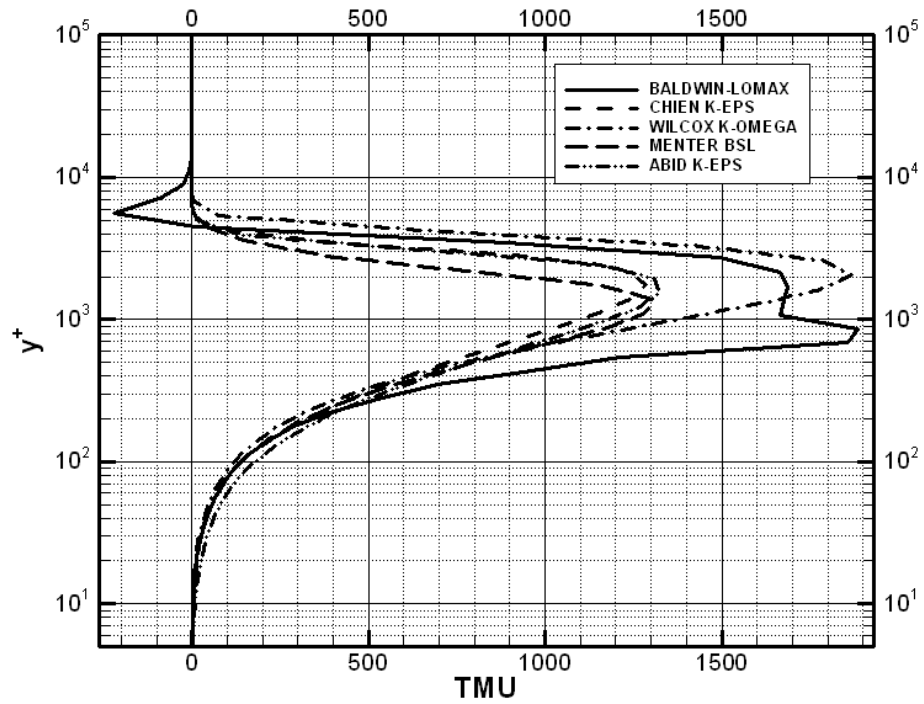


Figure 5.21 Turbulent Viscosity distribution on $x/c=0.9$

For the non-dimensional turbulent kinetic energy values, the peak points are resolved near regions of highest turbulent viscosity where y^+ values are close to 1×10^3 . *Chien k- ϵ* , *Abid k- ϵ* , *Wilcox k- ω* and *Menter BSL* models could be given in increasing order of highest k^+ values.

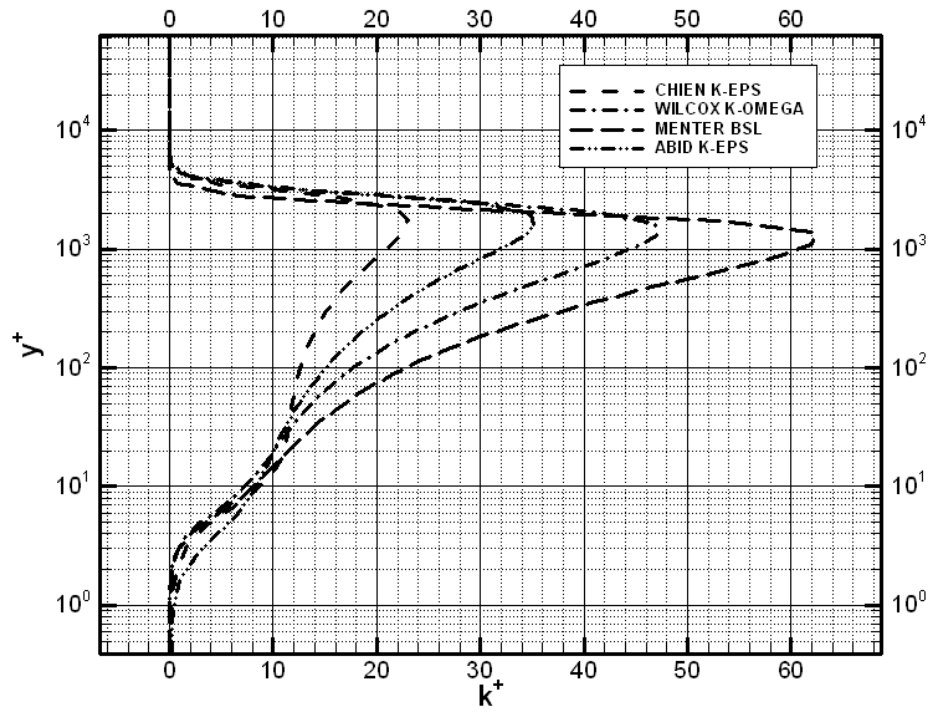


Figure 5.22 k^+ distribution on $x/c=0.9$

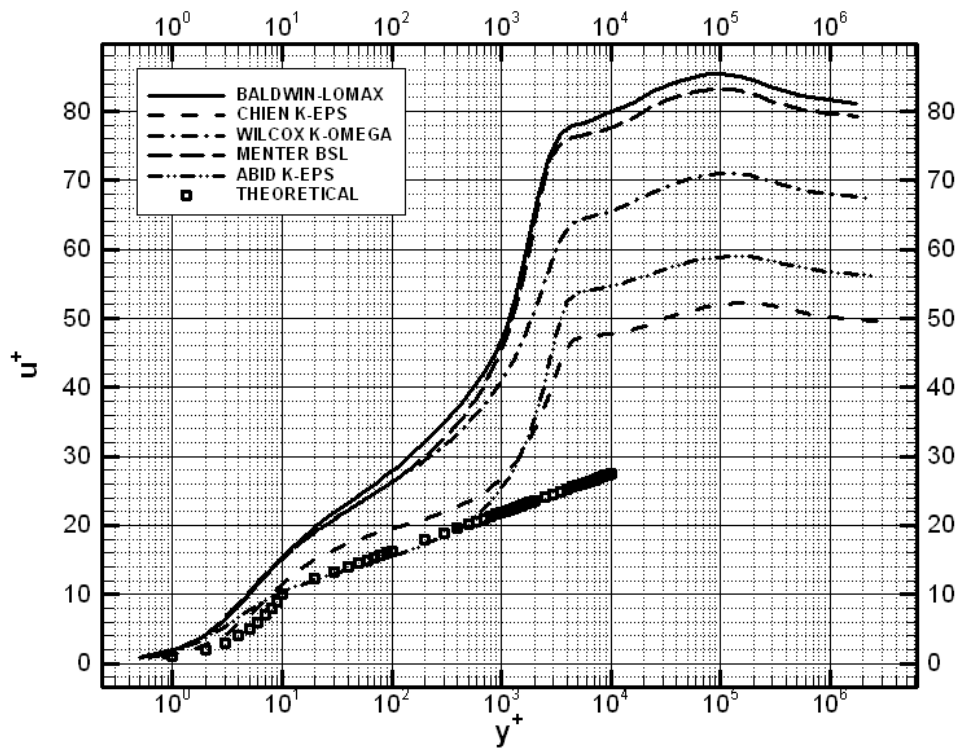


Figure 5.23 Turbulent Velocity Profiles on $x/c=0.9$

Turbulent velocity profiles given in Figure 5.23, presents the defect of the log-law layer due to the adverse pressure gradient effects occurring in the suction side of trailing edge. *Abid k-ε* shows a good agreement with the theoretical descriptions of viscous sub-layer and log-law region.

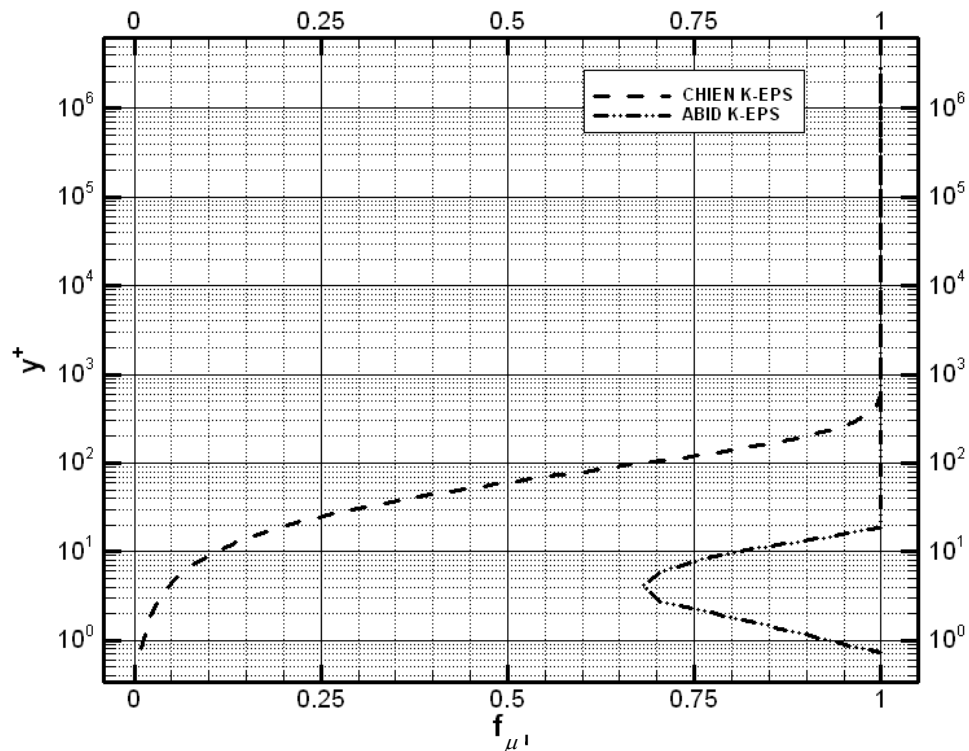


Figure 5.24 f_{μ} values for *Chien* and *Abid k-ε* on $x/c=0.9$

Due to the different boundary conditions, f_{μ} term appears to be in different characteristics near the wall region in Figure 5.24. Since ϵ boundary condition of Chien is zero, it would cause a high increase in turbulent viscosity, then logarithmic behavior could be achieved by manipulating turbulent viscosity with f_{μ} parameter.

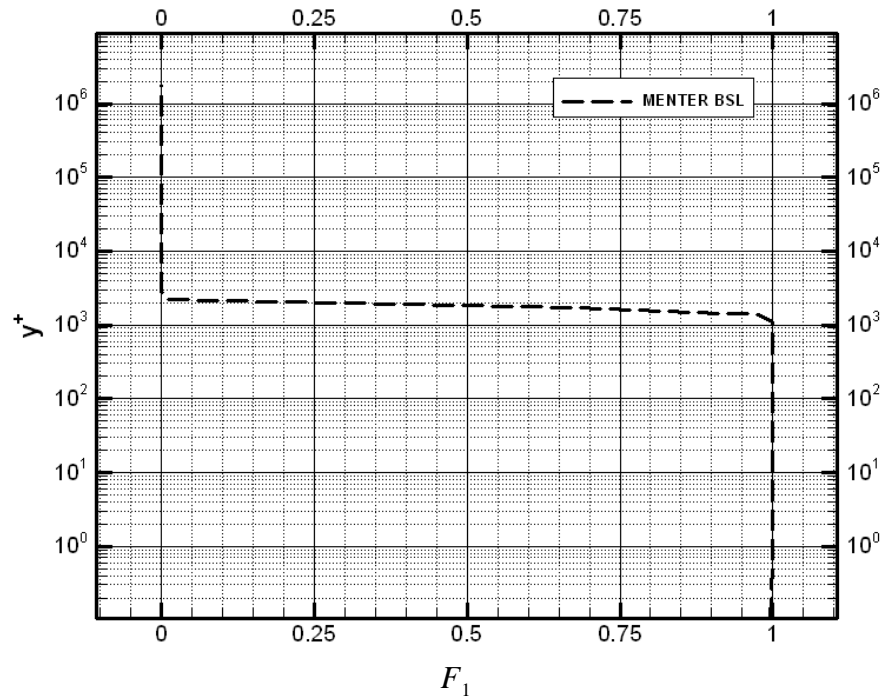


Figure 5.25 F_1 value transition for *Menter BSL* on $x/c=0.9$

Figure 5.25 shows the parameter F_1 , which manipulates the transition from $k-\omega$ to $k-\varepsilon$. The transition occurs at a location where y^+ is 2000. At the outer regions, parameter F_1 is equal to zero which stands for the standard $k-\varepsilon$ model whereas $k-\omega$ model is activated in regions close to the wall.

Contours of pressure, turbulent viscosity and pressure, destruction terms of turbulent kinetic energy for all turbulence models are visualized in the figures in Appendix E.

5.4.3 NACA63-2-415

The purpose of this test case is mainly the detection of the location of the stall point, prediction of the maximum C_l values and obtaining the lift, drag and moment curves. Computations are done for -16 to 20 degrees with angle of attack increments of 2 degrees. Flow conditions of Mach number of 0.3 and Reynolds number 9×10^6 is used in computations.

$M=0.3, Re=9e6, AoA=-16..20,+2$

The C_l values corresponding to different angle of attacks are plotted in Figure 5.26. Several computations are done by varying grid spacings in a direction normal to solid boundary.

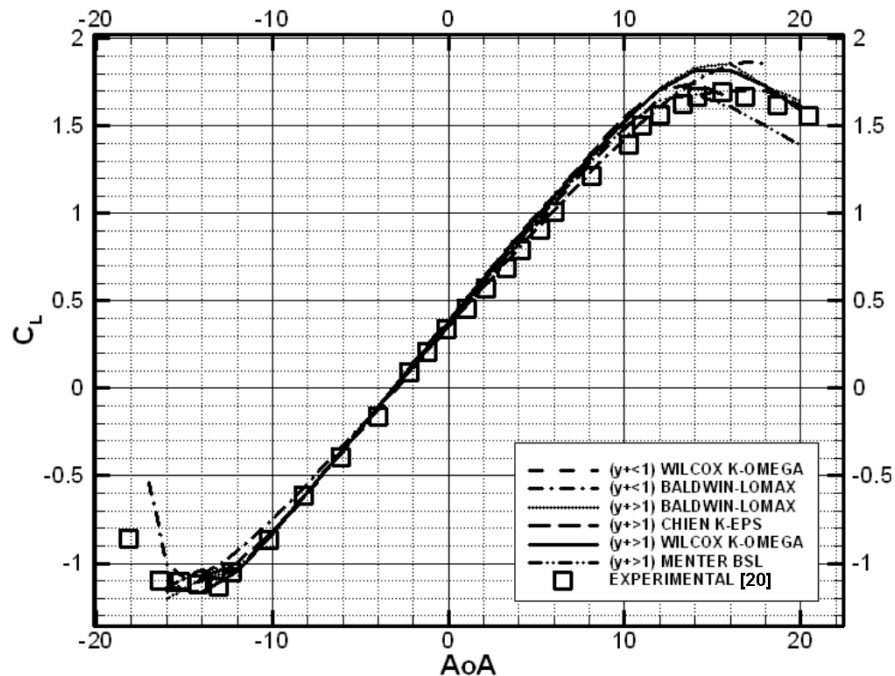


Figure 5.26 C_l versus AoA graph

The linear behavior of C_l versus angle of attack is obtained in every turbulence model. However, stall points are worth investigating in detail since the grid refinement in direction normal to the boundary layer changes the prediction success in a significant sense, as shown in Figure 5.27. In Figure 5.28, the stall point is detected by *Wilcox k- ω* model (with initial grid distance of approximately 2×10^{-6} which corresponds to y^+ values not more than 1) more accurately than the other models. In Figure 5.28, for the drag prediction refined grid of *Wilcox k- ω* gives good predictions of C_l - C_d data. Predictions of C_m appeared to be poor as can be seen from Figure 5.29.

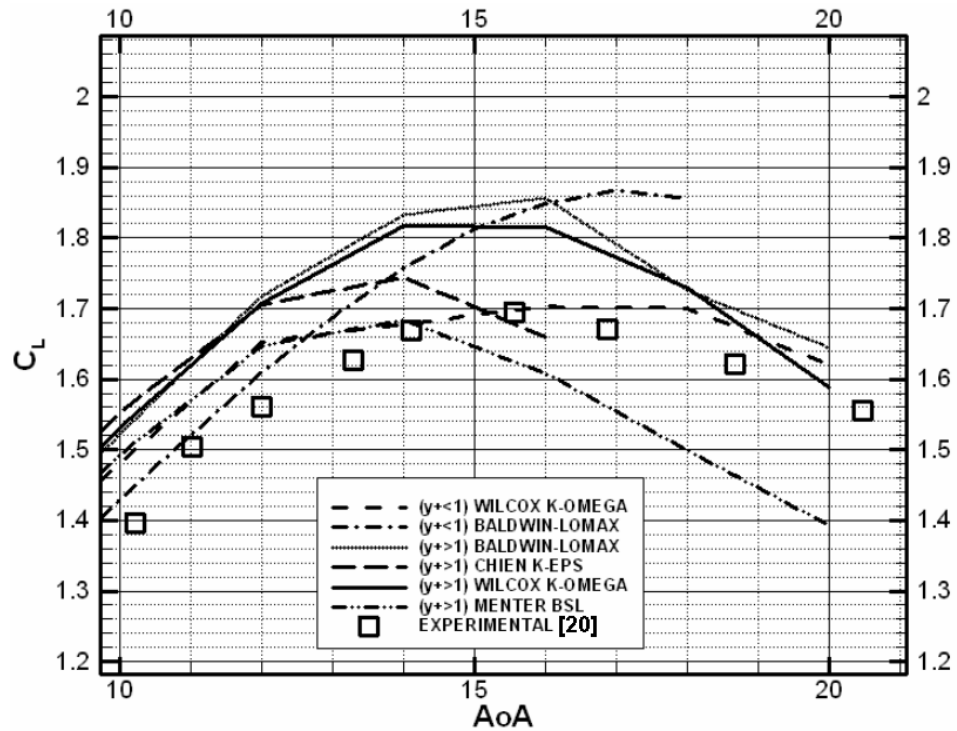


Figure 5.27 C_l versus AoA , Stall point detailed

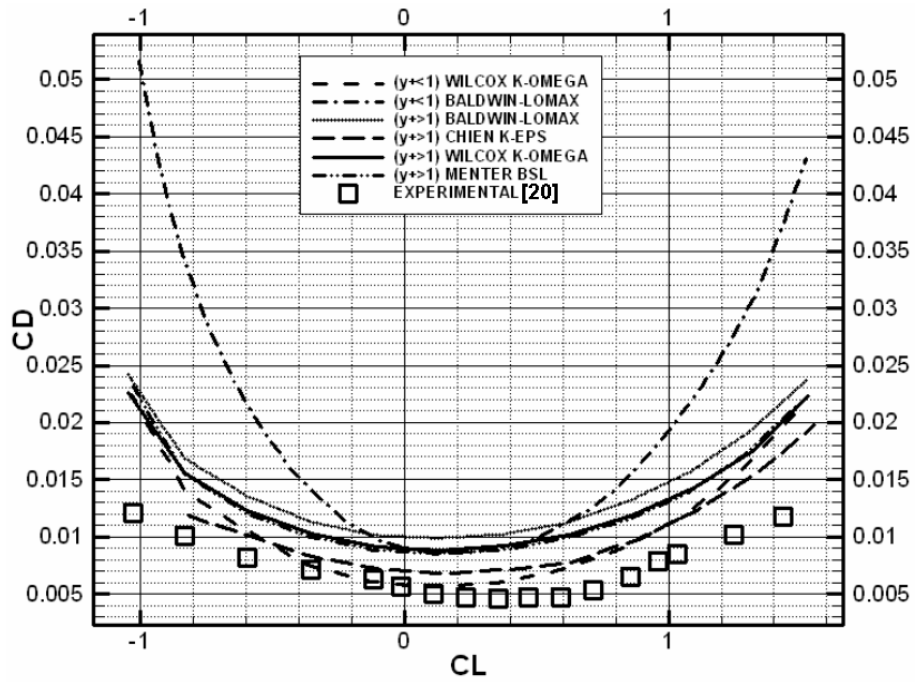


Figure 5.28 C_d versus C_l graph

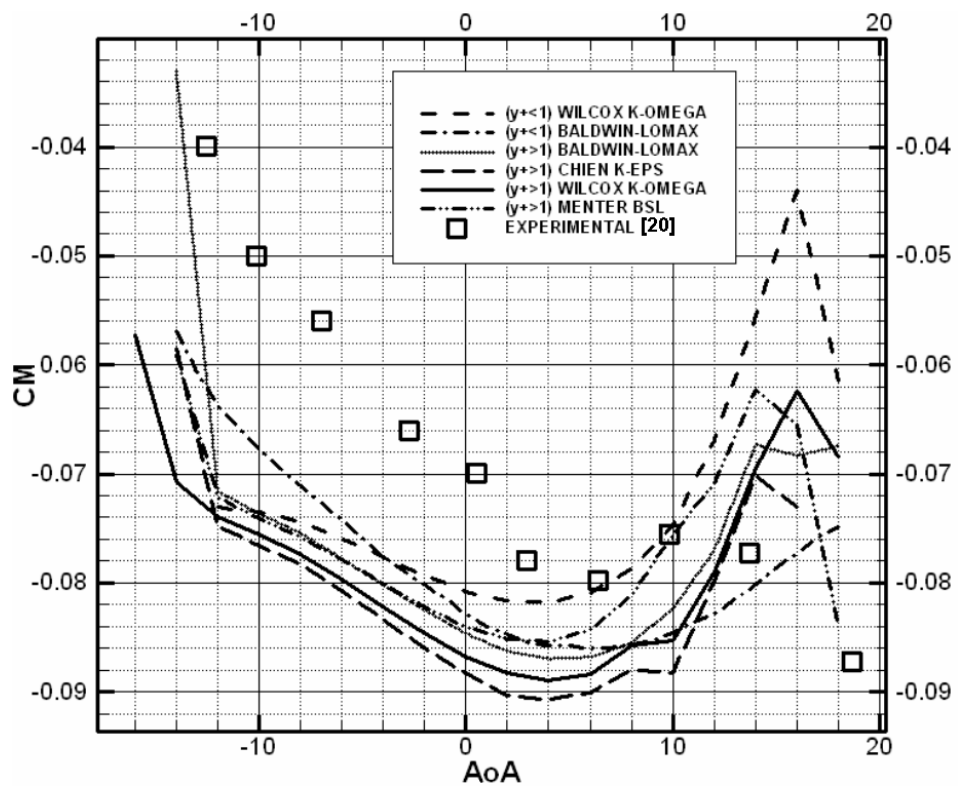


Figure 5.29 C_m versus AoA graph

5.5 Wing

5.5.1 ONERA M6 Wing

The flow over ONERA M6 Wing with a Mach number of 0.8395 and angle of attack of 3.06 degrees is tested. Reynolds number of 1.172×10^7 is used. C-O Grid type mesh is used with dimensions of 161 nodes in chordwise, 36 nodes in spanwise and 50 nodes to the outer boundary is used. First grid point is taken as 10^{-5} by considering the grid refinement test in NACA0012 case represented in Figure 5.14. A λ (lambda) shock formation is observed along the wing. The contours of pressure and turbulent viscosity are visualized in the Figures 5.30, 5.31 and 5.32.

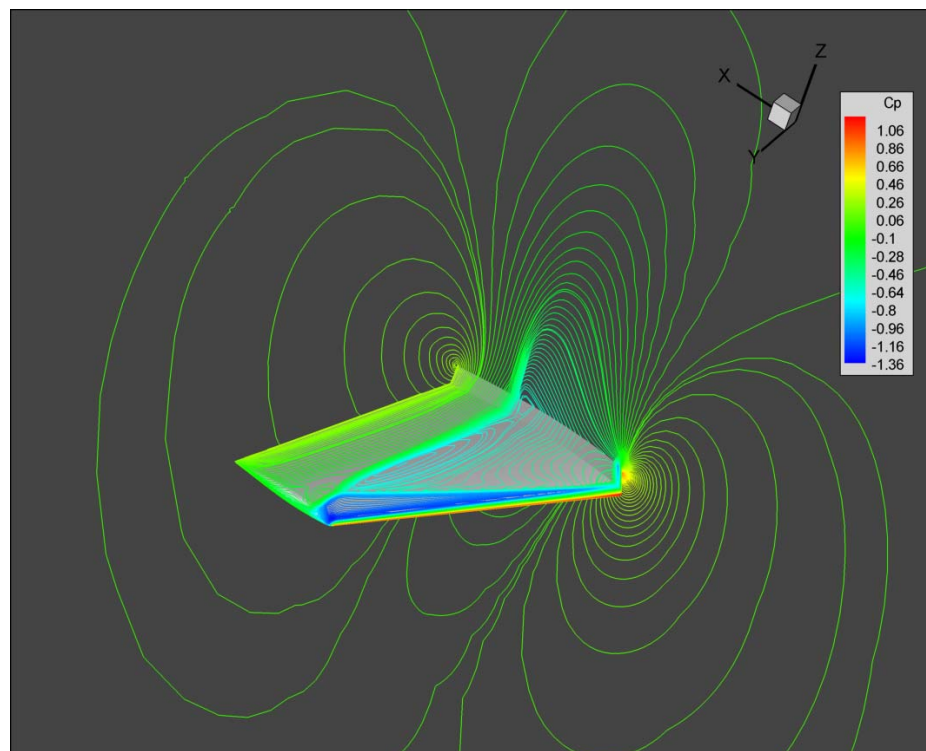


Figure 5.30 C_p contours

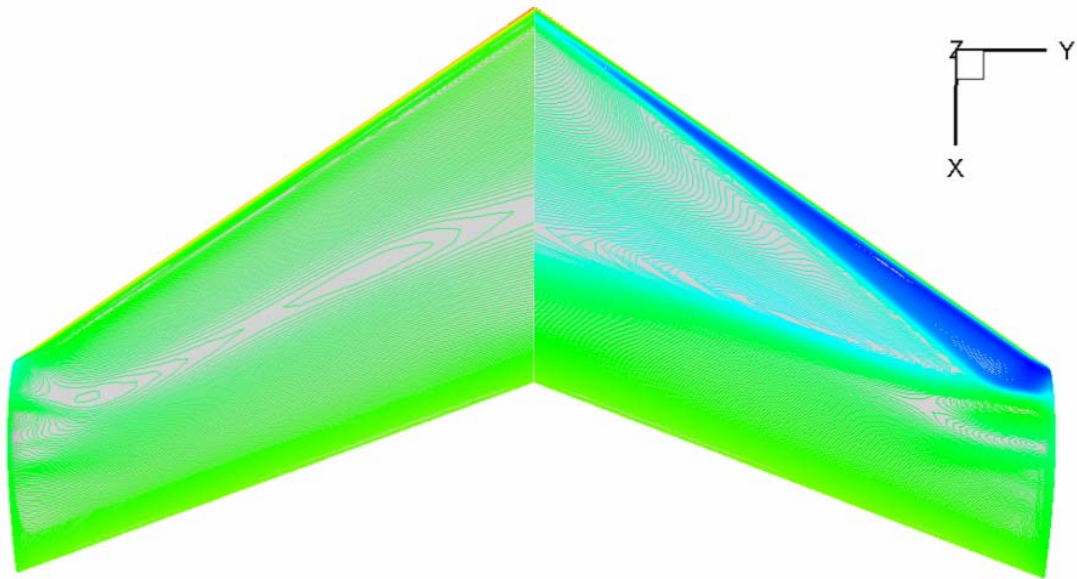


Figure 5.31 C_p contours Left – Lower side, Right – Upper side

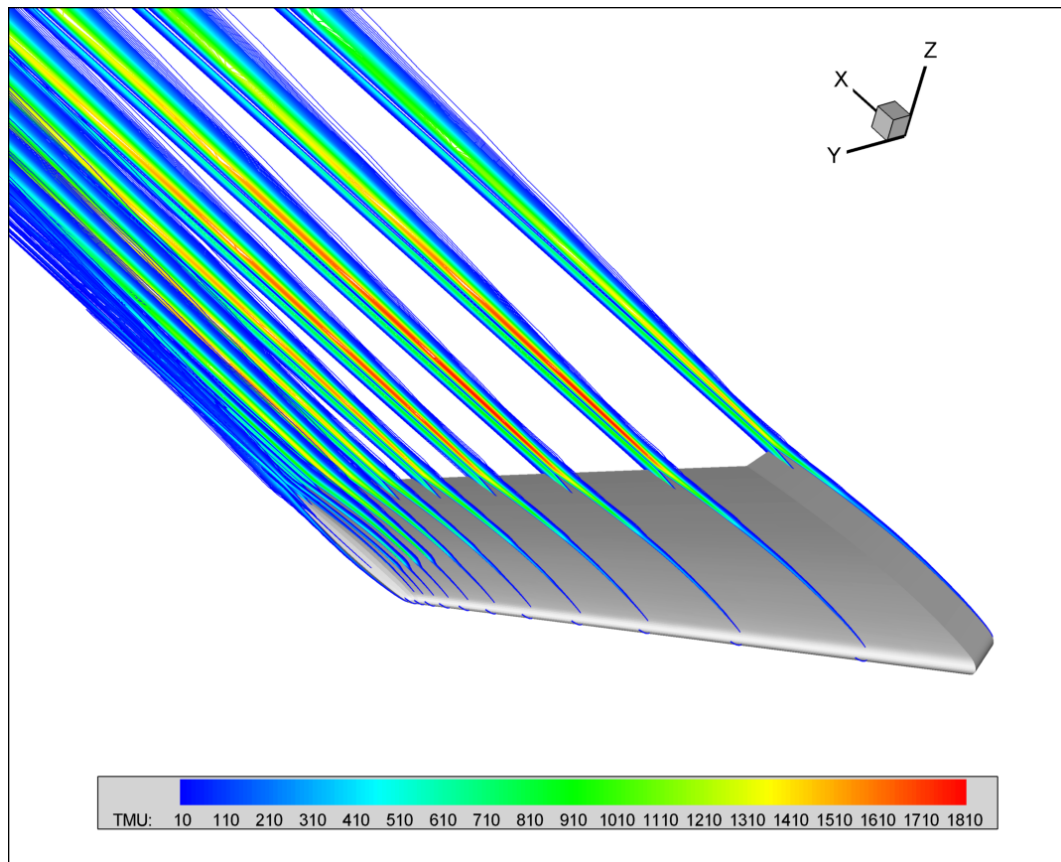


Figure 5.32 ONERA M6 WING, Turbulent Viscosity Contours

Johnson-King and Baldwin-Lomax results are provided from Kaynak, Çete and Şener's work [25]. Figures from Figure 5.33 to Figure 5.37 represent the coefficient of pressure distributions around the airfoil on several spanwise locations.

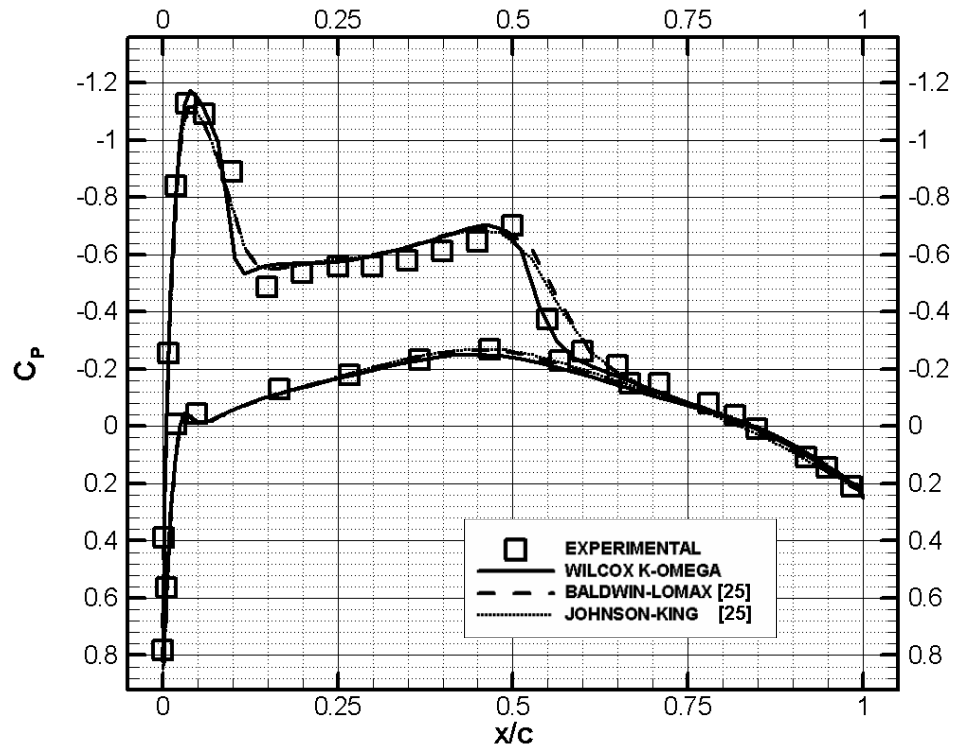


Figure 5.33 ONERA M6 WING, C_p distribution, $y/b=0.44$

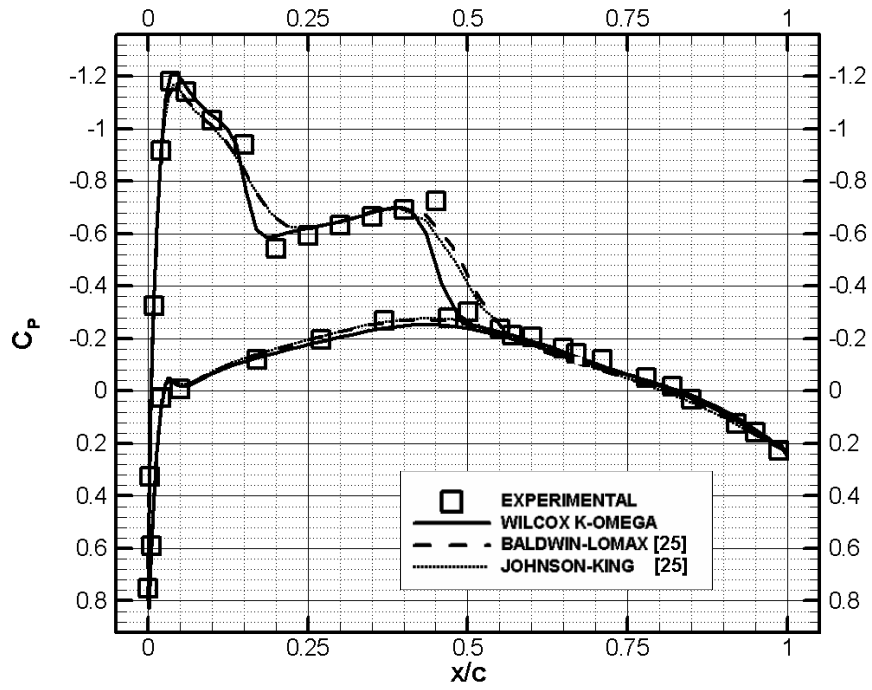


Figure 5.34 ONERA M6 WING, C_p distribution, $y/b=0.65$

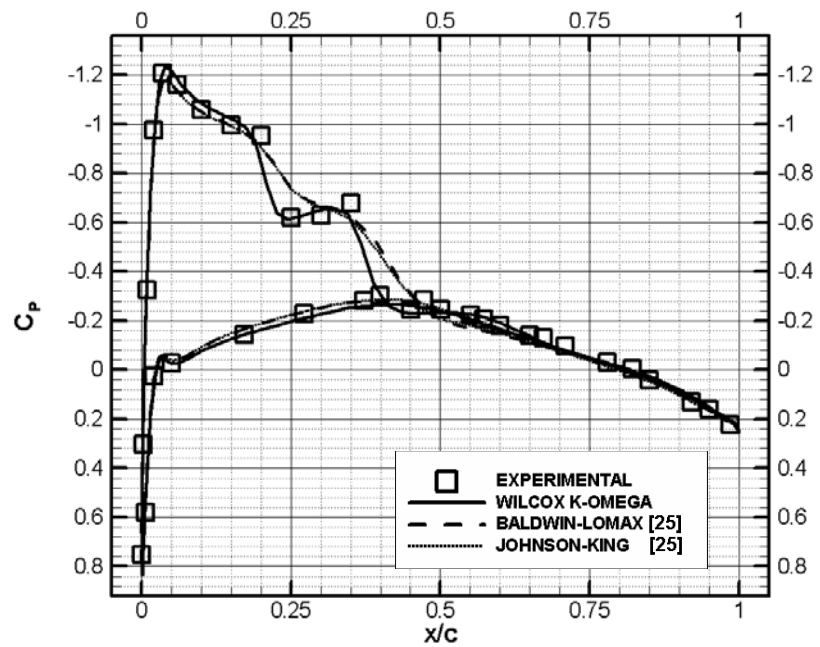


Figure 5.35 ONERA M6 WING, C_p distribution, $y/b=0.80$

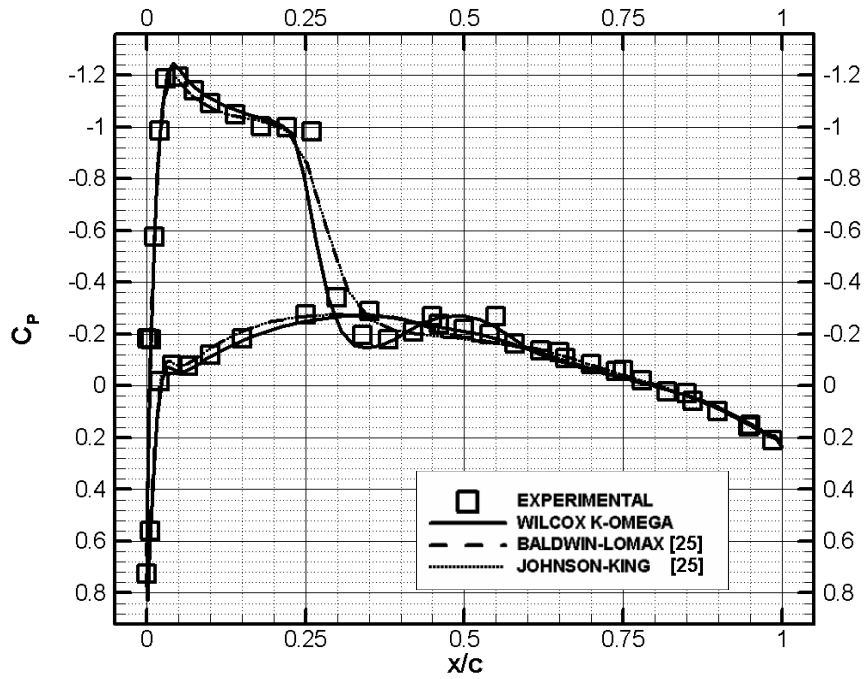


Figure 5.36 ONERA M6 WING, C_p distribution, $y/b=0.90$

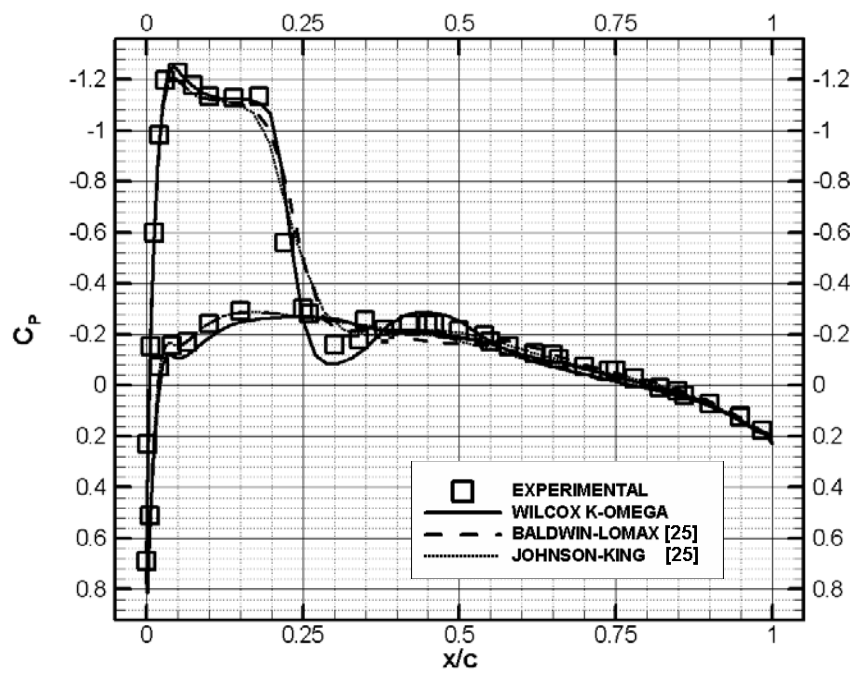


Figure 5.37 ONERA M6 WING, C_p distribution, $y/b=0.95$

CHAPTER 6

CONCLUSION

In this study, several turbulence models based on $k-\omega$ and $k-\varepsilon$ are implemented into a Navier-Stokes solver. During implementation stages, to adopt the significant step is to understand the base solver in detail and adapting the turbulence models into it. It was very difficult to implement a module that works independent of the solver. On the other hand, the module should take some values of flow and grid and deliver turbulent viscosity values for solution nodes.

For external flows over airfoils and wings, implementation of $k-\omega$ based models are appeared to be easier than implementation of $k-\varepsilon$ based models. As described in Chapter 4, $k-\varepsilon$ models have more correlations that are included in computations of turbulent viscosity than $k-\omega$ models. These correlations require the computations of y^+ , Re_k and Re_t values, which require the information of wall shear stress and distance to wall properties of solution nodes. Computations of these properties in absence of any wall surface, appears to be meaningless. No such correlations appear in the formulation of $k-\omega$ models which makes the implementation of these models much simpler. However boundary condition implementation for ω is a challenging subject on which many studies had been done and due to the simplicity in implementing the boundary condition for ε , $k-\varepsilon$ models could be preferred.

Analysis stages involve the interpretation of load values for different flow conditions on different airfoils. One should select a proper airfoil profile to construct a wing, which would be used for specific purposes. The load outputs obtained from computations will be a first indication of design decisions that are the predictions of C_p distributions, C_l , C_d and C_m values. The experience gained from the computations of flow over an airfoil shows that for resolving accurate distributions of pressure of coefficient, one should avoid a finer grid in the direction normal to the wall boundary, since excess turbulent viscosity formation is obtained. Other solution could be implementing of transition detection or introducing transition locations as an input, explicitly to the solver. Since the present work does not involve the transition detection, it is important to recommend a first grid point distance from the wall in the orders of 10^{-5} . On the other hand, for calculations of the load parameters of lift, drag and moment coefficients, this wall distance should be smaller since Figure 5.27 shows better results of predictions in smaller y^+ values for the first grid point. This value is generally obtained with an initial grid distance of 10^{-6} . The y^+ value of the first grid point is around 1 in this case which gives better predictions of load parameters especially in the stall conditions. For these computations, a model of blended $k-\omega$ and $k-\varepsilon$ model, *Menter BSL* model could be recommended.

For 3D applications, only *Wilcox $k-\omega$* model is investigated. In the presence of the results for the outputs mentioned above, the next model to be implemented appears as the *Menter BSL* model. In the recent years, *Spalart-Almaras* one-equation turbulence model of one-equation kind has gained success in external aerodynamic applications. The implementation of this model could also be another topic for future work.

On the other hand, solving one or two additional partial differential equations addition to the Navier-Stokes equations, for a high number of nodes

comparing with 2D airfoil grids could sometimes be more costly than solving algebraic equations. However, due to capability of solving a domain without considering any algebraic correlations involving wall distance or inner and outer layers, interpreting partial differential equations appear as a better solution in parallel and multi-block computing.

On a Pentium P4, 3.06 GHz. machine, the computation time for the use of $k-\omega$ models in a case of flow passing over NACA0012 airfoil with Mach number of 0.7 and angle of attack 1.79 calculated as nearly 600 seconds for a C type grid of 139x65 nodes, however this computation time rose up to twice itself for $k-\epsilon$ models since lower time step values should be used in order to get convergence. It would be appropriate to say that $k-\omega$ models appear to be more robust than $k-\epsilon$ models.

The results of the current completed project are being used in TAI for analysis and validation purposes. Further studies on *Wilcox* $k-\omega$ model will be handled in the following developments. Tunings and certain corrections will be implemented to have a better turbulence model that accurate transition detection and compressibility correction would be applied.

Further studies in wing computations and implementation of turbulence models into multi-block and chimera versions of the base solver are the main targets for future.

REFERENCES

- [1] University of Illinois at Urbana-Champaign, *Lecture Slides of Computational Astrophysics and Cosmology*, www.astro.uiuc.edu/classes/archive/astr496/s03_cac/graphics_0207.pdf, last access on; 08.07.2005
- [2] University of Kentucky, Advanced CFD Group, *Lecture Notes*, www.engr.uky.edu/~acfd/lctr-notes634.pdf, last access on; 08.07.2005
- [3] Karman, T. von. *Some remarks on the statistical theory of turbulence*, *Proc. 5th Int. Congr. Appl. Mech.*, Cambridge, MA, 347, 1938.
- [4] Hinze, J. O., *Turbulence*, McGraw-Hill, New York, 1959.
- [5] Chapman, G. T., Tobak, M., *Observations, Theoretical Ideas, and Modeling of Turbulent Flows-Past, Present and Future*, in *Theoretical Approaches to Turbulence*, Dwoyer et al. (eds), Springer-Verlag, New York, page 19-49, 1985.
- [6] Wilcox, D.C., *Turbulence Modeling for CFD*, Second edition, DCW Industries, Inc., 1998
- [7] von Karman Institute for Fluid Dynamics, *Lecture Series; Introduction to the Modeling of Turbulence*, March 17-21 1997
- [8] Krist, S.L., Biedron, R.T., Rumsey, C.L. 1998, *CFL3D User's Manual (Version 5.0), Turbulence Model Equations*, NASA Technical Memorandum NASA/TM-1998-208444, 271-306.

- [9] Pulliam, T.H., 1984, *Euler and Thin Layer Navier-Stokes Codes: ARC2D, ARC3D*, Notes for Computational Fluid Dynamics User's Workshop NASA Ames Research Center 1-8.
- [10] Patel, V.C., Rodi, W., Scheuerer G., 1984, *Turbulence Models for Near-Wall and Low Reynolds Number Flows: A Review*, AIAA Journal vol. 23, No: 9, pp 1308-1319.
- [11] Menter, F.R., (1993). AIAA-93-2906, *Zonal Two Equation $k-\omega$ Turbulence Models for Aerodynamic Flows*, AIAA 24th Fluid Dynamics Conference, July 6-9, 1993 / Orlando, Florida.
- [12] Beam, R.M., Warming, R.F, 1978, *An Implicit Factored Scheme for the Compressible Navier-Stokes Equations*, AIAA Journal, Vol. 16, No. 4, 1978, page 393-402.
- [13] Spalart, P.R., Allmaras S.R. 1992, *A One-Equation Turbulence Model for Aerodynamic Flows*, AIAA Journal AIAA-92-0439.
- [14] Pulliam, T.H., 1985, *Artificial Dissipation Models for the Euler Equations*, NASA Ames Research Center AIAA-85-0438.
- [15] Hoffman, K.A, Chaing, S.T., *Computational Fluid Dynamics, Volume 1*, Engineering Education System, August 2000.
- [16] Menter, F.R., 1993, *On the Influence of Freestream Values on Predictions with the $k-\omega$ Turbulence Model*, Eloret Institute.
- [17] Coles, D., 1978., *A model for Flow in the Viscous Sublayer*, Proceedings of the Workshop on Coherent Structure of Turbulent Boundary Layers, Leigh University, Bethlehem, Pa.
- [18] Schlichting, H., Kestin, J., 1979, *Boundary Layer Theory*, Seventh Edition, McGraw-Hill Book Company.

- [19] Maksymiuk, C.M., Pulliam, T.H., (1987). AIAA-87-0415, *Viscous Transonic Workshop Results Using ARC2D*, AIAA 25th Aerospace Sciences Meeting, January 12-15, 1987 / Reno, Nevada.
- [20] Abbott, I.H., Doenhoff, A.E. von, *Theory of Wing Sections*, Dover Books on Physics.
- [21] Baldwin, B. S., Lomax, H., *Thin Layer Approximation And Algebraic Model For Separated Turbulent Flows*, AIAA paper 78-257 AIAA 16th Aerospace Sciences Meeting, Huntsville, Alabama, 1978.
- [22] Cebeci, T., Smith, A. M. O., *Analysis of Turbulent Boundary Layers*, Academic Press, New York, 1974.
- [23] Baldwin, B. S., Barth, T. J., *A One Equation Turbulence Transport Model for High Reynolds Number Wall-Bounded Flows*, NASA-TM-102847, August 1990.
- [24] Obayashi, S., Fujii, K., *Practical Applications of New LU-ADI Scheme for Three-Dimensional Navier-Stokes Computation of Transonic Viscous Flows*, AIAA-86-0513, Reno, Nevada.
- [25] Kaynak, Ü., Çete, A.R., Yılmaz, Ş, *Accuracy Improvements for Transonic Wing Flows Using a Non-equilibrium Algebraic Turbulence Model*, 1998 World Aviation Conference, September 28-30, 1998, Anaheim, CA, Paper no:985573

APPENDIX A

Non-Dimensionalization steps for turbulence model equations

k equation for Wilcox *k*- ω and Menter BSL turbulence models

Production Term

$$\tilde{P}_k = \tilde{\mu}_T \cdot \tilde{\Omega}^2 = \mu_T \cdot \Omega^2 \cdot \left[\frac{\tilde{\mu}_\infty \cdot \tilde{a}_\infty^2}{\tilde{L}_R^2} \right] \quad (\text{A.1})$$

Destruction Term

$$\tilde{D}_k = \beta' \cdot \tilde{\rho} \cdot \tilde{k} \cdot \tilde{\omega} = \beta' \cdot \rho \cdot k \cdot \omega \cdot \left[\frac{\tilde{\rho}_\infty^2 \cdot \tilde{a}_\infty^4}{\tilde{\mu}_\infty} \right] \quad (\text{A.2})$$

Diffusion Term

$$\begin{aligned} \frac{\partial}{\partial \tilde{x}} \cdot \left(\left(\tilde{\mu} + \frac{\tilde{\mu}_T}{\sigma_k} \right) \cdot \frac{\partial \tilde{k}}{\partial \tilde{x}} \right) + \frac{\partial}{\partial \tilde{y}} \cdot \left(\left(\tilde{\mu} + \frac{\tilde{\mu}_T}{\sigma_k} \right) \cdot \frac{\partial \tilde{k}}{\partial \tilde{y}} \right) = \\ \left(\frac{\partial}{\partial x} \cdot \left(\left(\mu + \frac{\mu_T}{\sigma_k} \right) \cdot \frac{\partial k}{\partial x} \right) + \frac{\partial}{\partial y} \cdot \left(\left(\mu + \frac{\mu_T}{\sigma_k} \right) \cdot \frac{\partial k}{\partial y} \right) \right) \cdot \left[\frac{\tilde{\mu}_\infty \cdot \tilde{a}_\infty^2}{\tilde{L}_R^2} \right] \end{aligned} \quad (\text{A.3})$$

Total Derivative Term

$$\begin{aligned} \frac{\partial(\tilde{\rho} \cdot \tilde{k})}{\partial \tilde{t}} + \frac{\partial(\tilde{\rho} \cdot \tilde{u} \cdot \tilde{k})}{\partial \tilde{x}} + \frac{\partial(\tilde{\rho} \cdot \tilde{v} \cdot \tilde{k})}{\partial \tilde{y}} = \\ \left(\frac{\partial(\rho \cdot k)}{\partial t} + \frac{\partial(\rho \cdot u \cdot k)}{\partial x} + \frac{\partial(\rho \cdot v \cdot k)}{\partial y} \right) \cdot \left[\frac{\tilde{\rho}_\infty \cdot \tilde{a}_\infty^3}{\tilde{L}_R} \right] \end{aligned} \quad (\text{A.4})$$

Replacing non-dimensionalized variables into the original equation,

$$\begin{aligned} \left(\frac{\partial(\rho \cdot k)}{\partial t} + \frac{\partial(\rho \cdot u \cdot k)}{\partial x} + \frac{\partial(\rho \cdot v \cdot k)}{\partial y} \right) \cdot \left[\frac{\tilde{\rho}_\infty \cdot \tilde{a}_\infty^3}{\tilde{L}_R} \right] = \mu_T \cdot \Omega^2 \cdot \left[\frac{\tilde{\mu}_\infty \cdot \tilde{a}_\infty^2}{\tilde{L}_R^2} \right] - \beta' \cdot \rho \cdot k \cdot \omega \cdot \left[\frac{\tilde{\rho}_\infty^2 \cdot \tilde{a}_\infty^4}{\tilde{\mu}_\infty} \right] + \\ \left(\frac{\partial}{\partial x} \cdot \left(\left(\mu + \frac{\mu_T}{\sigma_k} \right) \cdot \frac{\partial k}{\partial x} \right) + \frac{\partial}{\partial y} \cdot \left(\left(\mu + \frac{\mu_T}{\sigma_k} \right) \cdot \frac{\partial k}{\partial y} \right) \right) \cdot \left[\frac{\tilde{\mu}_\infty \cdot \tilde{a}_\infty^2}{\tilde{L}_R^2} \right] \\ \left(\frac{\partial(\rho \cdot k)}{\partial t} + \frac{\partial(\rho \cdot u \cdot k)}{\partial x} + \frac{\partial(\rho \cdot v \cdot k)}{\partial y} \right) = \left[\begin{aligned} \mu_T \cdot \Omega^2 \cdot \left[\frac{\tilde{\mu}_\infty \cdot \tilde{a}_\infty^2}{\tilde{L}_R^2} \cdot \frac{\tilde{L}_R}{\tilde{\mu}_\infty \cdot \tilde{a}_\infty^2} \right] - \beta' \cdot \rho \cdot k \cdot \omega \cdot \left[\frac{\tilde{\rho}_\infty^2 \cdot \tilde{a}_\infty^4}{\tilde{\mu}_\infty} \cdot \frac{\tilde{L}_R}{\tilde{\mu}_\infty \cdot \tilde{a}_\infty^2} \right] + \\ \left(\frac{\partial}{\partial x} \cdot \left(\left(\mu + \frac{\mu_T}{\sigma_k} \right) \cdot \frac{\partial k}{\partial x} \right) + \frac{\partial}{\partial y} \cdot \left(\left(\mu + \frac{\mu_T}{\sigma_k} \right) \cdot \frac{\partial k}{\partial y} \right) \right) \cdot \left[\frac{\tilde{\mu}_\infty \cdot \tilde{a}_\infty^2}{\tilde{L}_R^2} \cdot \frac{\tilde{L}_R}{\tilde{\rho}_\infty \cdot \tilde{a}_\infty^2} \right] \end{aligned} \right] \end{aligned}$$

$$\begin{aligned} \left(\frac{\partial(\rho \cdot k)}{\partial t} + \frac{\partial(\rho \cdot u \cdot k)}{\partial x} + \frac{\partial(\rho \cdot v \cdot k)}{\partial y} \right) = \\ \left[\mu_T \cdot \Omega^2 - \beta' \cdot \rho \cdot k \cdot \omega \cdot \left(\frac{\text{Re}}{M_\infty} \right)^2 + \left(\frac{\partial}{\partial x} \cdot \left(\left(\mu + \frac{\mu_T}{\sigma_k} \right) \cdot \frac{\partial k}{\partial x} \right) + \frac{\partial}{\partial y} \cdot \left(\left(\mu + \frac{\mu_T}{\sigma_k} \right) \cdot \frac{\partial k}{\partial y} \right) \right) \right] \cdot \left[\frac{M_\infty}{\text{Re}} \right] \end{aligned} \quad (\text{A.5})$$

ω equation for Wilcox k - ω and Menter BSL turbulence models

Production Term

$$\tilde{P}_\omega = \zeta \cdot \tilde{\rho} \cdot \tilde{\Omega}^2 = \zeta \cdot \rho \cdot \Omega^2 \cdot \left[\frac{\tilde{\rho}_\infty \cdot \tilde{a}_\infty^2}{\tilde{L}_R^2} \right] \quad (\text{A.6})$$

Destruction Term

$$D_\omega = \beta \cdot \tilde{\rho} \cdot \tilde{\omega}^2 = \beta \cdot \rho \cdot \omega^2 \cdot \left[\frac{\tilde{\rho}_\infty^3 \cdot \tilde{a}_\infty^4}{\tilde{\mu}_\infty^2} \right] \quad (\text{A.7})$$

Diffusion Term

$$\begin{aligned} \frac{\partial}{\partial \tilde{x}} \cdot \left(\left(\tilde{\mu} + \frac{\tilde{\mu}_T}{\sigma_k} \right) \cdot \frac{\partial \tilde{\omega}}{\partial \tilde{x}} \right) + \frac{\partial}{\partial \tilde{y}} \cdot \left(\left(\tilde{\mu} + \frac{\tilde{\mu}_T}{\sigma_k} \right) \cdot \frac{\partial \tilde{\omega}}{\partial \tilde{y}} \right) = \\ \left(\frac{\partial}{\partial x} \cdot \left(\left(\mu + \frac{\mu_T}{\sigma_k} \right) \cdot \frac{\partial \omega}{\partial x} \right) + \frac{\partial}{\partial y} \cdot \left(\left(\mu + \frac{\mu_T}{\sigma_k} \right) \cdot \frac{\partial \omega}{\partial y} \right) \right) \cdot \left[\frac{\tilde{\rho}_\infty^2 \cdot \tilde{a}_\infty^2}{\tilde{L}_R^2} \right] \end{aligned} \quad (\text{A.8})$$

Total Derivative Term

$$\begin{aligned} \frac{\partial(\tilde{\rho} \cdot \tilde{\omega})}{\partial \tilde{t}} + \frac{\partial(\tilde{\rho} \cdot \tilde{u} \cdot \tilde{\omega})}{\partial \tilde{x}} + \frac{\partial(\tilde{\rho} \cdot \tilde{v} \cdot \tilde{\omega})}{\partial \tilde{y}} = \\ \left(\frac{\partial(\rho \cdot \omega)}{\partial t} + \frac{\partial(\rho \cdot u \cdot \omega)}{\partial x} + \frac{\partial(\rho \cdot v \cdot \omega)}{\partial y} \right) \cdot \left[\frac{\tilde{\rho}_\infty^2 \cdot \tilde{a}_\infty^3}{\tilde{L}_R \cdot \tilde{\mu}_\infty} \right] \end{aligned} \quad (\text{A.9})$$

Cross Diffusion Term (Only in Menter BSL Model)

$$\begin{aligned} 2 \cdot \tilde{\rho} \cdot (1 - F_1) \cdot \sigma_{\omega 2} \cdot \frac{1}{\tilde{\omega}} \cdot \left(\frac{\partial \tilde{k}}{\partial \tilde{x}} \cdot \frac{\partial \tilde{\omega}}{\partial \tilde{x}} + \frac{\partial \tilde{k}}{\partial \tilde{y}} \cdot \frac{\partial \tilde{\omega}}{\partial \tilde{y}} \right) = \\ 2 \cdot \rho \cdot (1 - F_1) \cdot \sigma_{\omega 2} \cdot \frac{1}{\omega} \cdot \left(\frac{\partial k}{\partial x} \cdot \frac{\partial \omega}{\partial x} + \frac{\partial k}{\partial y} \cdot \frac{\partial \omega}{\partial y} \right) \cdot \left[\frac{\tilde{\rho}_\infty \cdot \tilde{a}_\infty^2}{\tilde{L}_R^2} \right] \end{aligned} \quad (\text{A.10})$$

Then the following form is used as the non-dimensional ω equation

$$\begin{aligned} \left(\frac{\partial(\rho \cdot \omega)}{\partial t} + \frac{\partial(\rho \cdot u \cdot \omega)}{\partial x} + \frac{\partial(\rho \cdot v \cdot \omega)}{\partial y} \right) \cdot \left[\frac{\tilde{\rho}_\infty^2 \cdot \tilde{a}_\infty^3}{\tilde{L}_R \cdot \tilde{\mu}_\infty} \right] = \zeta \cdot \rho \cdot \Omega^2 \cdot \left[\frac{\tilde{\rho}_\infty \cdot \tilde{a}_\infty^2}{\tilde{L}_R^2} \right] - \beta \cdot \rho \cdot \omega^2 \cdot \left[\frac{\tilde{\rho}_\infty^3 \cdot \tilde{a}_\infty^4}{\tilde{\mu}_\infty^2} \right] + \\ \left(\frac{\partial}{\partial x} \cdot \left(\left(\mu + \frac{\mu_T}{\sigma_k} \right) \cdot \frac{\partial \omega}{\partial x} \right) + \frac{\partial}{\partial y} \cdot \left(\left(\mu + \frac{\mu_T}{\sigma_k} \right) \cdot \frac{\partial \omega}{\partial y} \right) \right) \cdot \left[\frac{\tilde{\rho}_\infty \cdot \tilde{a}_\infty^2}{\tilde{L}_R^2} \right] \end{aligned}$$

$$\left(\frac{\partial(\rho \cdot \omega)}{\partial t} + \frac{\partial(\rho \cdot u \cdot \omega)}{\partial x} + \frac{\partial(\rho \cdot v \cdot \omega)}{\partial y}\right) = \left[\zeta \cdot \rho \cdot \Omega^2 - \beta \cdot \rho \cdot \omega^2 \cdot \left[\frac{\tilde{\rho}_\infty^3 \cdot \tilde{a}_\infty^4}{\tilde{\mu}_\infty^2} \cdot \frac{\tilde{L}_R^2}{\tilde{\rho}_\infty \cdot \tilde{a}_\infty^2} \right] + \left(\frac{\partial}{\partial x} \cdot \left(\left(\mu + \frac{\mu_T}{\sigma_k} \right) \cdot \frac{\partial \omega}{\partial x} \right) + \frac{\partial}{\partial y} \cdot \left(\left(\mu + \frac{\mu_T}{\sigma_k} \right) \cdot \frac{\partial \omega}{\partial y} \right) \right) \right] \cdot \left[\frac{\tilde{\rho}_\infty \cdot \tilde{a}_\infty^2}{\tilde{L}_R^2} \cdot \frac{\tilde{L}_R \cdot \tilde{\mu}_\infty}{\tilde{\rho}_\infty^2 \cdot \tilde{a}_\infty^3} \right]$$

$$\begin{aligned} & \left(\frac{\partial(\rho \cdot \omega)}{\partial t} + \frac{\partial(\rho \cdot u \cdot \omega)}{\partial x} + \frac{\partial(\rho \cdot v \cdot \omega)}{\partial y}\right) \\ &= \left[\zeta \cdot \rho \cdot \Omega^2 - \beta \cdot \rho \cdot \omega^2 \cdot \left(\frac{\text{Re}}{M_\infty} \right)^2 + \left(\frac{\partial}{\partial x} \cdot \left(\left(\mu + \frac{\mu_T}{\sigma_k} \right) \cdot \frac{\partial \omega}{\partial x} \right) + \frac{\partial}{\partial y} \cdot \left(\left(\mu + \frac{\mu_T}{\sigma_k} \right) \cdot \frac{\partial \omega}{\partial y} \right) \right) \right] \cdot \left[\frac{M_\infty}{\text{Re}} \right] \end{aligned} \quad (\text{A.11})$$

For Menter BSL Model

$$\begin{aligned} \left(\frac{\partial(\rho \cdot \omega)}{\partial t} + \frac{\partial(\rho \cdot u \cdot \omega)}{\partial x} + \frac{\partial(\rho \cdot v \cdot \omega)}{\partial y}\right) \cdot \left[\frac{\tilde{\rho}_\infty^2 \cdot \tilde{a}_\infty^3}{\tilde{L}_R \cdot \tilde{\mu}_\infty} \right] &= \zeta \cdot \rho \cdot \Omega^2 \cdot \left[\frac{\tilde{\rho}_\infty \cdot \tilde{a}_\infty^2}{\tilde{L}_R^2} \right] - \beta \cdot \rho \cdot \omega^2 \cdot \left[\frac{\tilde{\rho}_\infty^3 \cdot \tilde{a}_\infty^4}{\tilde{\mu}_\infty^2} \right] + \\ & \left(\frac{\partial}{\partial x} \cdot \left(\left(\mu + \frac{\mu_T}{\sigma_k} \right) \cdot \frac{\partial \omega}{\partial x} \right) + \frac{\partial}{\partial y} \cdot \left(\left(\mu + \frac{\mu_T}{\sigma_k} \right) \cdot \frac{\partial \omega}{\partial y} \right) \right) \cdot \left[\frac{\tilde{\rho}_\infty \cdot \tilde{a}_\infty^2}{\tilde{L}_R^2} \right] + \\ & 2 \cdot \rho \cdot (1 - F_1) \cdot \sigma_{\omega 2} \cdot \frac{1}{\omega} \cdot \left(\frac{\partial k}{\partial x} \cdot \frac{\partial \omega}{\partial x} + \frac{\partial k}{\partial y} \cdot \frac{\partial \omega}{\partial y} \right) \cdot \left[\frac{\tilde{\rho}_\infty \cdot \tilde{a}_\infty^2}{\tilde{L}_R^2} \right] \end{aligned}$$

$$\left(\frac{\partial(\rho \cdot \omega)}{\partial t} + \frac{\partial(\rho \cdot u \cdot \omega)}{\partial x} + \frac{\partial(\rho \cdot v \cdot \omega)}{\partial y}\right) = \left[\zeta \cdot \rho \cdot \Omega^2 - \beta \cdot \rho \cdot \omega^2 \cdot \left[\frac{\tilde{\rho}_\infty^3 \cdot \tilde{a}_\infty^4}{\tilde{\mu}_\infty^2} \cdot \frac{\tilde{L}_R^2}{\tilde{\rho}_\infty \cdot \tilde{a}_\infty^2} \right] + \left(\frac{\partial}{\partial x} \cdot \left(\left(\mu + \frac{\mu_T}{\sigma_k} \right) \cdot \frac{\partial \omega}{\partial x} \right) + \frac{\partial}{\partial y} \cdot \left(\left(\mu + \frac{\mu_T}{\sigma_k} \right) \cdot \frac{\partial \omega}{\partial y} \right) \right) \right] \cdot \left[\frac{\tilde{\rho}_\infty \cdot \tilde{a}_\infty^2}{\tilde{L}_R^2} \cdot \frac{\tilde{L}_R \cdot \tilde{\mu}_\infty}{\tilde{\rho}_\infty^2 \cdot \tilde{a}_\infty^3} \right] + 2 \cdot \rho \cdot (1 - F_1) \cdot \sigma_{\omega 2} \cdot \frac{1}{\omega} \cdot \left(\frac{\partial k}{\partial x} \cdot \frac{\partial \omega}{\partial x} + \frac{\partial k}{\partial y} \cdot \frac{\partial \omega}{\partial y} \right)$$

$$\begin{aligned} & \left(\frac{\partial(\rho \cdot \omega)}{\partial t} + \frac{\partial(\rho \cdot u \cdot \omega)}{\partial x} + \frac{\partial(\rho \cdot v \cdot \omega)}{\partial y}\right) \\ &= \left[\zeta \cdot \rho \cdot \Omega^2 - \beta \cdot \rho \cdot \omega^2 \cdot \left(\frac{\text{Re}}{M_\infty} \right)^2 + \left(\frac{\partial}{\partial x} \cdot \left(\left(\mu + \frac{\mu_T}{\sigma_k} \right) \cdot \frac{\partial \omega}{\partial x} \right) + \frac{\partial}{\partial y} \cdot \left(\left(\mu + \frac{\mu_T}{\sigma_k} \right) \cdot \frac{\partial \omega}{\partial y} \right) \right) \right] \cdot \left[\frac{M_\infty}{\text{Re}} \right] \\ & + 2 \cdot \rho \cdot (1 - F_1) \cdot \sigma_{\omega 2} \cdot \frac{1}{\omega} \cdot \left(\frac{\partial k}{\partial x} \cdot \frac{\partial \omega}{\partial x} + \frac{\partial k}{\partial y} \cdot \frac{\partial \omega}{\partial y} \right) \end{aligned} \quad (\text{A.12})$$

Auxiliary Definitions

$$\begin{aligned}
 y^+ &= \frac{\tilde{u}_\tau \cdot \tilde{y}}{\tilde{\nu}} = \sqrt{\frac{\tilde{\tau}_w}{\tilde{\rho}}} \cdot \frac{\tilde{y}}{\tilde{\mu}} = \sqrt{\frac{\tilde{\tau}_w}{\tilde{\rho}}} \cdot \frac{\tilde{y} \cdot \tilde{\rho}}{\tilde{\mu}} = \frac{\sqrt{\tilde{\rho} \cdot \tilde{\tau}_w}}{\tilde{\mu}} \cdot \tilde{y} = \frac{\sqrt{\rho \cdot \tau_w}}{\mu} \cdot y \cdot \left[\frac{\sqrt{\tilde{\rho}_\infty \cdot \tilde{\mu}_\infty \cdot \tilde{a}_\infty}}{\tilde{\mu}_\infty} \cdot \tilde{L}_R \right] \\
 &= \frac{\sqrt{\rho \cdot \tau_w}}{\mu} \cdot y \cdot \left[\sqrt{\tilde{\rho}_\infty \cdot \frac{\tilde{L}_R \cdot \tilde{a}_\infty}{\tilde{\mu}_\infty}} \right] = \frac{\sqrt{\rho \cdot \tau_w}}{\mu} \cdot y \cdot \left[\frac{\text{Re}}{M_\infty} \right]^{1/2}
 \end{aligned}$$

$$k^+ = \frac{\tilde{k}}{\tilde{u}_\tau^2} = \frac{\tilde{k}}{\tilde{\tau}_w} = \frac{\tilde{k} \cdot \tilde{\rho}}{\tilde{\tau}_w} = \frac{k \cdot \rho}{\tau_w} \cdot \left[\frac{\tilde{a}_\infty^2 \cdot \tilde{\rho}_\infty}{\tilde{\mu}_\infty \cdot \tilde{a}_\infty} \cdot \tilde{L}_R \right] = \frac{k \cdot \rho}{\tau_w} \cdot \left[\frac{\tilde{a}_\infty \cdot \tilde{\rho}_\infty \cdot \tilde{L}_R}{\tilde{\mu}_\infty} \right] = \frac{k \cdot \rho}{\tau_w} \cdot \left[\frac{\text{Re}}{M_\infty} \right]$$

$$u^+ = \frac{\tilde{u}}{\tilde{u}_\tau} = \frac{\tilde{u}}{\sqrt{\frac{\tilde{\tau}_w}{\tilde{\rho}}}} = \sqrt{\frac{\rho}{\tau_w}} \cdot u \cdot \left[\tilde{a}_\infty \cdot \sqrt{\frac{\tilde{\rho}_\infty}{\tilde{\mu}_\infty \cdot \tilde{a}_\infty}} \cdot \tilde{L}_R \right] = \sqrt{\frac{\rho}{\tau_w}} \cdot u \cdot \left[\sqrt{\frac{\tilde{a}_\infty^2 \cdot \tilde{\rho}_\infty}{\tilde{\mu}_\infty \cdot \tilde{a}_\infty}} \cdot \tilde{L}_R \right] = \sqrt{\frac{\rho}{\tau_w}} \cdot u \cdot \left[\frac{\text{Re}}{M_\infty} \right]$$

$$C_f = \frac{\tilde{\tau}_w}{\frac{1}{2} \cdot \tilde{\rho}_\infty \cdot \tilde{u}_\infty^2} = \frac{\tau_w}{\frac{1}{2} \cdot \rho_\infty \cdot u_\infty^2} \cdot \left[\frac{\tilde{\mu}_\infty \cdot \tilde{a}_\infty}{\tilde{L}_R} \cdot \frac{1}{\tilde{\rho}_\infty \cdot \tilde{a}_\infty^2} \right] = \frac{\tau_w}{\frac{1}{2} \cdot \rho_\infty \cdot u_\infty^2} \cdot \left[\frac{M_\infty}{\text{Re}} \right]$$

$$\text{Re}_T = \frac{\tilde{\rho} \cdot \tilde{k}^2}{\tilde{\mu} \cdot \tilde{\varepsilon}} = \frac{\rho \cdot k^2}{\mu \cdot \varepsilon} \cdot \left[\frac{\tilde{\rho}_\infty \cdot \tilde{a}_\infty^4}{\tilde{\mu}_\infty} \cdot \frac{1}{\tilde{\rho}_\infty \cdot \tilde{a}_\infty^4} \right] = \frac{\rho \cdot k^2}{\mu \cdot \varepsilon}$$

$$\text{Re}_k = \frac{\tilde{\rho} \cdot \sqrt{\tilde{k}} \cdot \tilde{d}}{\tilde{\mu}} = \frac{\rho \cdot \sqrt{k} \cdot d}{\mu} \cdot \left[\frac{\tilde{\rho}_\infty \cdot \tilde{a}_\infty \cdot \tilde{L}_R}{\tilde{\mu}_\infty} \right] = \frac{\rho \cdot \sqrt{k} \cdot d}{\mu} \cdot \left[\frac{\text{Re}}{M_\infty} \right]$$

APPENDIX B

Transformation of turbulence model equations to generalized coordinates

As an example to the model equations, k equation of $k-\omega$ turbulence model will be transformed into generalized coordinates. This equation will be investigated in several parts.

$$\underbrace{\frac{\partial(\rho \cdot k)}{\partial t} + \frac{\partial(\rho \cdot u \cdot k)}{\partial x} + \frac{\partial(\rho \cdot v \cdot k)}{\partial y}}_I = \left[\underbrace{P_k - D_k}_{III} + \underbrace{\frac{\partial}{\partial x} \left(\left(\mu + \frac{\mu_T}{\sigma_k} \right) \cdot \frac{\partial k}{\partial x} \right) + \frac{\partial}{\partial y} \left(\left(\mu + \frac{\mu_T}{\sigma_k} \right) \cdot \frac{\partial k}{\partial y} \right)}_{II} \right] \cdot \left[\frac{M_\infty}{Re} \right]$$

I. Total Derivative Term

$$\begin{aligned} \frac{\partial(\rho \cdot k)}{\partial t} + \frac{\partial(\rho \cdot u \cdot k)}{\partial x} + \frac{\partial(\rho \cdot v \cdot k)}{\partial y} &= \frac{\partial(\rho \cdot k)}{\partial \tau} + \xi_\tau \cdot \frac{\partial(\rho \cdot k)}{\partial \xi} + \eta_\tau \cdot \frac{\partial(\rho \cdot k)}{\partial \eta} \\ &+ \xi_x \cdot \frac{\partial(\rho \cdot u \cdot k)}{\partial \xi} + \eta_x \cdot \frac{\partial(\rho \cdot u \cdot k)}{\partial \eta} \\ &+ \xi_y \cdot \frac{\partial(\rho \cdot v \cdot k)}{\partial \xi} + \eta_y \cdot \frac{\partial(\rho \cdot v \cdot k)}{\partial \eta} \end{aligned}$$

After applying the well known Chain Rule and dividing the total derivative equation to Jacobian term the following form is obtained,

$$\begin{aligned}
& \frac{1}{J} \cdot \left(\frac{\partial(\rho \cdot k)}{\partial t} + \frac{\partial(\rho \cdot u \cdot k)}{\partial x} + \frac{\partial(\rho \cdot v \cdot k)}{\partial y} \right) = \\
& \frac{\partial}{\partial \tau} \left(\frac{1}{J} \cdot \rho \cdot k \right) - \rho \cdot k \cdot \frac{\partial}{\partial \tau} \left(\frac{1}{J} \right) + \frac{\partial}{\partial \xi} \left(\frac{\xi_\tau}{J} \cdot \rho \cdot k \right) - \rho \cdot k \cdot \frac{\partial}{\partial \xi} \left(\frac{\xi_\tau}{J} \right) + \frac{\partial}{\partial \eta} \left(\frac{\eta_\tau}{J} \cdot \rho \cdot k \right) - \rho \cdot k \cdot \frac{\partial}{\partial \eta} \left(\frac{\eta_\tau}{J} \right) \\
& \quad + \frac{\partial}{\partial \xi} \left(\frac{\xi_x}{J} \cdot \rho \cdot u \cdot k \right) - \rho \cdot u \cdot k \cdot \frac{\partial}{\partial \xi} \left(\frac{\xi_x}{J} \right) + \frac{\partial}{\partial \eta} \left(\frac{\eta_x}{J} \cdot \rho \cdot u \cdot k \right) - \rho \cdot u \cdot k \cdot \frac{\partial}{\partial \eta} \left(\frac{\eta_x}{J} \right) \\
& \quad + \frac{\partial}{\partial \xi} \left(\frac{\xi_y}{J} \cdot \rho \cdot v \cdot k \right) - \rho \cdot v \cdot k \cdot \frac{\partial}{\partial \xi} \left(\frac{\xi_y}{J} \right) + \frac{\partial}{\partial \eta} \left(\frac{\eta_y}{J} \cdot \rho \cdot v \cdot k \right) - \rho \cdot v \cdot k \cdot \frac{\partial}{\partial \eta} \left(\frac{\eta_y}{J} \right)
\end{aligned}$$

grouping whole equation such that;

$$\begin{aligned}
& \frac{1}{J} \cdot \left(\frac{\partial(\rho \cdot k)}{\partial t} + \frac{\partial(\rho \cdot u \cdot k)}{\partial x} + \frac{\partial(\rho \cdot v \cdot k)}{\partial y} \right) = \\
& \left[\frac{\partial}{\partial \tau} \left(\frac{1}{J} \cdot \rho \cdot k \right) + \frac{\partial}{\partial \xi} \left(\frac{\xi_\tau}{J} \cdot \rho \cdot k \right) + \frac{\partial}{\partial \eta} \left(\frac{\eta_\tau}{J} \cdot \rho \cdot k \right) + \frac{\partial}{\partial \xi} \left(\frac{\xi_x}{J} \cdot \rho \cdot u \cdot k \right) + \frac{\partial}{\partial \eta} \left(\frac{\eta_x}{J} \cdot \rho \cdot u \cdot k \right) + \frac{\partial}{\partial \xi} \left(\frac{\xi_y}{J} \cdot \rho \cdot v \cdot k \right) + \frac{\partial}{\partial \eta} \left(\frac{\eta_y}{J} \cdot \rho \cdot v \cdot k \right) \right] + \\
& \left[-\rho \cdot k \cdot \frac{\partial}{\partial \tau} \left(\frac{1}{J} \right) - \rho \cdot k \cdot \frac{\partial}{\partial \xi} \left(\frac{\xi_\tau}{J} \right) - \rho \cdot k \cdot \frac{\partial}{\partial \eta} \left(\frac{\eta_\tau}{J} \right) - \rho \cdot u \cdot k \cdot \frac{\partial}{\partial \xi} \left(\frac{\xi_x}{J} \right) - \rho \cdot u \cdot k \cdot \frac{\partial}{\partial \eta} \left(\frac{\eta_x}{J} \right) - \rho \cdot v \cdot k \cdot \frac{\partial}{\partial \xi} \left(\frac{\xi_y}{J} \right) - \rho \cdot v \cdot k \cdot \frac{\partial}{\partial \eta} \left(\frac{\eta_y}{J} \right) \right]
\end{aligned}$$

The second group of terms in the right hand side of the equation is analytically zero. Grouping same derivatives,

$$\frac{1}{J} \cdot \left(\frac{\partial(\rho \cdot k)}{\partial t} + \frac{\partial(\rho \cdot u \cdot k)}{\partial x} + \frac{\partial(\rho \cdot v \cdot k)}{\partial y} \right) = \frac{\partial}{\partial \tau} \left(\frac{1}{J} \cdot \rho \cdot k \right) + \frac{\partial}{\partial \xi} \left(\rho \cdot k \cdot \frac{(\xi_\tau + \xi_x \cdot u + \xi_y \cdot v)}{J} \right) + \frac{\partial}{\partial \eta} \left(\rho \cdot k \cdot \frac{(\eta_\tau + \eta_x \cdot u + \eta_y \cdot v)}{J} \right)$$

Defining contravariant velocities,

$$\begin{aligned}
U &= \xi_\tau + \xi_x \cdot u + \xi_y \cdot v \\
V &= \eta_\tau + \eta_x \cdot u + \eta_y \cdot v
\end{aligned} \tag{B.1}$$

Then,

$$\frac{1}{J} \cdot \left(\frac{\partial(\rho \cdot k)}{\partial t} + \frac{\partial(\rho \cdot u \cdot k)}{\partial x} + \frac{\partial(\rho \cdot v \cdot k)}{\partial y} \right) = \frac{\partial}{\partial \tau} \left(\frac{\rho \cdot k}{J} \right) + \frac{\partial}{\partial \xi} \left(\frac{\rho \cdot U \cdot k}{J} \right) + \frac{\partial}{\partial \eta} \left(\frac{\rho \cdot V \cdot k}{J} \right) \tag{B.2}$$

II. Diffusion Term

$$\begin{aligned} \frac{\partial}{\partial x} \cdot \left(\left(\mu + \frac{\mu_T}{\sigma_k} \right) \cdot \frac{\partial k}{\partial x} \right) + \frac{\partial}{\partial y} \cdot \left(\left(\mu + \frac{\mu_T}{\sigma_k} \right) \cdot \frac{\partial k}{\partial y} \right) = \\ \xi_x \cdot \frac{\partial}{\partial \xi} \left[\left(\mu + \frac{\mu_T}{\sigma_k} \right) \cdot \left(\xi_x \cdot \frac{\partial k}{\partial \xi} + \eta_x \cdot \frac{\partial k}{\partial \eta} \right) \right] + \eta_x \cdot \frac{\partial}{\partial \eta} \left[\left(\mu + \frac{\mu_T}{\sigma_k} \right) \cdot \left(\xi_x \cdot \frac{\partial k}{\partial \xi} + \eta_x \cdot \frac{\partial k}{\partial \eta} \right) \right] \\ + \xi_y \cdot \frac{\partial}{\partial \xi} \left[\left(\mu + \frac{\mu_T}{\sigma_k} \right) \cdot \left(\xi_y \cdot \frac{\partial k}{\partial \xi} + \eta_y \cdot \frac{\partial k}{\partial \eta} \right) \right] + \eta_y \cdot \frac{\partial}{\partial \eta} \left[\left(\mu + \frac{\mu_T}{\sigma_k} \right) \cdot \left(\xi_y \cdot \frac{\partial k}{\partial \xi} + \eta_y \cdot \frac{\partial k}{\partial \eta} \right) \right] \end{aligned}$$

Performing a similar derivation as in total derivative term and dividing into Jacobian below expression is obtained,

$$\begin{aligned} \frac{1}{J} \cdot \left[\frac{\partial}{\partial x} \cdot \left(\left(\mu + \frac{\mu_T}{\sigma_k} \right) \cdot \frac{\partial k}{\partial x} \right) + \frac{\partial}{\partial y} \cdot \left(\left(\mu + \frac{\mu_T}{\sigma_k} \right) \cdot \frac{\partial k}{\partial y} \right) \right] = \\ \frac{\partial}{\partial \xi} \left[\frac{\xi_x}{J} \cdot \left(\mu + \frac{\mu_T}{\sigma_k} \right) \cdot \left(\xi_x \cdot \frac{\partial k}{\partial \xi} + \eta_x \cdot \frac{\partial k}{\partial \eta} \right) + \frac{\xi_y}{J} \cdot \left(\mu + \frac{\mu_T}{\sigma_k} \right) \cdot \left(\xi_y \cdot \frac{\partial k}{\partial \xi} + \eta_y \cdot \frac{\partial k}{\partial \eta} \right) \right] \\ + \frac{\partial}{\partial \eta} \left[\frac{\eta_x}{J} \cdot \left(\mu + \frac{\mu_T}{\sigma_k} \right) \cdot \left(\xi_x \cdot \frac{\partial k}{\partial \xi} + \eta_x \cdot \frac{\partial k}{\partial \eta} \right) + \frac{\eta_y}{J} \cdot \left(\mu + \frac{\mu_T}{\sigma_k} \right) \cdot \left(\xi_y \cdot \frac{\partial k}{\partial \xi} + \eta_y \cdot \frac{\partial k}{\partial \eta} \right) \right] \end{aligned}$$

If cross derivatives ($\partial_{\xi} \cdot \partial_{\eta}$) are neglected

$$\begin{aligned} \frac{1}{J} \cdot \left[\frac{\partial}{\partial x} \cdot \left(\left(\mu + \frac{\mu_T}{\sigma_k} \right) \cdot \frac{\partial k}{\partial x} \right) + \frac{\partial}{\partial y} \cdot \left(\left(\mu + \frac{\mu_T}{\sigma_k} \right) \cdot \frac{\partial k}{\partial y} \right) \right] = \\ \frac{\partial}{\partial \xi} \left[\frac{\xi_x^2}{J} \cdot \left(\mu + \frac{\mu_T}{\sigma_k} \right) \cdot \frac{\partial k}{\partial \xi} + \frac{\xi_y^2}{J} \cdot \left(\mu + \frac{\mu_T}{\sigma_k} \right) \cdot \frac{\partial k}{\partial \xi} \right] + \frac{\partial}{\partial \eta} \left[\frac{\eta_x^2}{J} \cdot \left(\mu + \frac{\mu_T}{\sigma_k} \right) \cdot \frac{\partial k}{\partial \eta} + \frac{\eta_y^2}{J} \cdot \left(\mu + \frac{\mu_T}{\sigma_k} \right) \cdot \frac{\partial k}{\partial \eta} \right] \end{aligned}$$

Then the diffusion term appears as such,

$$\begin{aligned} \frac{1}{J} \cdot \left[\frac{\partial}{\partial x} \cdot \left(\left(\mu + \frac{\mu_T}{\sigma_k} \right) \cdot \frac{\partial k}{\partial x} \right) + \frac{\partial}{\partial y} \cdot \left(\left(\mu + \frac{\mu_T}{\sigma_k} \right) \cdot \frac{\partial k}{\partial y} \right) \right] \\ = \frac{\partial}{\partial \xi} \left[\frac{1}{J} \cdot (\xi_x^2 + \xi_y^2) \cdot \left(\mu + \frac{\mu_T}{\sigma_k} \right) \cdot \frac{\partial k}{\partial \xi} \right] + \frac{\partial}{\partial \eta} \left[\frac{1}{J} \cdot (\eta_x^2 + \eta_y^2) \cdot \left(\mu + \frac{\mu_T}{\sigma_k} \right) \cdot \frac{\partial k}{\partial \eta} \right] \end{aligned} \quad (\text{B.3})$$

III. Production and Destruction Terms

There are no derivative terms to be processed in the computation scheme, so no explicit transformation is necessary for these terms. But it is important not to forget that the total derivative and diffusion terms are divided into Jacobian term. In order to satisfy the equality production and destruction terms must be divided into Jacobian term.

$$\frac{P_k}{J}, \frac{D_k}{J} \quad (\text{B.4})$$

Collecting equations, the transformed k equation could be obtained as,

$$\begin{aligned} \frac{\partial}{\partial \tau} \left(\frac{\rho \cdot k}{J} \right) + \frac{\partial}{\partial \xi} \left(\frac{\rho \cdot U \cdot k}{J} \right) + \frac{\partial}{\partial \eta} \left(\frac{\rho \cdot V \cdot k}{J} \right) = \\ \frac{P_k}{J} - \frac{D_k}{J} + \frac{\partial}{\partial \xi} \left[\frac{1}{J} \cdot (\xi_x^2 + \xi_y^2) \cdot \left(\mu + \frac{\mu_T}{\sigma_k} \right) \cdot \frac{\partial k}{\partial \xi} \right] + \frac{\partial}{\partial \eta} \left[\frac{1}{J} \cdot (\eta_x^2 + \eta_y^2) \cdot \left(\mu + \frac{\mu_T}{\sigma_k} \right) \cdot \frac{\partial k}{\partial \eta} \right] \end{aligned} \quad (\text{B.5})$$

One can obtain similar transformed equations of ε and ω variables. These equations pairs for k - ω and k - ε models could be written in vectorial form to have a suitable form for numerical scheme. The resulting forms for turbulence model equations are;

Main Solution Equation

$$\frac{\partial Q}{\partial \tau} + \frac{\partial F}{\partial \xi} + \frac{\partial G}{\partial \eta} = \frac{M_\infty}{\text{Re}} \left(\frac{\partial H}{\partial \xi} + \frac{\partial K}{\partial \eta} + M \right) \quad (\text{B.6})$$

k- ω Turbulence Models

$$Q = \frac{1}{J} \cdot \begin{bmatrix} \rho \cdot k \\ \rho \cdot \omega \end{bmatrix} \quad F = \frac{1}{J} \cdot \begin{bmatrix} \rho \cdot U \cdot k \\ \rho \cdot U \cdot \omega \end{bmatrix} \quad G = \frac{1}{J} \cdot \begin{bmatrix} \rho \cdot V \cdot k \\ \rho \cdot V \cdot \omega \end{bmatrix}$$

$$H = \frac{1}{J} \cdot \begin{bmatrix} (\xi_x^2 + \xi_y^2) \cdot \left(\mu + \frac{\mu_T}{\sigma_k} \right) \cdot \frac{\partial k}{\partial \xi} \\ (\xi_x^2 + \xi_y^2) \cdot \left(\mu + \frac{\mu_T}{\sigma_\omega} \right) \cdot \frac{\partial \omega}{\partial \xi} \end{bmatrix} \quad K = \frac{1}{J} \cdot \begin{bmatrix} (\eta_x^2 + \eta_y^2) \cdot \left(\mu + \frac{\mu_T}{\sigma_k} \right) \cdot \frac{\partial k}{\partial \eta} \\ (\eta_x^2 + \eta_y^2) \cdot \left(\mu + \frac{\mu_T}{\sigma_\omega} \right) \cdot \frac{\partial \omega}{\partial \eta} \end{bmatrix}$$

$$M = \frac{1}{J} \cdot \begin{bmatrix} \mu_T \cdot \Omega^2 - \beta' \cdot \rho \cdot k \cdot \omega \cdot \left(\frac{\text{Re}}{M_\infty} \right)^2 \\ \zeta \cdot \rho \cdot \Omega^2 - \beta \cdot \rho \cdot \omega^2 \cdot \left(\frac{\text{Re}}{M_\infty} \right)^2 \end{bmatrix}$$

Applicable for *Wilcox k- ω* formulation.

$$M = \frac{1}{J} \cdot \begin{bmatrix} \mu_T \cdot \Omega^2 - \beta' \cdot \rho \cdot k \cdot \omega \cdot \left(\frac{\text{Re}}{M_\infty} \right)^2 \\ \zeta \cdot \rho \cdot \Omega^2 - \beta \cdot \rho \cdot \omega^2 \cdot \left(\frac{\text{Re}}{M_\infty} \right)^2 + 2 \cdot \rho \cdot (1 - F_1) \cdot \sigma_{\omega 2} \cdot \frac{1}{\omega} \cdot \left(\frac{\partial k}{\partial x} \cdot \frac{\partial \omega}{\partial x} + \frac{\partial k}{\partial y} \cdot \frac{\partial \omega}{\partial y} \right) \end{bmatrix}$$

Applicable for *Menter BSL* formulation.

k- ε Turbulence Models

$$Q = \frac{1}{J} \cdot \begin{bmatrix} \rho \cdot k \\ \rho \cdot \varepsilon \end{bmatrix} \quad F = \frac{1}{J} \cdot \begin{bmatrix} \rho \cdot U \cdot k \\ \rho \cdot U \cdot \varepsilon \end{bmatrix} \quad G = \frac{1}{J} \cdot \begin{bmatrix} \rho \cdot V \cdot k \\ \rho \cdot V \cdot \varepsilon \end{bmatrix}$$

$$H = \frac{1}{J} \cdot \begin{bmatrix} (\xi_x^2 + \xi_y^2) \cdot \left(\mu + \frac{\mu_T}{\sigma_k} \right) \cdot \frac{\partial k}{\partial \xi} \\ (\xi_x^2 + \xi_y^2) \cdot \left(\mu + \frac{\mu_T}{\sigma_\varepsilon} \right) \cdot \frac{\partial \varepsilon}{\partial \xi} \end{bmatrix} \quad K = \frac{1}{J} \cdot \begin{bmatrix} (\eta_x^2 + \eta_y^2) \cdot \left(\mu + \frac{\mu_T}{\sigma_k} \right) \cdot \frac{\partial k}{\partial \eta} \\ (\eta_x^2 + \eta_y^2) \cdot \left(\mu + \frac{\mu_T}{\sigma_\varepsilon} \right) \cdot \frac{\partial \varepsilon}{\partial \eta} \end{bmatrix}$$

$$M = \frac{1}{J} \cdot \left[\begin{array}{c} \mu_T \cdot \Omega^2 - \rho \cdot \varepsilon \cdot \left(\frac{\text{Re}}{M_\infty} \right)^2 - 2.0 \cdot \mu \cdot \frac{k}{y^2} \\ C_{\varepsilon 1} \cdot f_1 \cdot \Omega^2 \cdot \mu_T \cdot \frac{\varepsilon}{k} - C_{\varepsilon 2} \cdot f_2 \cdot \rho \cdot \frac{\varepsilon^2}{k} \cdot \left(\frac{\text{Re}}{M_\infty} \right)^2 - 2.0 \cdot \mu \cdot \frac{\varepsilon}{y^2} \cdot \exp\left(-\frac{y^+}{2.0}\right) \end{array} \right]$$

Applicable for *Chien* k - ε formulation

$$M = \frac{1}{J} \cdot \left[\begin{array}{c} \mu_T \cdot \Omega^2 - \rho \cdot \varepsilon \cdot \left(\frac{\text{Re}}{M_\infty} \right)^2 \\ C_{\varepsilon 1} \cdot f_1 \cdot \Omega^2 \cdot \mu_T \cdot \frac{\varepsilon}{k} - C_{\varepsilon 2} \cdot f_2 \cdot \rho \cdot \frac{\varepsilon^2}{k} \cdot \left(\frac{\text{Re}}{M_\infty} \right)^2 \end{array} \right]$$

Applicable for *Abid* k - ε formulation

APPENDIX C

Calculation of Jacobian terms for Turbulence Models

Recalling the equation that is factored form of the solution for turbulence model Equations, (4.43)

$$\begin{aligned}
 & \left[1 + \frac{\theta \cdot \Delta \tau}{1 + \phi} \cdot \left(\frac{\partial}{\partial \eta} (B - V + S_\eta)^n - \frac{\partial^2}{\partial \eta^2} S^n - C^n \right) \right] \bullet \Delta Q^{n \otimes} = RHS^n \\
 & \left[1 + \frac{\theta \cdot \Delta \tau}{1 + \phi} \cdot \left(\frac{\partial}{\partial \xi} (A - U + R_\xi)^n - \frac{\partial^2}{\partial \xi^2} R^n \right) \right] \bullet \Delta Q^n = \Delta Q^{n \otimes} \quad (C.1) \\
 & RHS^n = \frac{\Delta \tau}{1 + \phi} \cdot \left(\frac{\partial}{\partial \xi} (-F^n + H^{*n}) + \frac{\partial}{\partial \eta} (-G^n + K^{*n}) + M^{*n} \right) + \frac{\phi}{1 + \phi} \cdot \Delta Q^{n-1}
 \end{aligned}$$

Jacobian Calculation for k- ω Models

$$A^n = \left(\frac{\partial F}{\partial Q} \right)^n = \begin{bmatrix} \frac{\partial F_1}{\partial Q_1} & \frac{\partial F_1}{\partial Q_2} \\ \frac{\partial F_2}{\partial Q_1} & \frac{\partial F_2}{\partial Q_2} \end{bmatrix} = \begin{bmatrix} \frac{\partial(\rho \cdot U \cdot k/J)}{\partial(\rho \cdot k/J)} & \frac{\partial(\rho \cdot U \cdot k/J)}{\partial(\rho \cdot \omega/J)} \\ \frac{\partial(\rho \cdot U \cdot \omega/J)}{\partial(\rho \cdot k/J)} & \frac{\partial(\rho \cdot U \cdot \omega/J)}{\partial(\rho \cdot \omega/J)} \end{bmatrix} = \begin{bmatrix} \frac{\partial(U \cdot Q_1)}{\partial Q_1} & \frac{\partial(U \cdot Q_1)}{\partial Q_2} \\ \frac{\partial(U \cdot Q_2)}{\partial Q_1} & \frac{\partial(U \cdot Q_2)}{\partial Q_2} \end{bmatrix} = \begin{bmatrix} U & 0 \\ 0 & U \end{bmatrix}$$

$$A^n = \left(\frac{\partial F}{\partial Q} \right)^n = \begin{bmatrix} U & 0 \\ 0 & U \end{bmatrix} \quad (C.2)$$

$$B^n = \left(\frac{\partial G}{\partial Q} \right)^n = \begin{bmatrix} \frac{\partial G_1}{\partial Q_1} & \frac{\partial G_1}{\partial Q_2} \\ \frac{\partial G_2}{\partial Q_1} & \frac{\partial G_2}{\partial Q_2} \end{bmatrix} = \begin{bmatrix} \frac{\partial(\rho \cdot V \cdot k/J)}{\partial(\rho \cdot k/J)} & \frac{\partial(\rho \cdot V \cdot k/J)}{\partial(\rho \cdot \omega/J)} \\ \frac{\partial(\rho \cdot V \cdot \omega/J)}{\partial(\rho \cdot k/J)} & \frac{\partial(\rho \cdot V \cdot \omega/J)}{\partial(\rho \cdot \omega/J)} \end{bmatrix} = \begin{bmatrix} \frac{\partial(V \cdot Q_1)}{\partial Q_1} & \frac{\partial(V \cdot Q_1)}{\partial Q_2} \\ \frac{\partial(V \cdot Q_2)}{\partial Q_1} & \frac{\partial(V \cdot Q_2)}{\partial Q_2} \end{bmatrix} = \begin{bmatrix} V & 0 \\ 0 & V \end{bmatrix}$$

$$B^n = \left(\frac{\partial G}{\partial Q} \right)^n = \begin{bmatrix} V & 0 \\ 0 & V \end{bmatrix} \quad (\text{C.3})$$

Jacobians of convection terms could easily be calculated while derivation of diffusion Jacobians are challenging since it involves second spatial derivatives.

In order to save space in derivations of Jacobians of diffusion terms, such definitions are made;

$$\Gamma_k = (\xi_x^2 + \xi_y^2) \cdot \left(\mu + \frac{\mu_t}{\sigma_k} \right), \quad \Gamma_\omega = (\xi_x^2 + \xi_y^2) \cdot \left(\mu + \frac{\mu_t}{\sigma_\omega} \right)$$

Then,

$$U^n = \left(\frac{\partial H^*}{\partial Q} \right)^n = \begin{bmatrix} \frac{\partial H^*_1}{\partial Q_1} & \frac{\partial H^*_1}{\partial Q_2} \\ \frac{\partial H^*_2}{\partial Q_1} & \frac{\partial H^*_2}{\partial Q_2} \end{bmatrix} = \begin{bmatrix} \frac{\partial \left(\frac{M_\infty \cdot \Gamma_k \cdot \partial k}{\text{Re} \cdot J \cdot \partial \xi} \right)}{\partial(\rho \cdot k/J)} & \frac{\partial \left(\frac{M_\infty \cdot \Gamma_k \cdot \partial k}{\text{Re} \cdot J \cdot \partial \xi} \right)}{\partial(\rho \cdot \omega/J)} \\ \frac{\partial \left(\frac{M_\infty \cdot \Gamma_\omega \cdot \partial \omega}{\text{Re} \cdot J \cdot \partial \xi} \right)}{\partial(\rho \cdot k/J)} & \frac{\partial \left(\frac{M_\infty \cdot \Gamma_\omega \cdot \partial \omega}{\text{Re} \cdot J \cdot \partial \xi} \right)}{\partial(\rho \cdot \omega/J)} \end{bmatrix} = \begin{bmatrix} I & II \\ III & IV \end{bmatrix}$$

This Jacobian term will be examined in four parts;

1st term

$$\begin{aligned}
& \frac{\partial \left(\frac{M_\infty \cdot \Gamma_k}{\text{Re} \cdot J} \cdot \frac{\partial k}{\partial \xi} \right)}{\partial \left(\frac{\rho \cdot k}{J} \right)} = \frac{\partial \left(\frac{M_\infty \cdot \Gamma_k}{\text{Re} \cdot J} \cdot \frac{\partial \left(\frac{\rho \cdot k}{J} \cdot \frac{J}{\rho} \right)}{\partial \xi} \right)}{\partial \left(\frac{\rho \cdot k}{J} \right)} = \frac{\partial \left(\frac{M_\infty \cdot \Gamma_k}{\text{Re} \cdot J} \cdot \frac{\partial \left(Q_1 \cdot \frac{J}{\rho} \right)}{\partial \xi} \right)}{\partial Q_1} \\
& = \frac{\partial \left(\frac{M_\infty \cdot \Gamma_k}{\text{Re} \cdot J} \cdot \left(Q_1 \cdot \frac{\partial \left(\frac{J}{\rho} \right)}{\partial \xi} + \frac{J}{\rho} \cdot \frac{\partial \left(Q_1 \right)}{\partial \xi} \right) \right)}{\partial Q_1} = \frac{M_\infty \cdot \Gamma_k}{\text{Re} \cdot J} \cdot \frac{\partial \left(\frac{J}{\rho} \right)}{\partial \xi} + \frac{M_\infty \cdot \Gamma_k}{\text{Re} \cdot J} \cdot \frac{J}{\rho} \cdot \frac{\partial^2 Q_1}{\partial Q_1 \partial \xi} \\
& = \frac{M_\infty \cdot \Gamma_k}{\text{Re} \cdot J} \cdot \frac{\partial \left(\frac{J}{\rho} \right)}{\partial \xi} + \frac{M_\infty \cdot \Gamma_k}{\text{Re} \cdot J} \cdot \frac{J}{\rho} \cdot \frac{\partial}{\partial \xi} \left(\frac{\partial Q_1}{\partial Q_1} \right) = \frac{M_\infty \cdot \Gamma_k}{\text{Re} \cdot J} \cdot \frac{\partial \left(\frac{J}{\rho} \right)}{\partial \xi} + \frac{M_\infty \cdot \Gamma_k}{\text{Re} \cdot J} \cdot \frac{J}{\rho} \cdot \frac{\partial}{\partial \xi} \quad (1) \\
& = \frac{M_\infty \cdot \Gamma_k}{\text{Re} \cdot J} \cdot \frac{\partial \left(\frac{J}{\rho} \right)}{\partial \xi}
\end{aligned}$$

Since the expressions inside the “ ∂ ” operators has independent vector representations namely, (Q_1 and Q_2), term 2 and 3 has zero values. Similar derivation for term 4 appears as;

$$\frac{M_\infty \cdot \Gamma_\omega}{\text{Re} \cdot J} \cdot \frac{\partial \left(\frac{J}{\rho} \right)}{\partial \xi}$$

Then the Jacobian term appears as

$$U^n = \left(\frac{\partial H^*}{\partial Q} \right)^n = \frac{M_\infty}{\text{Re}} \cdot \begin{bmatrix} \frac{\Gamma_k}{J} \cdot \frac{\partial \left(\frac{J}{\rho} \right)}{\partial \xi} & 0 \\ 0 & \frac{\Gamma_\omega}{J} \cdot \frac{\partial \left(\frac{J}{\rho} \right)}{\partial \xi} \end{bmatrix} \quad (\text{C.4})$$

The Jacobian named, R that is derived from the second derivative part of the diffusion term appears as

$$R^n = \left(\frac{\partial H^*}{\partial Q_\xi} \right)^n = \begin{bmatrix} \frac{\partial H^*_1}{\partial Q_{\xi_1}} & \frac{\partial H^*_1}{\partial Q_{\xi_2}} \\ \frac{\partial H^*_2}{\partial Q_{\xi_1}} & \frac{\partial H^*_2}{\partial Q_{\xi_2}} \end{bmatrix}$$

Here Q_ξ is

$$Q_\xi = \frac{1}{J} \cdot \begin{bmatrix} \frac{\partial(\rho \cdot k)}{\partial \xi} \\ \frac{\partial(\rho \cdot \omega)}{\partial \xi} \end{bmatrix}$$

In a similar fashion to the first diffusion term

$$R^n = \left(\frac{\partial H^*}{\partial Q_\xi} \right)^n = \begin{bmatrix} \frac{\partial H^*_1}{\partial Q_{\xi_1}} & \frac{\partial H^*_1}{\partial Q_{\xi_2}} \\ \frac{\partial H^*_2}{\partial Q_{\xi_1}} & \frac{\partial H^*_2}{\partial Q_{\xi_2}} \end{bmatrix} = \begin{bmatrix} \frac{\partial \left(\frac{M_\infty \cdot \Gamma_k \cdot \partial k}{\text{Re} \cdot J \cdot \partial \xi} \right)}{\frac{\partial(\rho \cdot k/J)}{\partial \xi}} & \frac{\partial \left(\frac{M_\infty \cdot \Gamma_k \cdot \partial k}{\text{Re} \cdot J \cdot \partial \xi} \right)}{\frac{\partial(\rho \cdot \omega/J)}{\partial \xi}} \\ \frac{\partial \left(\frac{M_\infty \cdot \Gamma_\omega \cdot \partial \omega}{\text{Re} \cdot J \cdot \partial \xi} \right)}{\frac{\partial(\rho \cdot k/J)}{\partial \xi}} & \frac{\partial \left(\frac{M_\infty \cdot \Gamma_\omega \cdot \partial \omega}{\text{Re} \cdot J \cdot \partial \xi} \right)}{\frac{\partial(\rho \cdot \omega/J)}{\partial \xi}} \end{bmatrix} = \begin{bmatrix} I & II \\ III & IV \end{bmatrix}$$

This term will also be studied in 4 parts.

1st term

$$\begin{aligned}
& \frac{\partial \left(\frac{M_\infty \cdot \Gamma_k}{\text{Re} \cdot J} \cdot \frac{\partial k}{\partial \xi} \right)}{\partial \left(\frac{\rho \cdot k}{J} \right) / \partial \xi} = \frac{\partial \left(\frac{M_\infty \cdot \Gamma_k}{\text{Re} \cdot J} \cdot \frac{\partial \left(\frac{\rho \cdot k}{J} \cdot \frac{J}{\rho} \right)}{\partial \xi} \right)}{\partial \left(\frac{\rho \cdot k}{J} \right) / \partial \xi} = \frac{\partial \left(\frac{M_\infty \cdot \Gamma_k}{\text{Re} \cdot J} \cdot \frac{\partial \left(Q_1 \cdot \frac{J}{\rho} \right)}{\partial \xi} \right)}{\partial Q_1 / \partial \xi} \\
& = \frac{\partial \left(\frac{M_\infty \cdot \Gamma_k}{\text{Re} \cdot J} \cdot \left(Q_1 \cdot \frac{\partial \left(\frac{J}{\rho} \right)}{\partial \xi} + \frac{J}{\rho} \cdot \frac{\partial (Q_1)}{\partial \xi} \right) \right)}{\partial Q_1 / \partial \xi} = \frac{M_\infty \cdot \Gamma_k \cdot Q_1 \cdot \frac{\partial \left(\frac{J}{\rho} \right)}{\partial \xi}}{\partial Q_1 / \partial \xi} + \frac{M_\infty \cdot \Gamma_k \cdot J}{\text{Re} \cdot J \cdot \rho} \\
& = \frac{M_\infty \cdot \Gamma_k \cdot J}{\text{Re} \cdot J \cdot \rho}
\end{aligned}$$

As described in previous derivation of Jacobian, the expressions inside the “ ∂ ” operators has independent vector representations namely, (Q_1 and Q_2), term 2 and 3 has zero values. Similar to previous expression, 4th term could be derived as;

$$\frac{M_\infty \cdot \Gamma_\omega \cdot J}{\text{Re} \cdot J \cdot \rho}$$

Then,

$$R^n = \left(\frac{\partial H^*}{\partial Q_\xi} \right)^n = \frac{M_\infty}{\text{Re}} \cdot \begin{bmatrix} \frac{\Gamma_k \cdot J}{J \cdot \rho} & 0 \\ 0 & \frac{\Gamma_\omega \cdot J}{J \cdot \rho} \end{bmatrix} \quad (\text{C.5})$$

The other Jacobians of diffusion will be written directly by taking the derivations of Equations (C.4) and (C.5) as a base.

After making some necessary definitions,

$$\Gamma'_k = (\eta_x^2 + \eta_y^2) \cdot \left(\mu + \frac{\mu_t}{\sigma_k} \right), \quad \Gamma'_\omega = (\eta_x^2 + \eta_y^2) \cdot \left(\mu + \frac{\mu_t}{\sigma_\omega} \right)$$

$$V^n = \left(\frac{\partial K^*}{\partial Q} \right)^n = \frac{M_\infty}{\text{Re}} \cdot \begin{bmatrix} \frac{\Gamma'_k}{J} \cdot \frac{\partial \left(\frac{J}{\rho} \right)}{\partial \eta} & 0 \\ 0 & \frac{\Gamma'_\omega}{J} \cdot \frac{\partial \left(\frac{J}{\rho} \right)}{\partial \eta} \end{bmatrix} \quad (\text{C.6})$$

$$S^n = \left(\frac{\partial K^*}{\partial Q_\eta} \right)^n = \frac{M_\infty}{\text{Re}} \cdot \begin{bmatrix} \frac{\Gamma'_k}{J} \cdot \frac{J}{\rho} & 0 \\ 0 & \frac{\Gamma'_\omega}{J} \cdot \frac{J}{\rho} \end{bmatrix} \quad (\text{C.7})$$

The source matrix M and its Jacobian matrix C, differ in representations for *Wilcox k- ω* and *Menter BSL* models.

The derivation of Jacobians of source matrix which includes the destruction and production terms of variables includes the determination of the stability of the models. In the source Jacobian term matrix C, the treatment explicit and implicit representations of production and destruction terms will be investigated. Also by equating the inverse diagonal elements of 4x4 matrix C to zero, one can get a solution of uncoupled formulation of turbulence models.

If the M matrix for *Wilcox k- ω* is written in terms of vectors Q_1 and Q_2 then,

$$\begin{aligned} M^* &= \frac{1}{J} \cdot \frac{M_\infty}{\text{Re}} \cdot \begin{bmatrix} \mu_T \cdot \Omega^2 - \beta' \cdot \rho \cdot k \cdot \omega \cdot \left(\frac{\text{Re}}{M_\infty} \right)^2 \\ \zeta \cdot \rho \cdot \Omega^2 - \beta \cdot \rho \cdot \omega^2 \cdot \left(\frac{\text{Re}}{M_\infty} \right)^2 \end{bmatrix} = \frac{M_\infty}{\text{Re}} \cdot \begin{bmatrix} \frac{\rho \cdot k}{J \cdot \omega} \cdot \Omega^2 - \beta' \cdot \frac{\rho \cdot k}{J} \cdot \omega \cdot \left(\frac{\text{Re}}{M_\infty} \right)^2 \\ \zeta \cdot \frac{\rho}{J} \cdot \Omega^2 - \beta \cdot \frac{\rho \cdot \omega^2}{J} \cdot \left(\frac{\text{Re}}{M_\infty} \right)^2 \end{bmatrix} \\ &= \frac{M_\infty}{\text{Re}} \cdot \begin{bmatrix} \frac{\rho \cdot k / J}{\rho \cdot \omega / J} \cdot \Omega^2 - \beta' \cdot \frac{\rho \cdot k}{J} \cdot \frac{\rho \cdot \omega}{J} \cdot \frac{J}{\rho} \cdot \left(\frac{\text{Re}}{M_\infty} \right)^2 \\ \zeta \cdot \frac{\rho}{J} \cdot \Omega^2 - \beta \cdot \frac{\rho^2 \cdot \omega^2}{J^2} \cdot \frac{J}{\rho} \cdot \left(\frac{\text{Re}}{M_\infty} \right)^2 \end{bmatrix} = \frac{M_\infty}{\text{Re}} \cdot \begin{bmatrix} \frac{\rho \cdot Q_1}{J \cdot Q_2} \cdot \Omega^2 - \beta' \cdot Q_1 \cdot Q_2 \cdot \frac{J}{\rho} \cdot \left(\frac{\text{Re}}{M_\infty} \right)^2 \\ \zeta \cdot \frac{\rho}{J} \cdot \Omega^2 - \beta \cdot Q_2^2 \cdot \frac{J}{\rho} \cdot \left(\frac{\text{Re}}{M_\infty} \right)^2 \end{bmatrix} \end{aligned}$$

Then Jacobian term could be derived as,

$$\begin{aligned}
C^n &= \left(\frac{\partial M^*}{\partial Q} \right)^n = \begin{bmatrix} \frac{\partial M_1^*}{\partial Q_1} & \frac{\partial M_1^*}{\partial Q_2} \\ \frac{\partial M_2^*}{\partial Q_1} & \frac{\partial M_2^*}{\partial Q_2} \end{bmatrix} \\
&= \frac{M_\infty}{\text{Re}} \cdot \begin{bmatrix} \frac{\partial \left(\frac{\rho}{J} \cdot \frac{Q_1}{Q_2} \cdot \Omega^2 - \beta' \cdot Q_1 \cdot Q_2 \cdot \frac{J}{\rho} \cdot \left(\frac{\text{Re}}{M_\infty} \right)^2 \right)}{\partial Q_1} & \frac{\partial \left(\frac{\rho}{J} \cdot \frac{Q_1}{Q_2} \cdot \Omega^2 - \beta' \cdot Q_1 \cdot Q_2 \cdot \frac{J}{\rho} \cdot \left(\frac{\text{Re}}{M_\infty} \right)^2 \right)}{\partial Q_2} \\ \frac{\partial \left(\zeta \cdot \frac{\rho}{J} \cdot \Omega^2 - \beta \cdot Q_2^2 \cdot \frac{J}{\rho} \cdot \left(\frac{\text{Re}}{M_\infty} \right)^2 \right)}{\partial Q_1} & \frac{\partial \left(\zeta \cdot \frac{\rho}{J} \cdot \Omega^2 - \beta \cdot Q_2^2 \cdot \frac{J}{\rho} \cdot \left(\frac{\text{Re}}{M_\infty} \right)^2 \right)}{\partial Q_2} \end{bmatrix} \\
&= \frac{M_\infty}{\text{Re}} \cdot \begin{bmatrix} \frac{\rho}{J} \cdot \frac{1}{Q_2} \cdot \Omega^2 - \beta' \cdot 1 \cdot Q_2 \cdot \frac{J}{\rho} \cdot \left(\frac{\text{Re}}{M_\infty} \right)^2 & -\frac{\rho}{J} \cdot \frac{Q_1}{Q_2^2} \cdot \Omega^2 - \beta' \cdot Q_1 \cdot 1 \cdot \frac{J}{\rho} \cdot \left(\frac{\text{Re}}{M_\infty} \right)^2 \\ 0 - 0 & 0 - 2.0 \cdot \beta \cdot Q_2 \cdot \frac{J}{\rho} \cdot \left(\frac{\text{Re}}{M_\infty} \right)^2 \end{bmatrix} \\
&= \frac{M_\infty}{\text{Re}} \cdot \begin{bmatrix} \frac{\Omega^2}{\omega} - \beta' \cdot \omega \cdot \left(\frac{\text{Re}}{M_\infty} \right)^2 & -\frac{k}{\omega^2} \cdot \Omega^2 - \beta' \cdot k \cdot \left(\frac{\text{Re}}{M_\infty} \right)^2 \\ 0 & -2.0 \cdot \beta \cdot \omega \cdot \left(\frac{\text{Re}}{M_\infty} \right)^2 \end{bmatrix} \\
C^n &= \left(\frac{\partial M^*}{\partial Q} \right)^n = \frac{M_\infty}{\text{Re}} \cdot \begin{bmatrix} \frac{\Omega^2}{\omega} - \beta' \cdot \omega \cdot \left(\frac{\text{Re}}{M_\infty} \right)^2 & -\frac{k}{\omega^2} \cdot \Omega^2 - \beta' \cdot k \cdot \left(\frac{\text{Re}}{M_\infty} \right)^2 \\ 0 & -2.0 \cdot \beta \cdot \omega \cdot \left(\frac{\text{Re}}{M_\infty} \right)^2 \end{bmatrix} \quad (\text{C.8})
\end{aligned}$$

If the production terms are represented in explicit form, the expressions derived from the production terms drop from the source Jacobian matrix.

$$C^n = \frac{M_\infty}{\text{Re}} \cdot \begin{bmatrix} -\beta' \cdot \omega \cdot \left(\frac{\text{Re}}{M_\infty} \right)^2 & -\beta' \cdot k \cdot \left(\frac{\text{Re}}{M_\infty} \right)^2 \\ 0 & -2.0 \cdot \beta \cdot \omega \cdot \left(\frac{\text{Re}}{M_\infty} \right)^2 \end{bmatrix}$$

The following expression represents implicit production terms but an uncoupled formulation.

$$C^n = \frac{M_\infty}{\text{Re}} \cdot \begin{bmatrix} \frac{\Omega^2}{\omega} - \beta' \cdot \omega \cdot \left(\frac{\text{Re}}{M_\infty}\right)^2 & 0 \\ 0 & -2.0 \cdot \beta \cdot \omega \cdot \left(\frac{\text{Re}}{M_\infty}\right)^2 \end{bmatrix}$$

A third representation of source Jacobian forms by taking production terms explicit and an uncoupled formulation.

$$C^n = \frac{M_\infty}{\text{Re}} \cdot \begin{bmatrix} -\beta' \cdot \omega \cdot \left(\frac{\text{Re}}{M_\infty}\right)^2 & 0 \\ 0 & -2.0 \cdot \beta \cdot \omega \cdot \left(\frac{\text{Re}}{M_\infty}\right)^2 \end{bmatrix}$$

These differences in Jacobians are investigated in the work of Spalart and Allmaras [13]. The investigations of them have shown that, regarding the positivity of source terms is achieved when the production terms are taken explicit while destruction terms treated as implicit which is called as the third strategy. The last appearance of source Jacobian term is used in the implementation.

For *Menter BSL* model the source term source Jacobian C appears as,

$$C^n = \frac{M_\infty}{\text{Re}} \cdot \begin{bmatrix} -\beta' \cdot \omega \cdot \left(\frac{\text{Re}}{M_\infty}\right)^2 & 0 \\ 0 & -\left[2 \cdot \rho \cdot (1 - F_1) \cdot \sigma_{\omega^2} \cdot \frac{1}{\omega^2} \cdot \left(\frac{\partial k}{\partial x} \cdot \frac{\partial \omega}{\partial x} + \frac{\partial k}{\partial y} \cdot \frac{\partial \omega}{\partial y}\right)\right] - 2.0 \cdot \beta \cdot \omega \cdot \left(\frac{\text{Re}}{M_\infty}\right)^2 \end{bmatrix}$$

Above representation of source Jacobian term is advised in [11, page 6].

Jacobian Calculation for k-ε Models

The core structure of two equation models could be regarded in a similar fashion whereas the source terms and Jacobians of these source terms appear in complete difference. The boundary conditions also differ in great amount. At this point only the source Jacobian calculations will be presented.

$$\begin{aligned}
 M &= \frac{M_\infty}{\text{Re}} \cdot \left[\begin{array}{c} \frac{\mu_T}{J} \cdot \Omega^2 - \frac{\rho \cdot \varepsilon}{J} \cdot \left(\frac{\text{Re}}{M_\infty} \right)^2 - 2.0 \cdot \mu \cdot \frac{k/J}{y^2} \\ C_{\varepsilon 1} \cdot f_1 \cdot \Omega^2 \cdot \frac{\mu_T}{J} \cdot \frac{\varepsilon}{k} - C_{\varepsilon 2} \cdot f_2 \cdot \frac{\rho}{J} \cdot \frac{\varepsilon^2}{k} \cdot \left(\frac{\text{Re}}{M_\infty} \right)^2 - 2.0 \cdot \mu \cdot \frac{\varepsilon/J}{y^2} \cdot \exp\left(-\frac{y^+}{2.0}\right) \end{array} \right] \\
 &= \frac{M_\infty}{\text{Re}} \cdot \left[\begin{array}{c} \frac{C_\mu \cdot f_\mu \cdot \rho k^2 / \varepsilon}{J} \cdot \Omega^2 - \frac{\rho \cdot \varepsilon}{J} \cdot \left(\frac{\text{Re}}{M_\infty} \right)^2 - 2.0 \cdot \mu \cdot \frac{k/J}{y^2} \\ C_{\varepsilon 1} \cdot f_1 \cdot \Omega^2 \cdot \frac{C_\mu \cdot f_\mu \cdot \rho k^2 / \varepsilon}{J} \cdot \frac{\varepsilon}{k} - C_{\varepsilon 2} \cdot f_2 \cdot \frac{\rho}{J} \cdot \frac{\varepsilon^2}{k} \cdot \left(\frac{\text{Re}}{M_\infty} \right)^2 - 2.0 \cdot \mu \cdot \frac{\varepsilon/J}{y^2} \cdot \exp\left(-\frac{y^+}{2.0}\right) \end{array} \right] \\
 &= \frac{M_\infty}{\text{Re}} \cdot \left[\begin{array}{c} C_\mu \cdot f_\mu \cdot \frac{\frac{\rho^2 \cdot k^2}{J^2}}{\frac{\rho \cdot \varepsilon}{J}} \cdot \Omega^2 - \frac{\rho \cdot \varepsilon}{J} \cdot \left(\frac{\text{Re}}{M_\infty} \right)^2 - 2.0 \cdot \mu \cdot \frac{\rho \cdot k/J}{\rho \cdot y^2} \\ C_{\varepsilon 1} \cdot f_1 \cdot \Omega^2 \cdot C_\mu \cdot f_\mu \cdot \frac{\rho \cdot k}{J} - C_{\varepsilon 2} \cdot f_2 \cdot \frac{\frac{\rho^2 \cdot \varepsilon^2}{J^2}}{\frac{\rho \cdot k}{J}} \cdot \left(\frac{\text{Re}}{M_\infty} \right)^2 - 2.0 \cdot \mu \cdot \frac{\rho \cdot \varepsilon/J}{\rho \cdot y^2} \cdot \exp\left(-\frac{y^+}{2.0}\right) \end{array} \right] \\
 &= \frac{M_\infty}{\text{Re}} \cdot \left[\begin{array}{c} C_\mu \cdot f_\mu \cdot \frac{Q_1^2}{Q_2} \cdot \Omega^2 - Q_2 \cdot \left(\frac{\text{Re}}{M_\infty} \right)^2 - 2.0 \cdot \mu \cdot \frac{Q_1}{\rho \cdot y^2} \\ C_{\varepsilon 1} \cdot f_1 \cdot \Omega^2 \cdot C_\mu \cdot f_\mu \cdot Q_1 - C_{\varepsilon 2} \cdot f_2 \cdot \frac{Q_2^2}{Q_1} \cdot \left(\frac{\text{Re}}{M_\infty} \right)^2 - 2.0 \cdot \mu \cdot \frac{Q_2}{\rho \cdot y^2} \cdot \exp\left(-\frac{y^+}{2.0}\right) \end{array} \right]
 \end{aligned}$$

$$C^n = \left(\frac{\partial M^*}{\partial Q} \right)^n = \begin{bmatrix} \frac{\partial M_1^*}{\partial Q_1} & \frac{\partial M_1^*}{\partial Q_2} \\ \frac{\partial M_2^*}{\partial Q_1} & \frac{\partial M_2^*}{\partial Q_2} \end{bmatrix}$$

$$\begin{aligned}
& \frac{M_\infty}{\text{Re}} \left[\begin{array}{cc} \frac{\partial \left(C_\mu \cdot f_\mu \cdot \frac{Q^2}{Q} \cdot \Omega - Q \cdot \left(\frac{\text{Re}}{M_\infty} \right)^2 - 20 \cdot \mu \cdot \frac{Q}{\rho y^2} \right)}{\partial Q} & \frac{\partial \left(C_\mu \cdot f_\mu \cdot \frac{Q^2}{Q} \cdot \Omega - Q \cdot \left(\frac{\text{Re}}{M_\infty} \right)^2 - 20 \cdot \mu \cdot \frac{Q}{\rho y^2} \right)}{\partial Q} \\ \frac{\partial \left(C_{\epsilon 1} \cdot f_1 \cdot \Omega^2 \cdot C_\mu \cdot f_\mu \cdot Q - C_{\epsilon 2} \cdot f_2 \cdot \frac{Q^2}{Q} \cdot \left(\frac{\text{Re}}{M_\infty} \right)^2 - 20 \cdot \mu \cdot \frac{Q}{\rho y^2} \cdot \exp\left(-\frac{y^+}{20}\right) \right)}{\partial Q} & \frac{\partial \left(C_{\epsilon 1} \cdot f_1 \cdot \Omega^2 \cdot C_\mu \cdot f_\mu \cdot Q - C_{\epsilon 2} \cdot f_2 \cdot \frac{Q^2}{Q} \cdot \left(\frac{\text{Re}}{M_\infty} \right)^2 - 20 \cdot \mu \cdot \frac{Q}{\rho y^2} \cdot \exp\left(-\frac{y^+}{20}\right) \right)}{\partial Q} \end{array} \right] \\
& \frac{M_\infty}{\text{Re}} \left[\begin{array}{cc} C_\mu \cdot f_\mu \cdot 2.0 \cdot \frac{Q_1}{Q_2} \cdot \Omega^2 - 2.0 \cdot \frac{\mu}{\rho \cdot y^2} & -C_\mu \cdot f_\mu \cdot \frac{Q_1^2}{Q_2^2} \cdot \Omega^2 - \left(\frac{\text{Re}}{M_\infty} \right)^2 \\ C_{\epsilon 1} \cdot f_1 \cdot \Omega^2 \cdot C_\mu \cdot f_\mu + C_{\epsilon 2} \cdot f_2 \cdot \frac{Q_2^2}{Q_1^2} \cdot \left(\frac{\text{Re}}{M_\infty} \right)^2 & -2.0 \cdot C_{\epsilon 2} \cdot f_2 \cdot \frac{Q_2}{Q_1} \cdot \left(\frac{\text{Re}}{M_\infty} \right)^2 - 2.0 \cdot \frac{\mu}{\rho \cdot y^2} \cdot \exp\left(-\frac{y^+}{20}\right) \end{array} \right] \\
& \frac{M_\infty}{\text{Re}} \left[\begin{array}{cc} C_\mu \cdot f_\mu \cdot 2.0 \cdot \frac{k}{\varepsilon} \cdot \Omega^2 - 2.0 \cdot \frac{\mu}{\rho \cdot y^2} & -C_\mu \cdot f_\mu \cdot \frac{k^2}{\varepsilon^2} \cdot \Omega^2 - \left(\frac{\text{Re}}{M_\infty} \right)^2 \\ C_{\epsilon 1} \cdot f_1 \cdot \Omega^2 \cdot C_\mu \cdot f_\mu + C_{\epsilon 2} \cdot f_2 \cdot \frac{\varepsilon^2}{k^2} \cdot \left(\frac{\text{Re}}{M_\infty} \right)^2 & -2.0 \cdot C_{\epsilon 2} \cdot f_2 \cdot \frac{\varepsilon}{k} \cdot \left(\frac{\text{Re}}{M_\infty} \right)^2 - 2.0 \cdot \frac{\mu}{\rho \cdot y^2} \cdot \exp\left(-\frac{y^+}{20}\right) \end{array} \right]
\end{aligned}$$

As described in Turbulence models section, the D and E terms for *Abid* k - ε model is zero. Dropping these terms from the source Jacobian matrix developed for *Chien* k - ε model gives the matrix for *Abid* k - ε .

$$C^n = \frac{M_\infty}{\text{Re}} \left[\begin{array}{cc} C_\mu \cdot f_\mu \cdot 2.0 \cdot \frac{k}{\varepsilon} \cdot \Omega^2 - 2.0 \cdot \frac{\mu}{\rho \cdot y^2} & -C_\mu \cdot f_\mu \cdot \frac{k^2}{\varepsilon^2} \cdot \Omega^2 - \left(\frac{\text{Re}}{M_\infty} \right)^2 \\ C_{\epsilon 1} \cdot f_1 \cdot \Omega^2 \cdot C_\mu \cdot f_\mu + C_{\epsilon 2} \cdot f_2 \cdot \frac{\varepsilon^2}{k^2} \cdot \left(\frac{\text{Re}}{M_\infty} \right)^2 & -2.0 \cdot C_{\epsilon 2} \cdot f_2 \cdot \frac{\varepsilon}{k} \cdot \left(\frac{\text{Re}}{M_\infty} \right)^2 \end{array} \right]$$

APPENDIX D

Discretization of Turbulence Model equations

ξ sweep

$$\left[1 + \frac{\theta \cdot \Delta \tau}{1 + \phi} \cdot \left(\frac{\partial}{\partial \eta} (B - V + S_\eta)^n - \frac{\partial^2}{\partial \eta^2} S^n - C^n \right) \right] \bullet \Delta Q^{n \otimes} = RHS^n \quad (D.1)$$

The following notations are presented due to simplicity in derivations,

$$t^* = \frac{\theta \cdot \Delta \tau}{1 + \phi}, \quad q = \Delta Q^{n \otimes}$$

The discretization work will be accomplished in 6 steps,

$$\left[1 + t^* \cdot \left(\frac{\partial}{\partial \eta} (B - V + S_\eta)^n - \frac{\partial^2}{\partial \eta^2} S^n - C^n \right) \right] \bullet q = RHS^n$$

$$\underbrace{q}_1 + \underbrace{t^* \cdot \delta_\eta^{upwind} \cdot (B \cdot q)}_2 - \underbrace{t^* \cdot \delta_\eta \cdot (V \cdot q)}_3 + \underbrace{t^* \cdot \delta_\eta \cdot (S_\eta \cdot q)}_4 - \underbrace{t^* \cdot \delta_\eta^2 \cdot (S \cdot q)}_5 - \underbrace{t^* \cdot (C \cdot q)}_6 = RHS^n$$

1) $q_{j,k}$

$$2) t^* \cdot \delta_\eta^{upwind} \cdot (B \cdot q) = t^* \cdot \frac{(B \cdot q)_{j,k+1} - (B \cdot q)_{j,k-1}}{2} - t^* \cdot \left[\frac{(|B| \cdot q)_{j,k+1} - 2 \cdot (|B| \cdot q)_{j,k} - (|B| \cdot q)_{j,k-1}}{2} \right]$$

$$3) -t^* \cdot \delta_\eta \cdot (V \cdot q) = -t^* \cdot \frac{M_\infty}{Re} \cdot \frac{\partial}{\partial \eta} \begin{bmatrix} \frac{\Gamma'_k}{J} \cdot \frac{\partial (J/\rho \cdot q_1)}{\partial \eta} & 0 \\ 0 & \frac{\Gamma'_\omega}{J} \cdot \frac{\partial (J/\rho \cdot q_2)}{\partial \eta} \end{bmatrix}$$

$$= -t^* \cdot \frac{M_\infty}{\text{Re}} \cdot \begin{bmatrix} \frac{\partial}{\partial \eta} \left(\frac{\Gamma'_k}{J} \cdot \frac{\partial (J/\rho \cdot q_1)}{\partial \eta} \right) & 0 \\ 0 & \frac{\partial}{\partial \eta} \left(\frac{\Gamma'_\omega}{J} \cdot \frac{\partial (J/\rho \cdot q_2)}{\partial \eta} \right) \end{bmatrix}$$

$$= -t^* \cdot \frac{M_\infty}{\text{Re}} \cdot \begin{bmatrix} \frac{\left(\frac{\Gamma'_k}{J} \cdot \frac{\partial (J/\rho \cdot q_1)}{\partial \eta} \right)_{j,k+\frac{1}{2}} - \left(\frac{\Gamma'_k}{J} \cdot \frac{\partial (J/\rho \cdot q_1)}{\partial \eta} \right)_{j,k-\frac{1}{2}}}{\Delta \eta} & 0 \\ 0 & \frac{\left(\frac{\Gamma'_\omega}{J} \cdot \frac{\partial (J/\rho \cdot q_2)}{\partial \eta} \right)_{j,k+\frac{1}{2}} - \left(\frac{\Gamma'_\omega}{J} \cdot \frac{\partial (J/\rho \cdot q_2)}{\partial \eta} \right)_{j,k-\frac{1}{2}}}{\Delta \eta} \end{bmatrix}$$

($\Delta \eta = 1$)

$$= -t^* \cdot \frac{M_\infty}{\text{Re}} \cdot \begin{bmatrix} \left(\frac{\Gamma'_k}{J} \right)_{j,k+\frac{1}{2}} \cdot \left(\left(\frac{J}{\rho} \cdot q_1 \right)_{j,k+1} - \left(\frac{J}{\rho} \cdot q_1 \right)_{j,k} \right) - \left(\frac{\Gamma'_k}{J} \right)_{j,k-\frac{1}{2}} \cdot \left(\left(\frac{J}{\rho} \cdot q_1 \right)_{j,k} - \left(\frac{J}{\rho} \cdot q_1 \right)_{j,k-1} \right) & 0 \\ 0 & \sim \end{bmatrix}$$

$$= -t^* \cdot \frac{M_\infty}{\text{Re}} \cdot \left[\left(\frac{\Gamma'_k}{J} \right)_{j,k+\frac{1}{2}} \cdot \left(\frac{J}{\rho} \right)_{j,k+1} \right] \cdot q_{1,j,k+1} - \left[\left(\frac{\Gamma'_k}{J} \right)_{j,k+\frac{1}{2}} + \left(\frac{\Gamma'_k}{J} \right)_{j,k-\frac{1}{2}} \right] \cdot \left(\frac{J}{\rho} \right)_{j,k} \cdot q_{1,j,k} + \left[\left(\frac{\Gamma'_k}{J} \right)_{j,k-\frac{1}{2}} \cdot \left(\frac{J}{\rho} \right)_{j,k-1} \right] \cdot q_{1,j,k-1} \quad 0 \quad \sim$$

If the matrix is divided into three parts with respect to discretization indices,

$$= -t^* \cdot \frac{M_\infty}{\text{Re}} \cdot \underbrace{\begin{bmatrix} \left(\frac{\Gamma'_k}{J} \right)_{j,k+\frac{1}{2}} \cdot \left(\frac{J}{\rho} \right)_{j,k+1} & 0 \\ 0 & \left(\frac{\Gamma'_\omega}{J} \right)_{j,k+\frac{1}{2}} \cdot \left(\frac{J}{\rho} \right)_{j,k+1} \end{bmatrix}}_{V_{\eta KP}} \cdot q_{j,k+1}$$

$$+ t^* \cdot \frac{M_\infty}{\text{Re}} \cdot \underbrace{\begin{bmatrix} \left(\left(\frac{\Gamma'_k}{J} \right)_{j,k+\frac{1}{2}} + \left(\frac{\Gamma'_k}{J} \right)_{j,k-\frac{1}{2}} \right) \cdot \left(\frac{J}{\rho} \right)_{j,k} & 0 \\ 0 & \left(\left(\frac{\Gamma'_\omega}{J} \right)_{j,k+\frac{1}{2}} + \left(\frac{\Gamma'_\omega}{J} \right)_{j,k-\frac{1}{2}} \right) \cdot \left(\frac{J}{\rho} \right)_{j,k} \end{bmatrix}}_{V_{\eta K}} \cdot q_{j,k}$$

$$\begin{aligned}
& -t^* \cdot \frac{M_\infty}{\text{Re}} \cdot \underbrace{\begin{bmatrix} \left(\frac{\Gamma'_k}{J}\right)_{j,k-\frac{1}{2}} \cdot \left(\frac{J}{\rho}\right)_{j,k-1} & 0 \\ 0 & \left(\frac{\Gamma'_\omega}{J}\right)_{j,k-\frac{1}{2}} \cdot \left(\frac{J}{\rho}\right)_{j,k-1} \end{bmatrix}}_{V_{\eta KR}} \cdot q_{j,k-1} \\
& = t^* \cdot \left(-V_{\eta KP} \cdot q_{j,k+1} + V_{\eta K} \cdot q_{j,k} - V_{\eta KR} \cdot q_{j,k-1} \right)
\end{aligned}$$

$$\begin{aligned}
4) \quad t^* \cdot \delta_\eta \cdot (S_\eta \cdot q) & = t^* \cdot \frac{M_\infty}{\text{Re}} \cdot \frac{\partial}{\partial \eta} \begin{bmatrix} \frac{\partial}{\partial \eta} \left(\Gamma'_k \cdot \frac{1}{\rho} \right) \cdot q_1 & 0 \\ 0 & \frac{\partial}{\partial \eta} \left(\Gamma'_\omega \cdot \frac{1}{\rho} \right) \cdot q_2 \end{bmatrix} \\
& = t^* \cdot \frac{M_\infty}{\text{Re}} \cdot \begin{bmatrix} \delta_\eta^2 \left(\frac{\Gamma'_k}{\rho} \right) \cdot q_1 + \delta_\eta \left(\frac{\Gamma'_k}{\rho} \right) \cdot \delta_\eta q_1 & 0 \\ 0 & \delta_\eta^2 \left(\frac{\Gamma'_\omega}{\rho} \right) \cdot q_2 + \delta_\eta \left(\frac{\Gamma'_\omega}{\rho} \right) \cdot \delta_\eta q_2 \end{bmatrix}
\end{aligned}$$

Similar approach regarding the indices is done for this matrix formation,

$$\begin{aligned}
& = t^* \cdot \frac{M_\infty}{\text{Re}} \cdot \underbrace{\begin{bmatrix} \left(\frac{\Gamma'_k}{\rho}\right)_{j,k+1} - 2 \cdot \left(\frac{\Gamma'_k}{\rho}\right)_{j,k} + \left(\frac{\Gamma'_k}{\rho}\right)_{j,k-1} & 0 \\ 0 & \left(\frac{\Gamma'_\omega}{\rho}\right)_{j,k+1} - 2 \cdot \left(\frac{\Gamma'_\omega}{\rho}\right)_{j,k} + \left(\frac{\Gamma'_\omega}{\rho}\right)_{j,k-1} \end{bmatrix}}_{S_{\eta K}} \cdot q_{j,k} \\
& + t^* \cdot \frac{M_\infty}{4 \cdot \text{Re}} \cdot \underbrace{\begin{bmatrix} \left(\frac{\Gamma'_k}{\rho}\right)_{j,k+1} - \left(\frac{\Gamma'_k}{\rho}\right)_{j,k-1} & 0 \\ 0 & \left(\frac{\Gamma'_\omega}{\rho}\right)_{j,k+1} - \left(\frac{\Gamma'_\omega}{\rho}\right)_{j,k-1} \end{bmatrix}}_{S_{\eta KP}} \cdot q_{j,k+1} \\
& - t^* \cdot \frac{M_\infty}{4 \cdot \text{Re}} \cdot \underbrace{\begin{bmatrix} \left(\frac{\Gamma'_k}{\rho}\right)_{j,k+1} - \left(\frac{\Gamma'_k}{\rho}\right)_{j,k-1} & 0 \\ 0 & \left(\frac{\Gamma'_\omega}{\rho}\right)_{j,k+1} - \left(\frac{\Gamma'_\omega}{\rho}\right)_{j,k-1} \end{bmatrix}}_{S_{\eta KR} - S_{\eta KP}} \cdot q_{j,k-1} \\
& = t^* \cdot \left(S_{\eta KP} \cdot q_{j,k+1} + S_{\eta K} \cdot q_{j,k} - S_{\eta KR} \cdot q_{j,k-1} \right)
\end{aligned}$$

$$5) -t^* \cdot \delta_\eta^2 \cdot (S \cdot q) = -t^* \cdot (S_{j,k+1} \cdot q_{j,k+1} - 2 \cdot S_{j,k} \cdot q_{j,k} + S_{j,k-1} \cdot q_{j,k-1})$$

$$6) -t^* \cdot (C_{j,k} \cdot q_{j,k})$$

Right hand side discretization

$$RHS^n = \frac{\Delta\tau}{1+\phi} \cdot \left(\frac{\partial}{\partial\xi} (-F^n + H^{*n}) + \frac{\partial}{\partial\eta} (-G^n + K^{*n}) + M^{*n} \right) + \frac{\phi}{1+\phi} \cdot \Delta Q^{n-1} \quad (D.2)$$

$$t^{**} = \frac{\Delta\tau}{1+\phi}$$

$$RHS^n = \underbrace{-t^{**} \cdot \delta_\xi^{upwind} F}_1 + \underbrace{t^{**} \cdot \delta_\xi H^*}_2 - \underbrace{t^{**} \cdot \delta_\eta^{upwind} G}_3 + \underbrace{t^{**} \cdot \delta_\eta K^*}_4 + \underbrace{t^{**} \cdot M^*}_5 + \underbrace{\frac{\phi}{1+\phi} \cdot \Delta Q^{n-1}}_6$$

$$1) -t^{**} \cdot \delta_\xi^{upwind} F = -t^{**} \cdot \frac{F_{j+1,k} - F_{j-1,k}}{2} + t^{**} \cdot \left[\frac{|F|_{j+1,k} - 2 \cdot |F|_{j,k} - |F|_{j-1,k}}{2} \right]$$

$$2) t^{**} \cdot \delta_\xi H^* = t^{**} \cdot \frac{M_\infty}{\text{Re}} \cdot \delta_\xi \left[\begin{array}{l} \frac{\Gamma_k}{J} \cdot \frac{\partial k}{\partial \xi} \\ \frac{\Gamma_\omega}{J} \cdot \frac{\partial \omega}{\partial \xi} \end{array} \right]$$

$$= t^{**} \cdot \frac{M_\infty}{\text{Re}} \cdot \left[\begin{array}{l} \left(\frac{\Gamma_k}{J} \right)_{j+\frac{1}{2},k} \cdot (k_{j+1,k} - k_{j,k}) - \left(\frac{\Gamma_k}{J} \right)_{j-\frac{1}{2},k} \cdot (k_{j,k} - k_{j-1,k}) \\ \left(\frac{\Gamma_\omega}{J} \right)_{j+\frac{1}{2},k} \cdot (\omega_{j+1,k} - \omega_{j,k}) - \left(\frac{\Gamma_\omega}{J} \right)_{j-\frac{1}{2},k} \cdot (\omega_{j,k} - \omega_{j-1,k}) \end{array} \right]$$

$$H^\bullet = \frac{M_\infty}{\text{Re}} \cdot \left[\begin{array}{l} \left(\frac{\Gamma_k}{J} \right)_{j+\frac{1}{2},k} \cdot (k_{j+1,k} - k_{j,k}) - \left(\frac{\Gamma_k}{J} \right)_{j-\frac{1}{2},k} \cdot (k_{j,k} - k_{j-1,k}) \\ \left(\frac{\Gamma_\omega}{J} \right)_{j+\frac{1}{2},k} \cdot (\omega_{j+1,k} - \omega_{j,k}) - \left(\frac{\Gamma_\omega}{J} \right)_{j-\frac{1}{2},k} \cdot (\omega_{j,k} - \omega_{j-1,k}) \end{array} \right]$$

$$3) -t^{**} \cdot \delta_{\eta}^{upwind} G = -t^{**} \cdot \frac{G_{j,k+1} - G_{j,k-1}}{2} + t^{**} \cdot \left[\frac{|G|_{j,k+1} - 2 \cdot |G|_{j,k} - |G|_{j,k-1}}{2} \right]$$

$$4) t^{**} \cdot \delta_{\eta} K^* = t^{**} \cdot \frac{M_{\infty}}{\text{Re}} \cdot \delta_{\eta} \begin{bmatrix} \frac{\Gamma'_k}{J} \cdot \frac{\partial k}{\partial \eta} \\ \frac{\Gamma'_{\omega}}{J} \cdot \frac{\partial \omega}{\partial \eta} \end{bmatrix}$$

$$= t^{**} \cdot \frac{M_{\infty}}{\text{Re}} \cdot \begin{bmatrix} \left(\frac{\Gamma'_k}{J} \right)_{j,k+\frac{1}{2}} \cdot (k_{j,k+1} - k_{j,k}) - \left(\frac{\Gamma'_k}{J} \right)_{j,k-\frac{1}{2}} \cdot (k_{j,k} - k_{j,k-1}) \\ \left(\frac{\Gamma'_{\omega}}{J} \right)_{j,k+\frac{1}{2}} \cdot (\omega_{j,k+1} - \omega_{j,k}) - \left(\frac{\Gamma'_{\omega}}{J} \right)_{j,k-\frac{1}{2}} \cdot (\omega_{j,k} - \omega_{j,k-1}) \end{bmatrix}$$

$$K^* = \frac{M_{\infty}}{\text{Re}} \cdot \begin{bmatrix} \left(\frac{\Gamma'_k}{J} \right)_{j,k+\frac{1}{2}} \cdot (k_{j,k+1} - k_{j,k}) - \left(\frac{\Gamma'_k}{J} \right)_{j,k-\frac{1}{2}} \cdot (k_{j,k} - k_{j,k-1}) \\ \left(\frac{\Gamma'_{\omega}}{J} \right)_{j,k+\frac{1}{2}} \cdot (\omega_{j,k+1} - \omega_{j,k}) - \left(\frac{\Gamma'_{\omega}}{J} \right)_{j,k-\frac{1}{2}} \cdot (\omega_{j,k} - \omega_{j,k-1}) \end{bmatrix}$$

$$5) t^{**} \cdot M^*_{j,k}$$

$$6) \frac{\phi}{1+\phi} \cdot \Delta Q_{j,k}^{n-1}.$$

η sweep

$$\left[1 + \frac{\theta \cdot \Delta \tau}{1+\phi} \cdot \left(\frac{\partial}{\partial \xi} (A - U + R_{\xi})^n - \frac{\partial^2}{\partial \xi^2} R^n \right) \right] \bullet \Delta Q^n = \Delta Q^{n \otimes} \quad (\text{D.3})$$

$$\left[1 + \frac{\theta \cdot \Delta \tau}{1+\phi} \cdot \left(\frac{\partial}{\partial \xi} (A - U + R_{\xi})^n - \frac{\partial^2}{\partial \xi^2} R^n \right) \right] \bullet q = \Delta Q^{n \otimes}$$

$$\underbrace{q}_1 + \underbrace{t^* \cdot \delta_{\xi}^{upwind} \cdot (A \cdot q)}_2 - \underbrace{t^* \cdot \delta_{\xi} \cdot (U \cdot q)}_3 + \underbrace{t^* \cdot \delta_{\xi} \cdot (R_{\xi} \cdot q)}_4 - \underbrace{t^* \cdot \delta_{\xi}^2 \cdot (R \cdot q)}_5 = \Delta Q^{n \otimes}$$

The following notations are presented due to simplicity in derivations,

$$t^* = \frac{\theta \cdot \Delta \tau}{1 + \phi}, \quad q = \Delta Q^n$$

1) $q_{j,k}$

$$2) t^* \cdot \delta_{\xi}^{supwind} \cdot (A \cdot q) = t^* \cdot \frac{(A \cdot q)_{j+1,k} - (A \cdot q)_{j-1,k}}{2} - t^* \cdot \left[\frac{(|A| \cdot q)_{j+1,k} - 2 \cdot (|A| \cdot q)_{j,k} - (|A| \cdot q)_{j-1,k}}{2} \right]$$

$$-t^* \cdot \delta_{\xi} \cdot (U \cdot q) = -t^* \cdot \frac{M_{\infty}}{\text{Re}} \cdot \frac{\partial}{\partial \xi} \begin{bmatrix} \frac{\Gamma_k}{J} \cdot \frac{\partial (J/\rho \cdot q_1)}{\partial \xi} & 0 \\ 0 & \frac{\Gamma_{\omega}}{J} \cdot \frac{\partial (J/\rho \cdot q_2)}{\partial \xi} \end{bmatrix}$$

$$3) = -t^* \cdot \frac{M_{\infty}}{\text{Re}} \cdot \begin{bmatrix} \frac{\partial}{\partial \xi} \left(\frac{\Gamma_k}{J} \cdot \frac{\partial (J/\rho \cdot q_1)}{\partial \xi} \right) & 0 \\ 0 & \frac{\partial}{\partial \xi} \left(\frac{\Gamma_{\omega}}{J} \cdot \frac{\partial (J/\rho \cdot q_2)}{\partial \xi} \right) \end{bmatrix}$$

$$= -t^* \cdot \frac{M_{\infty}}{\text{Re}} \cdot \begin{bmatrix} \frac{\left(\frac{\Gamma_k}{J} \cdot \frac{\partial (J/\rho \cdot q_1)}{\partial \xi} \right)_{j+\frac{1}{2},k} - \left(\frac{\Gamma_k}{J} \cdot \frac{\partial (J/\rho \cdot q_1)}{\partial \xi} \right)_{j-\frac{1}{2},k}}{\Delta \xi} & 0 \\ 0 & \frac{\left(\frac{\Gamma_{\omega}}{J} \cdot \frac{\partial (J/\rho \cdot q_2)}{\partial \xi} \right)_{j+\frac{1}{2},k} - \left(\frac{\Gamma_{\omega}}{J} \cdot \frac{\partial (J/\rho \cdot q_2)}{\partial \xi} \right)_{j-\frac{1}{2},k}}{\Delta \xi} \end{bmatrix}$$

($\Delta \xi = 1$)

$$= -t^* \cdot \frac{M_{\infty}}{\text{Re}} \cdot \begin{bmatrix} \left(\frac{\Gamma_k}{J} \right)_{j+\frac{1}{2},k} \cdot \left(\left(\frac{J}{\rho} \cdot q_1 \right)_{j+1,k} - \left(\frac{J}{\rho} \cdot q_1 \right)_{j,k} \right) - \left(\frac{\Gamma_k}{J} \right)_{j-\frac{1}{2},k} \cdot \left(\left(\frac{J}{\rho} \cdot q_1 \right)_{j,k} - \left(\frac{J}{\rho} \cdot q_1 \right)_{j-1,k} \right) & 0 \\ 0 & \sim \end{bmatrix}$$

$$= -t^* \cdot \frac{M_{\infty}}{\text{Re}} \cdot \begin{bmatrix} \left[\left(\frac{\Gamma_k}{J} \right)_{j+\frac{1}{2},k} \cdot \left(\frac{J}{\rho} \right)_{j+1,k} \right] \cdot q_{1j+1,k} - \left[\left(\frac{\Gamma_k}{J} \right)_{j+\frac{1}{2},k} + \left(\frac{\Gamma_k}{J} \right)_{j-\frac{1}{2},k} \right] \cdot \left(\frac{J}{\rho} \right)_{j,k} \cdot q_{1j,k} + \left[\left(\frac{\Gamma_k}{J} \right)_{j-\frac{1}{2},k} \cdot \left(\frac{J}{\rho} \right)_{j-1,k} \right] \cdot q_{1j-1,k} & 0 \\ 0 & \sim \end{bmatrix}$$

Dividing the matrix into three parts,

$$\begin{aligned}
&= -t^* \cdot \frac{M_\infty}{\text{Re}} \cdot \underbrace{\begin{bmatrix} \left(\frac{\Gamma_k}{J}\right)_{j+\frac{1}{2},k} \cdot \left(\frac{J}{\rho}\right)_{j+1,k} & & 0 \\ & 0 & \left(\frac{\Gamma_\omega}{J}\right)_{j+\frac{1}{2},k} \cdot \left(\frac{J}{\rho}\right)_{j+1,k} \end{bmatrix}}_{U_{\xi P}} \cdot q_{j+1,k} \\
&+ t^* \cdot \frac{M_\infty}{\text{Re}} \cdot \underbrace{\begin{bmatrix} \left(\left(\frac{\Gamma_k}{J}\right)_{j+\frac{1}{2},k} + \left(\frac{\Gamma_k}{J}\right)_{j-\frac{1}{2},k} \right) \cdot \left(\frac{J}{\rho}\right)_{j,k} & & 0 \\ & 0 & \left(\left(\frac{\Gamma_\omega}{J}\right)_{j+\frac{1}{2},k} + \left(\frac{\Gamma_\omega}{J}\right)_{j-\frac{1}{2},k} \right) \cdot \left(\frac{J}{\rho}\right)_{j,k} \end{bmatrix}}_{U_{\xi J}} \cdot q_{j,k} \\
&- t^* \cdot \frac{M_\infty}{\text{Re}} \cdot \underbrace{\begin{bmatrix} \left(\frac{\Gamma_k}{J}\right)_{j-\frac{1}{2},k} \cdot \left(\frac{J}{\rho}\right)_{j-1,k} & & 0 \\ & 0 & \left(\frac{\Gamma_\omega}{J}\right)_{j-\frac{1}{2},k} \cdot \left(\frac{J}{\rho}\right)_{j-1,k} \end{bmatrix}}_{U_{\xi R}} \cdot q_{j-1,k} \\
&= t^* \cdot \left(-U_{\xi P} \cdot q_{j+1,k} + U_{\xi J} \cdot q_{j,k} - U_{\xi R} \cdot q_{j-1,k} \right) \\
&t^* \cdot \delta_\xi \cdot (R_\xi \cdot q) = t^* \cdot \frac{M_\infty}{\text{Re}} \cdot \frac{\partial}{\partial \xi} \begin{bmatrix} \frac{\partial}{\partial \xi} \left(\Gamma_k \cdot \frac{1}{\rho} \right) \cdot q_1 & & 0 \\ & 0 & \frac{\partial}{\partial \xi} \left(\Gamma_\omega \cdot \frac{1}{\rho} \right) \cdot q_2 \end{bmatrix} \\
4) &= t^* \cdot \frac{M_\infty}{\text{Re}} \cdot \begin{bmatrix} \delta_\xi^2 \left(\frac{\Gamma_k}{\rho} \right) \cdot q_1 + \delta_\xi \left(\frac{\Gamma_k}{\rho} \right) \cdot \delta_\xi q_1 & & 0 \\ & 0 & \delta_\xi^2 \left(\frac{\Gamma_\omega}{\rho} \right) \cdot q_2 + \delta_\xi \left(\frac{\Gamma_\omega}{\rho} \right) \cdot \delta_\xi q_2 \end{bmatrix} \\
&= t^* \cdot \frac{M_\infty}{\text{Re}} \cdot \underbrace{\begin{bmatrix} \left(\frac{\Gamma_k}{\rho}\right)_{j+1,k} & -2 \cdot \left(\frac{\Gamma_k}{\rho}\right)_{j,k} & + \left(\frac{\Gamma_k}{\rho}\right)_{j-1,k} & & 0 \\ & 0 & & \left(\frac{\Gamma_\omega}{\rho}\right)_{j+1,k} & -2 \cdot \left(\frac{\Gamma_\omega}{\rho}\right)_{j,k} & + \left(\frac{\Gamma_\omega}{\rho}\right)_{j-1,k} \end{bmatrix}}_{R_{\xi J}} \cdot q_{j,k}
\end{aligned}$$

$$\begin{aligned}
& + t^* \cdot \frac{M_\infty}{4 \cdot \text{Re}} \cdot \underbrace{\begin{bmatrix} \left(\frac{\Gamma_k}{\rho}\right)_{j+1,k} & -\left(\frac{\Gamma_k}{\rho}\right)_{j-1,k} & 0 \\ 0 & \left(\frac{\Gamma_\omega}{\rho}\right)_{j+1,k} & -\left(\frac{\Gamma_\omega}{\rho}\right)_{j+1,k} \end{bmatrix}}_{R_{\xi JP}} \cdot q_{j+1,k} \\
& - t^* \cdot \frac{M_\infty}{4 \cdot \text{Re}} \cdot \underbrace{\begin{bmatrix} \left(\frac{\Gamma_k}{\rho}\right)_{j+1,k} & -\left(\frac{\Gamma_k}{\rho}\right)_{j-1,k} & 0 \\ 0 & \left(\frac{\Gamma_\omega}{\rho}\right)_{j+1,k} & -\left(\frac{\Gamma_\omega}{\rho}\right)_{j+1,k} \end{bmatrix}}_{R_{\xi R} = R_{\xi P}} \cdot q_{j-1,k} \\
& = t^* \cdot (R_{\xi JP} \cdot q_{j+1,k} + R_{\xi J} \cdot q_{j,k} - R_{\xi JR} \cdot q_{j-1,k})
\end{aligned}$$

$$5) -t^* \cdot \delta_\xi^2 \cdot (R \cdot q) = -t^* \cdot (R_{j+1,k} \cdot q_{j+1,k} - 2 \cdot R_{j,k} \cdot q_{j,k} + R_{j-1,k} \cdot q_{j-1,k})$$

ξ sweep

$$\begin{aligned}
& \left[-t^* \cdot \frac{B_{j,k-1}}{2} - t^* \cdot \frac{|B|_{j,k-1}}{2} - t^* \cdot V_{\eta KR} - t^* \cdot S_{\eta KR} - t^* \cdot S_{j,k-1} \right] \cdot q_{j,k-1} \\
& + \left[I + t^* \cdot |B|_{j,k} + t^* \cdot V_{\eta K} + t^* \cdot S_{\eta K} + 2 \cdot t^* \cdot S_{j,k} - t^* \cdot C_{j,k} \right] \cdot q_{j,k} \\
& \left[t^* \cdot \frac{B_{j,k+1}}{2} - t^* \cdot \frac{|B|_{j,k+1}}{2} - t^* \cdot V_{\eta KP} + t^* \cdot S_{\eta KP} - t^* \cdot S_{j,k+1} \right] \cdot q_{j,k+1} \\
& = RHS \\
& = -t^{**} \cdot \frac{F_{j+1,k} - F_{j-1,k}}{2} + \left[\frac{|F|_{j+1,k} - 2 \cdot |F|_{j,k} - |F|_{j-1,k}}{2} \right] + t^{**} \cdot H \bullet \\
& - t^{**} \cdot \frac{G_{j,k+1} - G_{j,k-1}}{2} + \left[\frac{|G|_{j,k+1} - 2 \cdot |G|_{j,k} - |G|_{j,k-1}}{2} \right] + t^{**} \cdot K \bullet \\
& + t^{**} \cdot M^*_{j,k} + \frac{\phi}{1 + \phi} \cdot \Delta Q_{j,k}^{n-1}
\end{aligned}$$

η sweep

$$\begin{aligned}
 & \left[-t^* \cdot \frac{A_{j-1,k}}{2} - t^* \cdot \frac{|A|_{j-1,k}}{2} - t^* \cdot U_{\xi JR} - t^* \cdot R_{\xi JR} - t^* \cdot R_{j-1,k} \right] \cdot q_{j-1,k} \\
 & + \left[I + t^* \cdot |A|_{j,k} + t^* \cdot U_{\xi J} + t^* \cdot R_{\xi J} + 2 \cdot t^* \cdot R_{j,k} \right] \cdot q_{j,k} \\
 & \left[t^* \cdot \frac{A_{j+1,k}}{2} - t^* \cdot \frac{|A|_{j+1,k}}{2} - t^* \cdot U_{\xi JP} + t^* \cdot R_{\xi JP} - t^* \cdot R_{j+1,k} \right] \cdot q_{j+1,k} \\
 & = \Delta Q_{j,k}^n \otimes
 \end{aligned}$$

APPENDIX E

Contour results for RAE2822 $M=0.725$, $AoA=2.92$ case

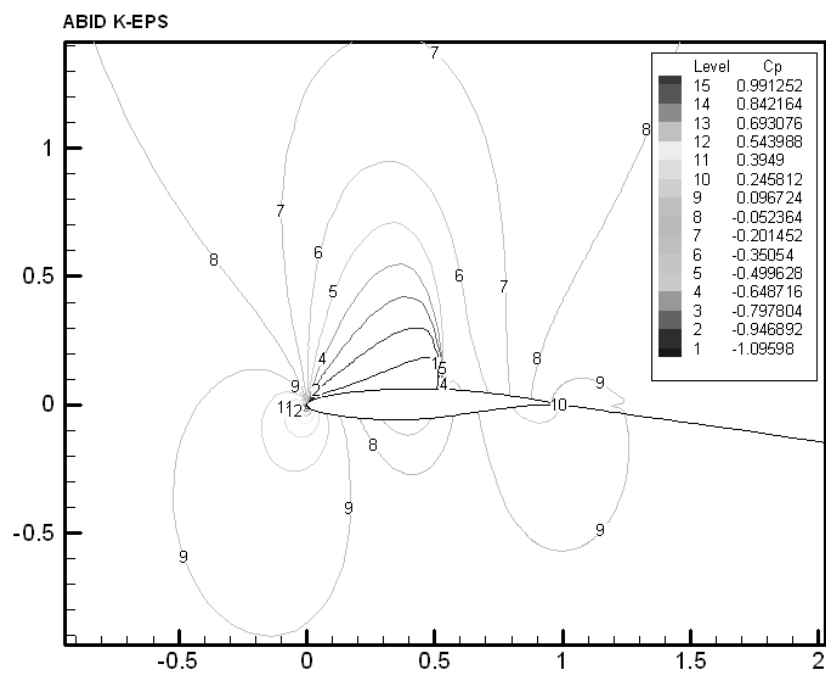


Figure 0.1 C_p contours, *Abid k-ε*

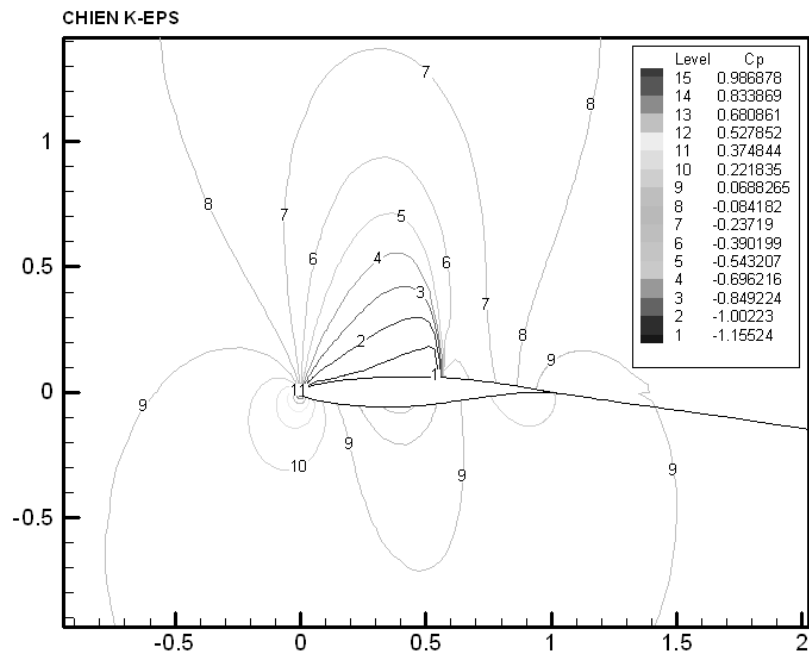


Figure 0.2 C_p contours, *Chien k- ϵ*

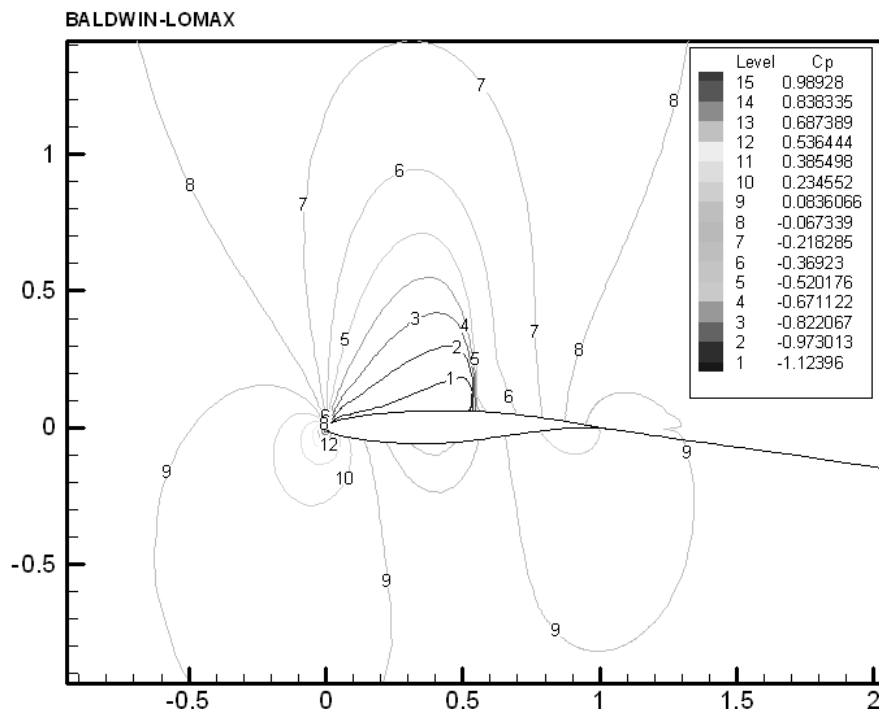


Figure 0.3 C_p contours, *Baldwin-Lomax*

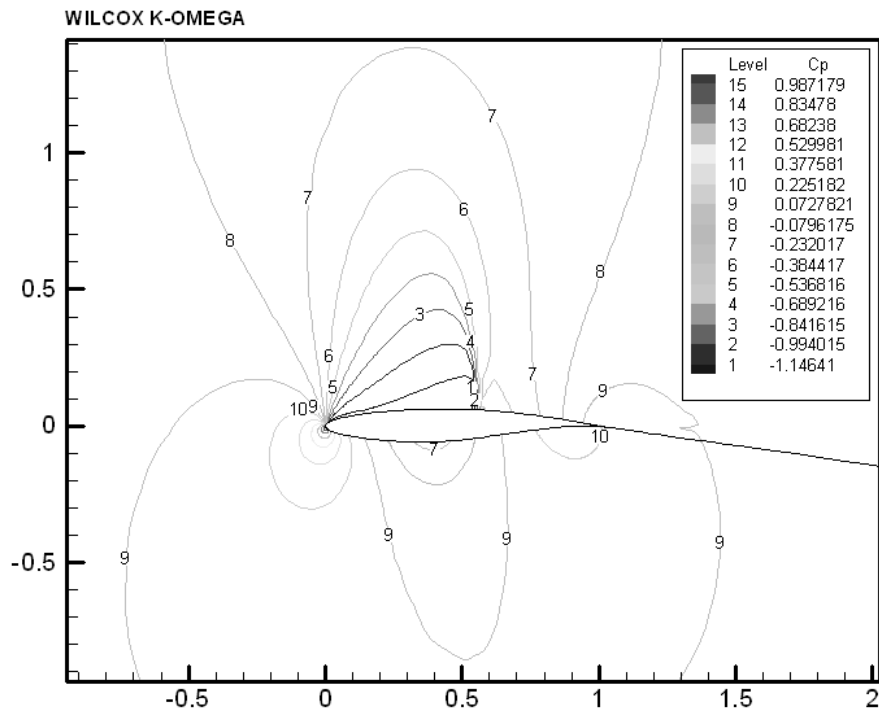


Figure 0.4 C_p contours, *Wilcox k- ω*

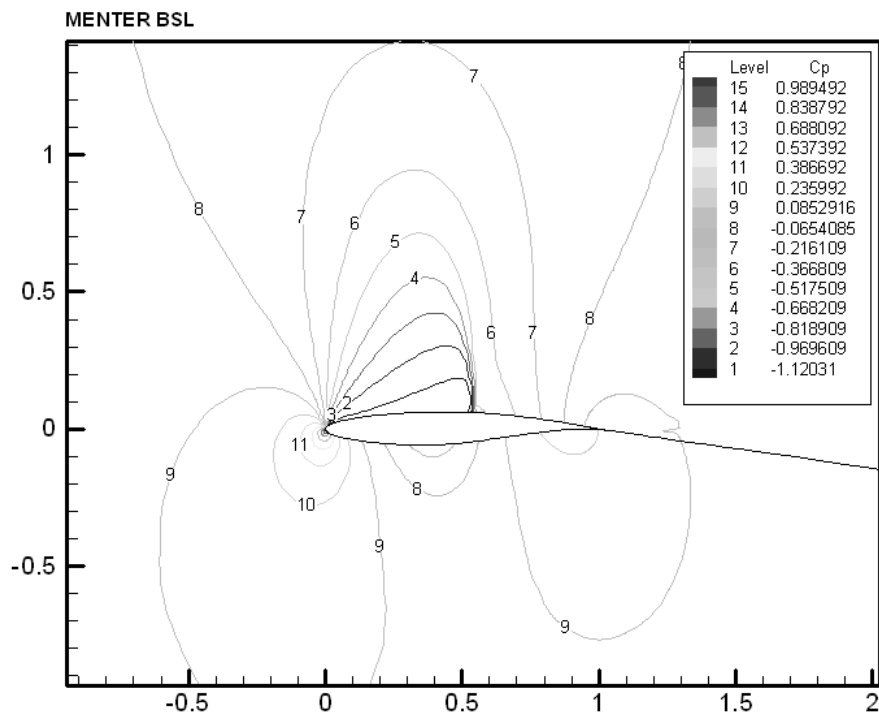


Figure 0.5 C_p contours, *Menter BSL*

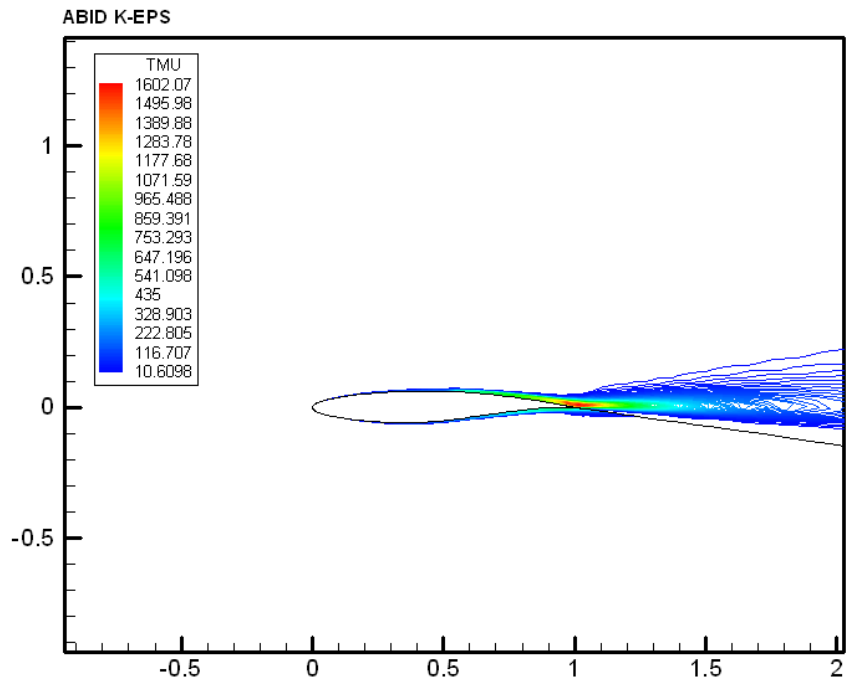


Figure 0.6 μ_T contours, *Abid k-ε*

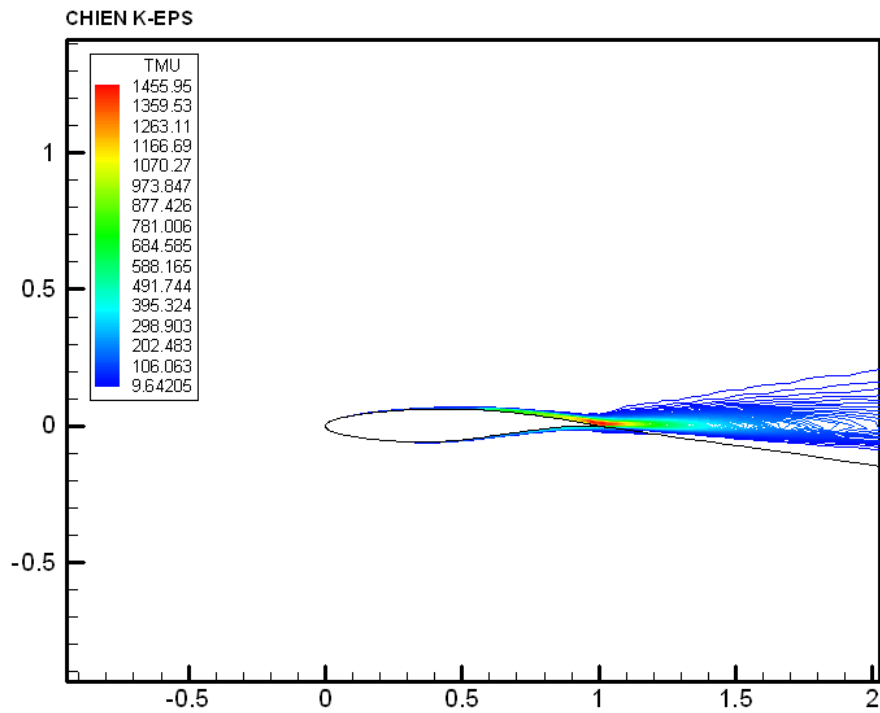


Figure 0.7 μ_T contours, *Chien k-ε*

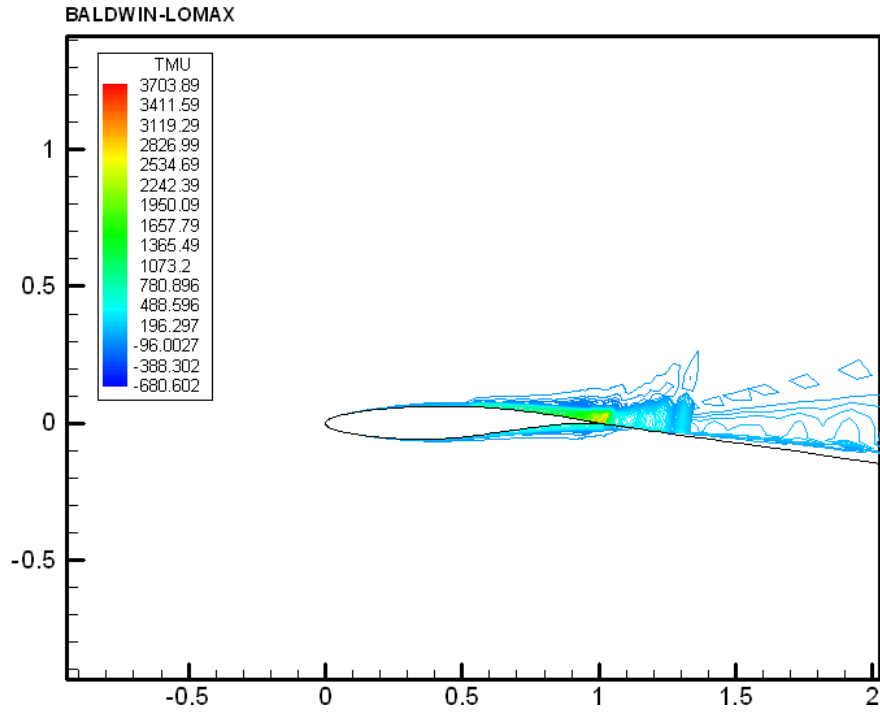


Figure 0.8 μ_T contours, *Baldwin-Lomax*

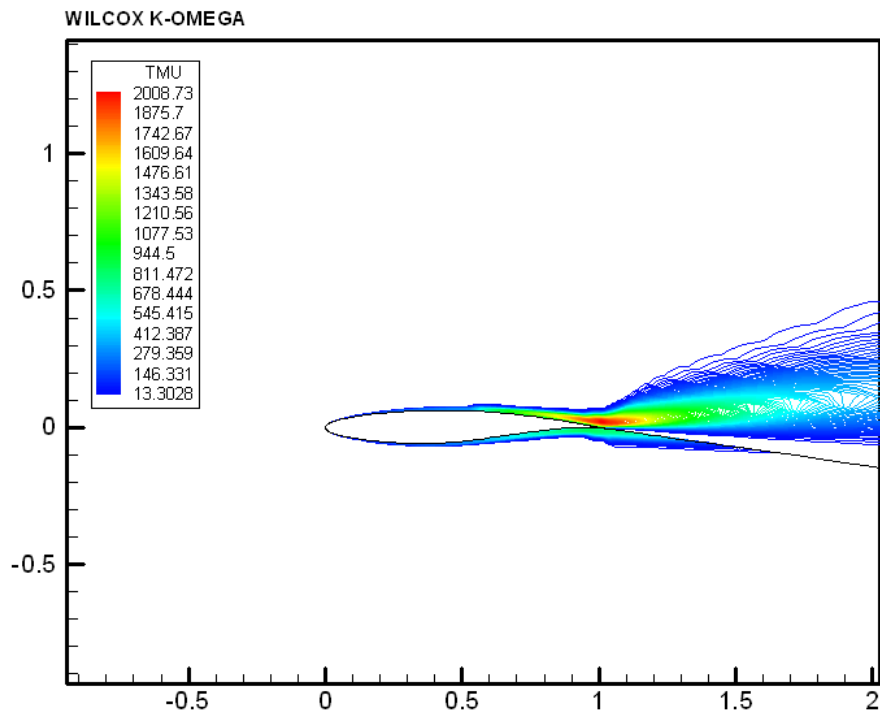


Figure 0.9 μ_T contours, *Wilcox k- ω*

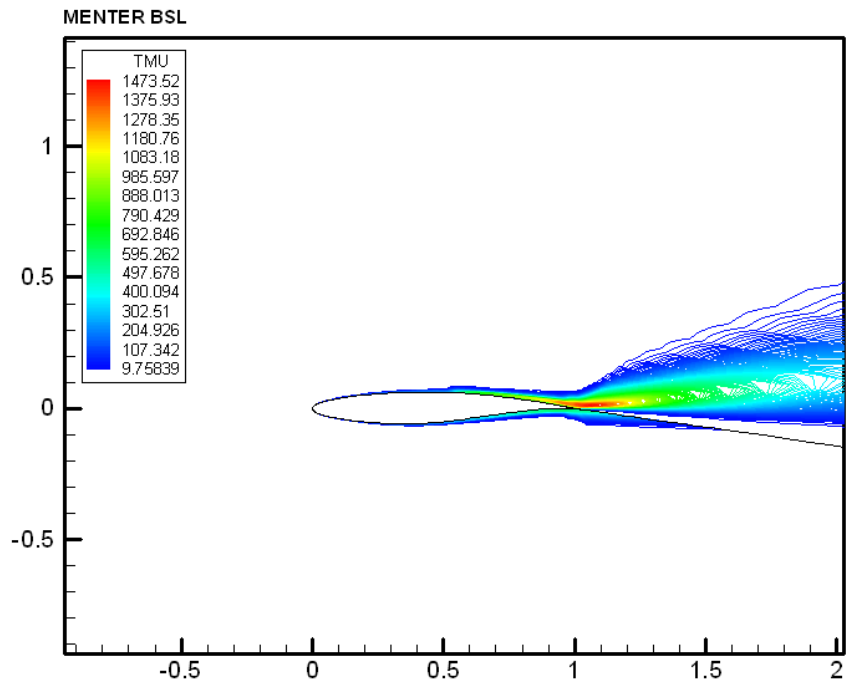


Figure 0.10 μ_T contours, *Menter BSL*

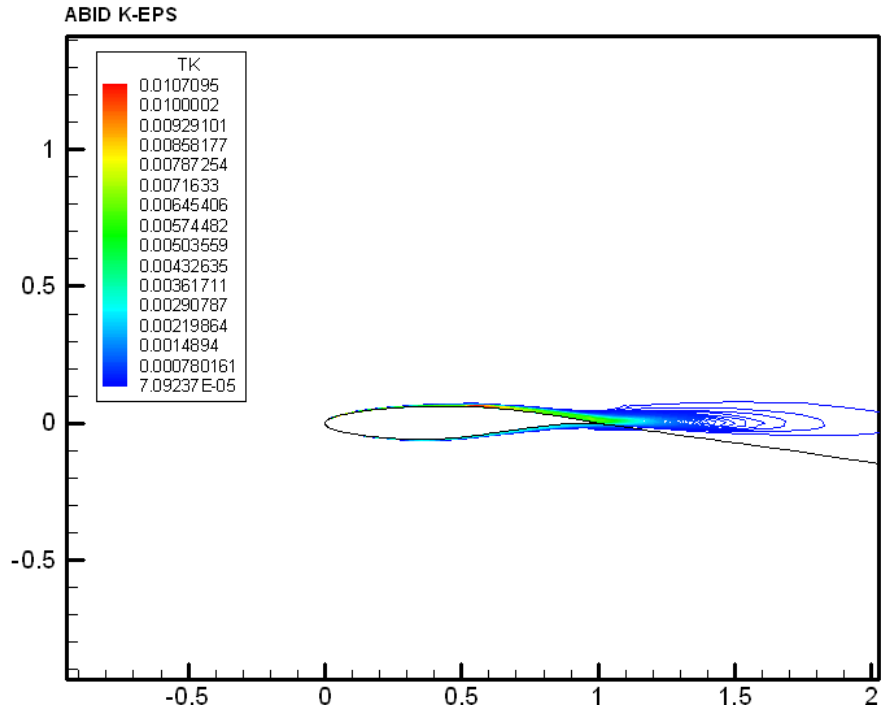


Figure 0.11 k contours, *Abid k- ϵ*

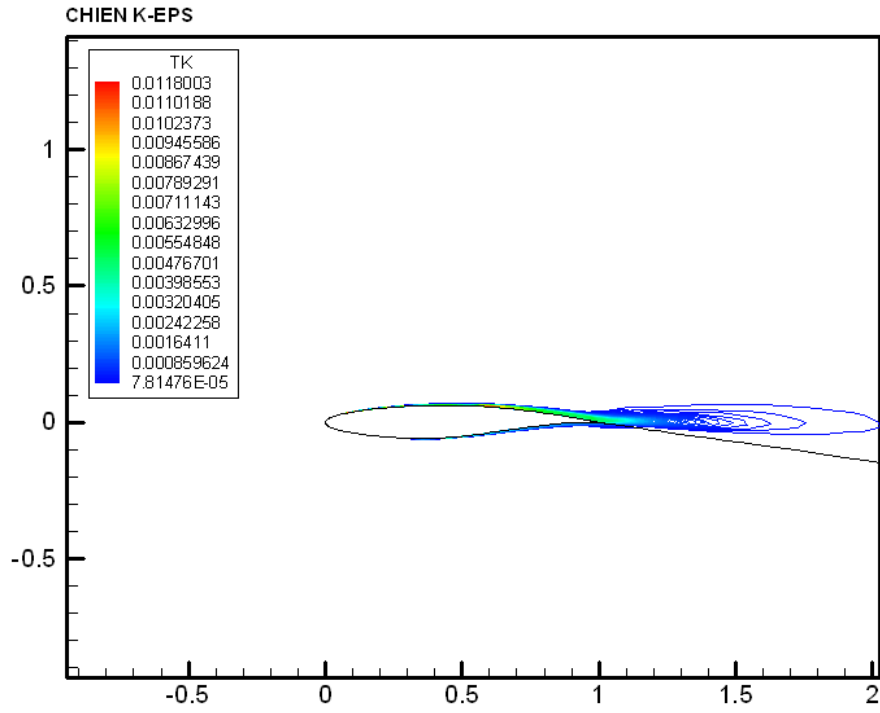


Figure 0.12 k contours, *Chien $k-\epsilon$*

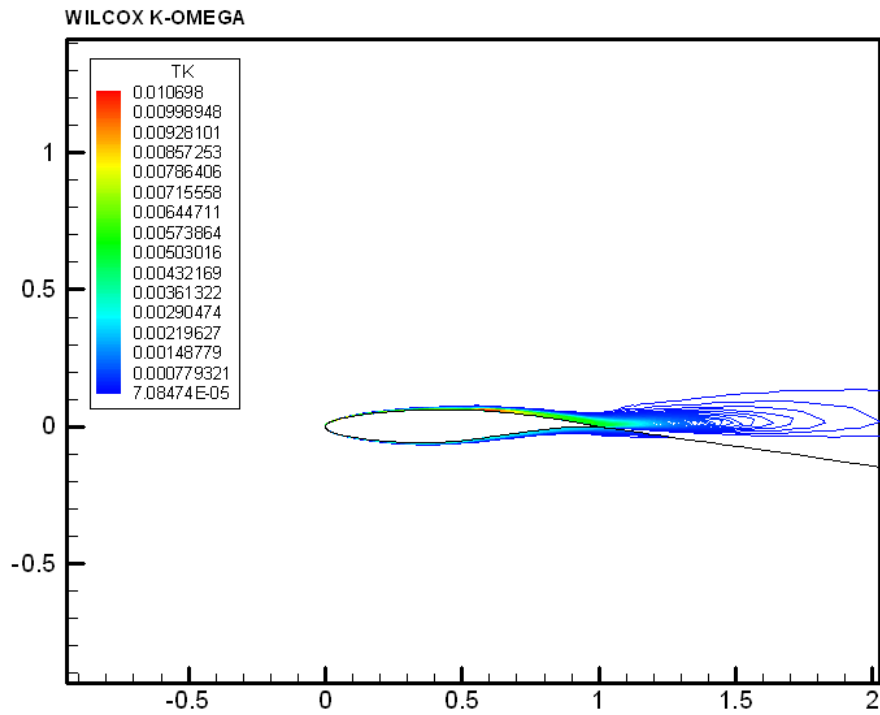


Figure 0.13 k contours, *Wilcox $k-\omega$*

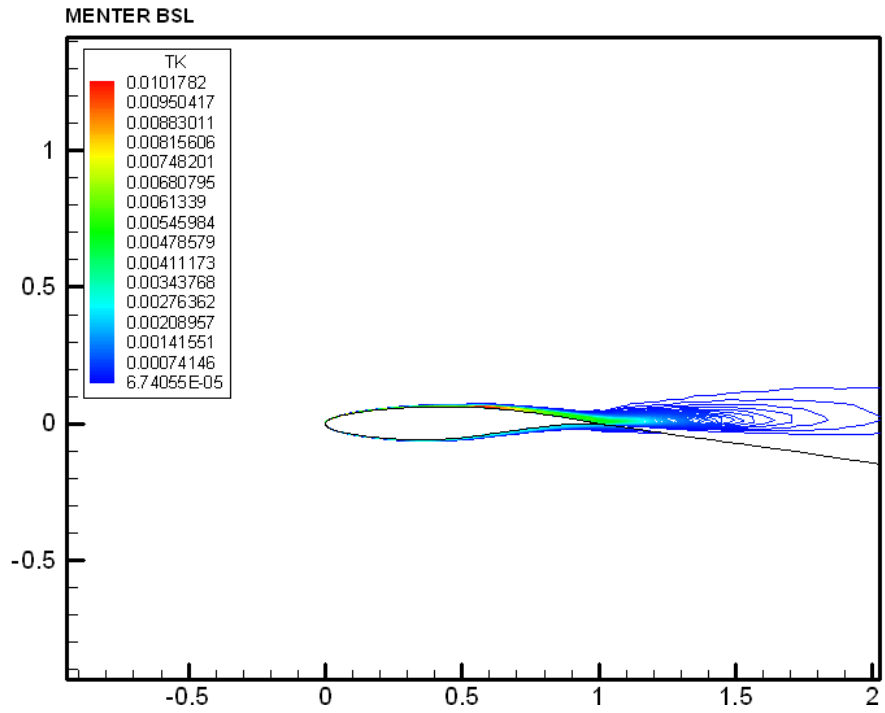


Figure 0.14 k contours, *Menter BSL*

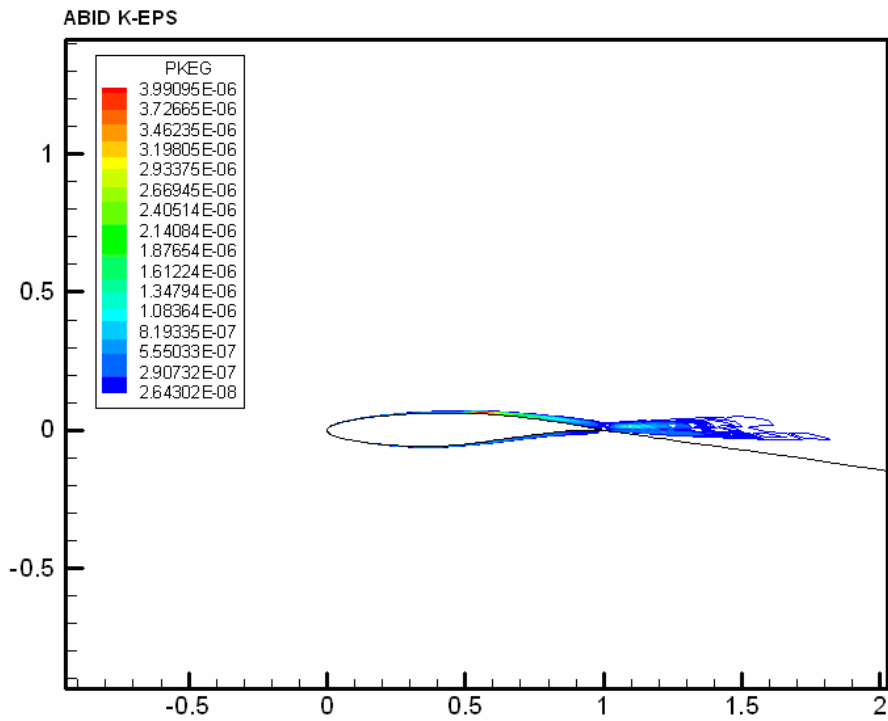


Figure 0.15 k production contours, *Abid $k-\epsilon$*

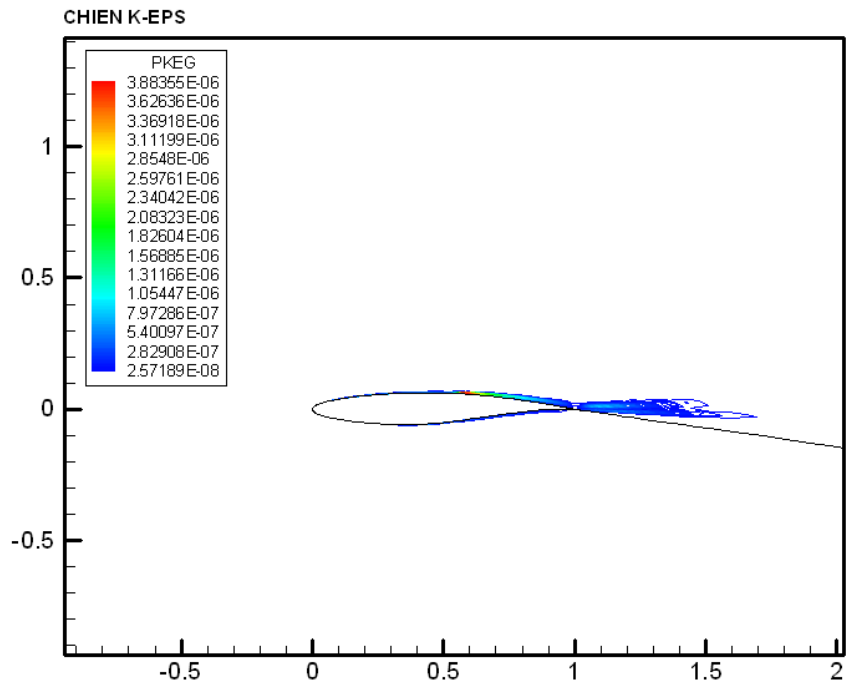


Figure 0.16 k production contours, *Chien $k-\epsilon$*

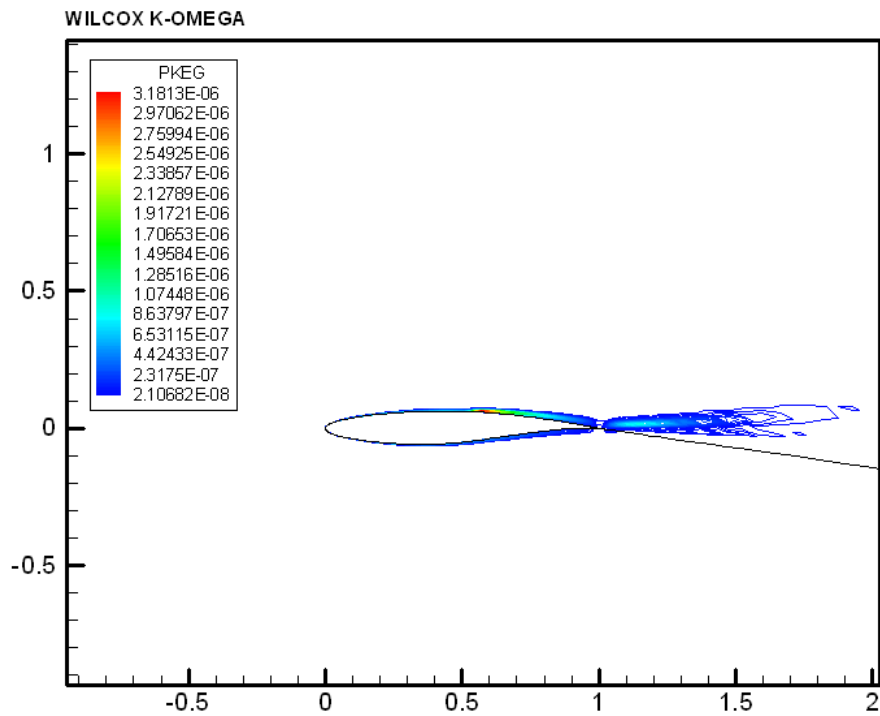


Figure 0.17 k production contours, *Wilcox $k-\omega$*

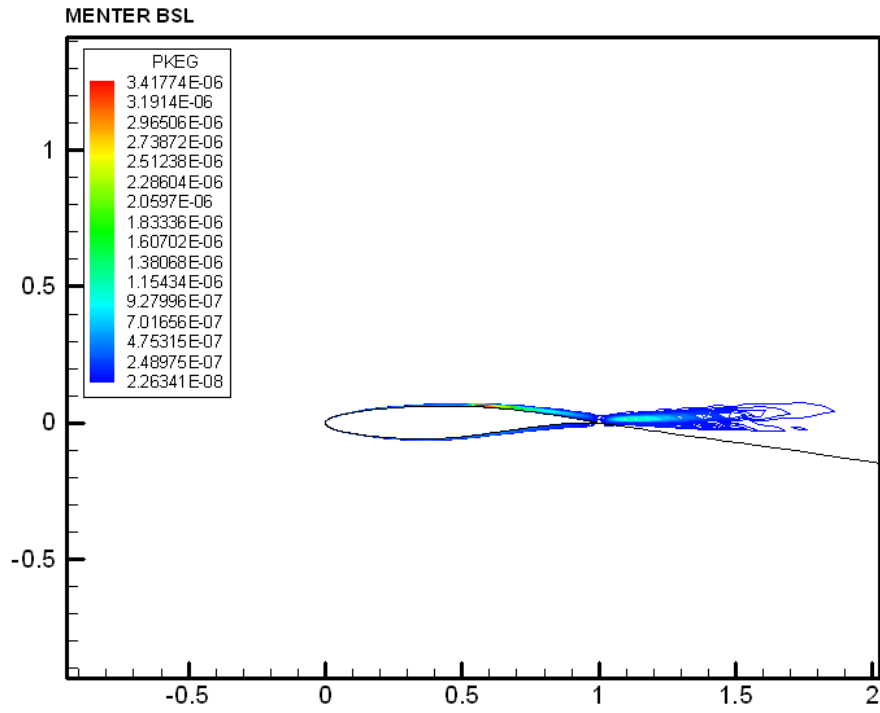


Figure 0.18 k production contours, *Menter BSL*

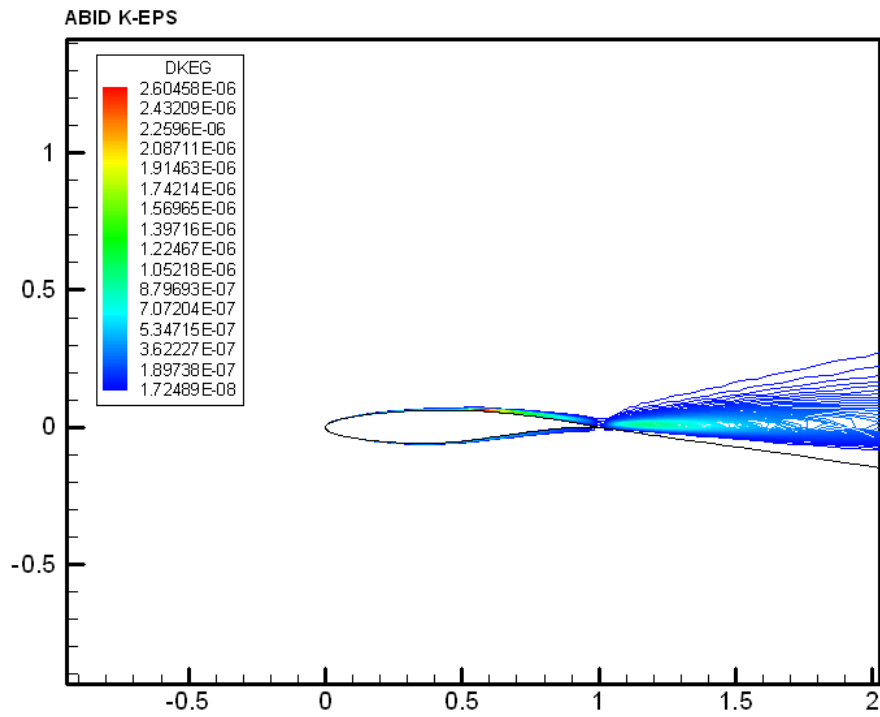


Figure 0.19 k destruction contours, *Abid k-ε*

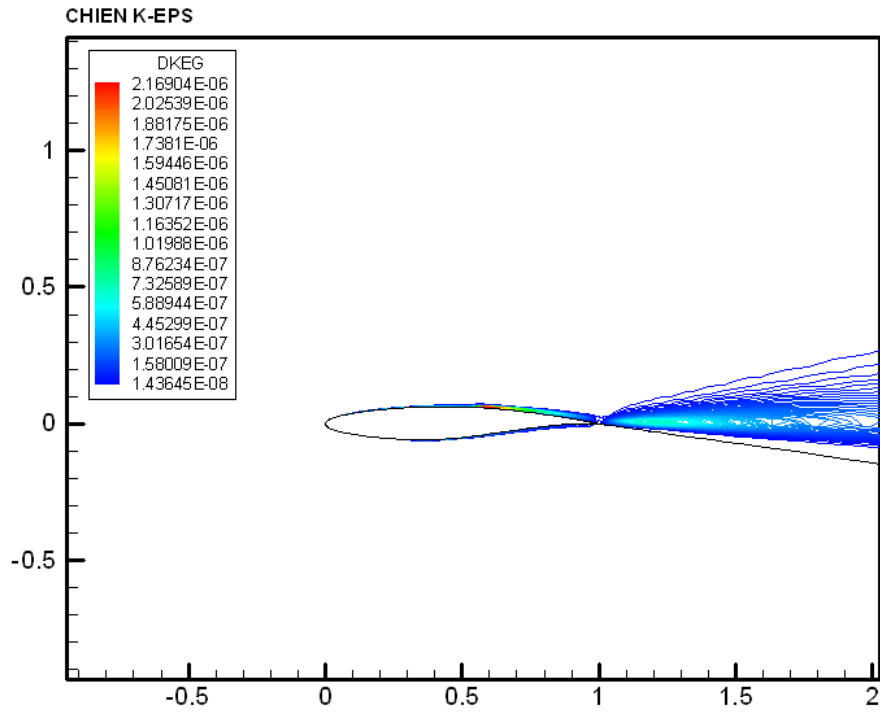


Figure 0.20 k destruction contours, *Chien $k-\epsilon$*

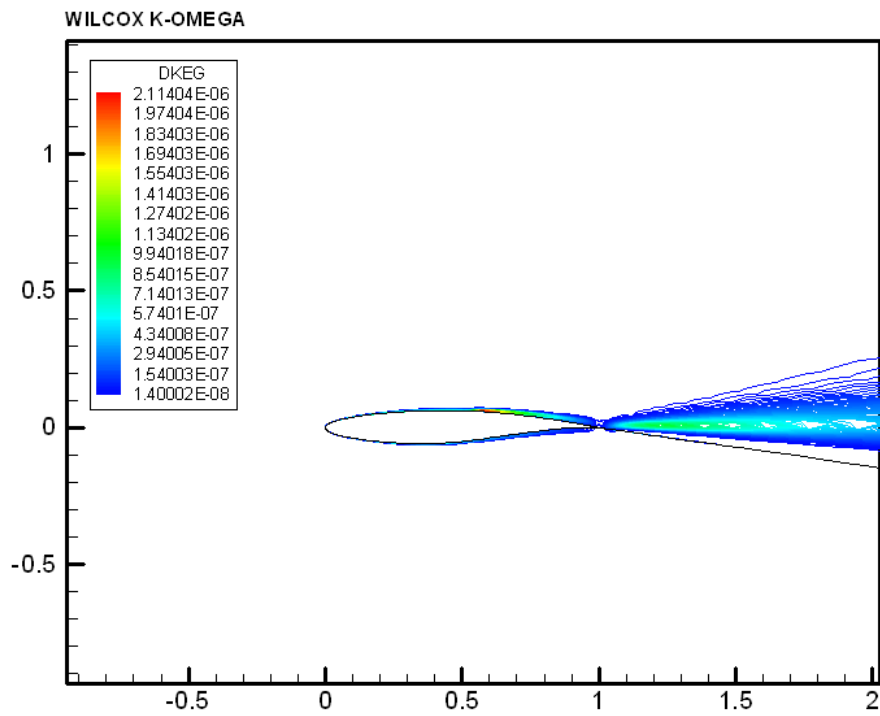


Figure 0.21 k destruction contours, *Wilcox $k-\omega$*

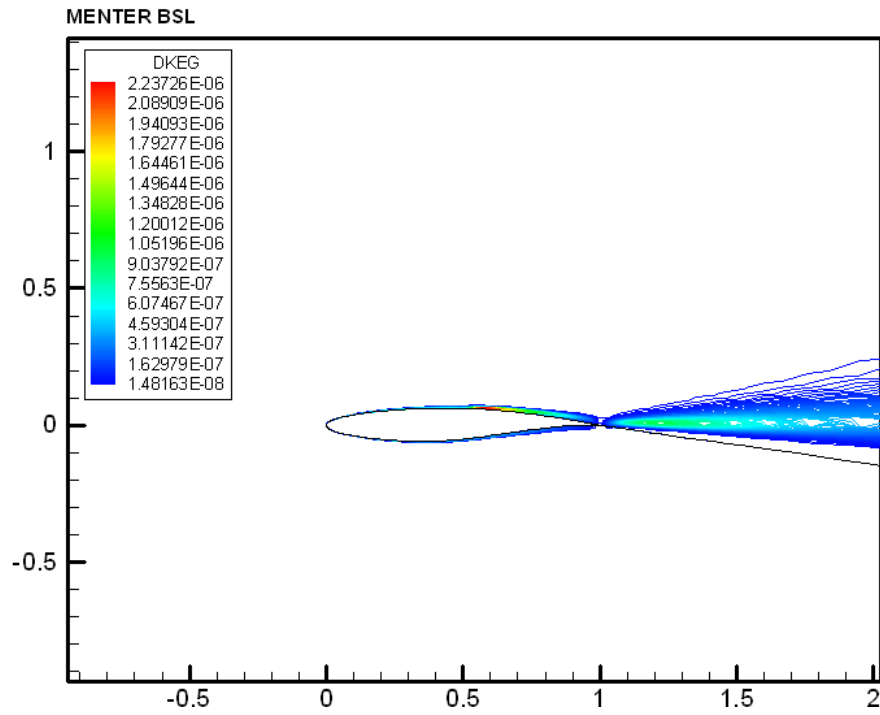


Figure 0.22 k destruction contours, *Menter BSL*